

Alma Mater Studiorum – Università di Bologna

**DOTTORATO DI RICERCA IN
SCIENZE VETERINARIE**

Ciclo XXIX

Settore Concorsuale di afferenza: Cliniche chirurgica e ostetrica veterinaria 07-H5

Settore Scientifico disciplinare: Clinica ostetrica e ginecologia veterinaria VET-10

**Morphology and microscopy of equine umbilical cord and
characterization of Mesenchymal Stem Cells isolated from
foetal adnexa**

Presentata da:

Dott.ssa Aliai Lanci

Coordinatore Dottorato

Chiar.mo Prof. Arcangelo Gentile

Relatore

Chiar.ma Prof.ssa Carolina Castagnetti

Correlatore

Chiar.ma Prof.ssa Eleonora Iacono

Esame finale anno 2017

TABLE OF CONTENTS

ABSTRACT	1
INTRODUCTION.....	2
<i>SECTION I- Studies on equine umbilical cord</i>	8
CHAPTER 1	8
✓ Study of umbilical cord in the equine species	8
✓ Macroscopic characteristics of the umbilical cord in standardbred, thoroughbred and saddlebred horses	11
✓ Preliminary descriptive study of equine placenta generated after transfer of in vivo and in vitro produced embryos	26
CHAPTER 2	29
✓ Microscopic characteristics of the umbilical cord in the equine species.....	29
<i>SECTION II- Studies on equine Mesenchymal Stem Cells</i>	48
CHAPTER 3	48
✓ Expression of proinflammatory cytokines by equine Mesenchymal Stem Cells from foetal adnexa: preliminary data	48
✓ Ultrastructural characteristics and immune profile of Mesenchymal Stem Cells derived from equine foetal adnexa.....	51
CHAPTER 4	80
✓ Wharton's jelly derived Mesenchymal Stem Cells: comparing human and horse.....	80
CHAPTER 5	104
✓ Ultrastructural comparison between equine adult and foetal Mesenchymal Stem Cells.....	104

<i>SECTION III- Clinical Application</i>	133
CHAPTER 6	133
✓ Effects of amniotic fluid Mesenchymal Stem Cells in carboxymethyl cellulose gel on healing of spontaneous pressure sores: clinical outcome in seven hospitalized neonatal foals.	133
CHAPTER 7	143
✓ Effects of Wharton’s jelly Mesenchymal Stem Cells on pressure sore of a six-month-old filly.....	143
GENERAL RESULTS AND DISCUSSION	167
CONCLUSIONS	173

ABSTRACT

The purpose of this PhD thesis is to perform a dissertation about the equine umbilical cord (UC), with particular attention to its macroscopic characteristics moving into its microscopic features. Furthermore, equine UC was microscopically and immunohistochemically described. The coiling makes the UC a structure both flexible and strong, and provides resistance to external forces, which could compromise blood flow. Data obtained from the present study could be considered as a normal range of number of coils and UCI in the equine physiological pregnancies. The second and major component of this dissertation was focused on umbilical cord as a Mesenchymal Stem Cells (MSCs) niche. In particular, the ultrastructural characterization and immune profile of equine MSCs derived from foetal tissues (Wharton's jelly and blood) were investigated; equine foetal MSCs were then compared to human foetal MSCs and equine adult MSCs. The third section included the clinical applications of MSCs derived from AF and WJ on cutaneous wounds of different ages' foals. The employ of foetal MSCs on cutaneous wounds decreased their healing both in neonatal foals and six-month foals, in comparison with other traditional treatments. In conclusion, one of the most important feature of placenta's evaluation is the observation of normal characteristic of the equine UC. Furthermore, since the UC is a discarded material after delivery, it represents an excellent non-invasive alternative source of MSCs with reliable migration and differentiation capacities, and it is a convenient cell source for autologous or allogeneic regenerative therapies. Finally, it is important a constant update about regenerative medicine and the development of research in this field considering that the horse serves as a perfect model for humans.

Key words: equine, umbilical cord, Mesenchymal Stem Cells

INTRODUCTION

The umbilical cord (UC) represents an important connection between mother and fetus and it is designed to protect blood flow to the fetus during pregnancy. This particular property is due to the UC intervascular stroma, a mucous connective tissue, also called Wharton's jelly (WJ). It develops from extraembryonic mesoderm, binds and encases the umbilical vessels, protecting them from twisting and compression during pregnancy (Ferguson and Dodson, 2009). Wharton's jelly also has angiogenic and metabolic roles for the umbilical circulation. Some authors demonstrated that, in humans, an alteration of its composition could be related to foetal pathologic conditions (Labarrere et al., 1985; Ghezzi et al., 2001; Kulkarni et al., 2007).

The equine umbilical cord, divided into amniotic portion toward foetal side and allantoic portion towards placental side, should be attached to the dorsal side at the base of one of the horns. It consists of 2 veins and 2 arteries in the allantoic portion, and two arteries and one vein in the amniotic portion (Withwell and Jeffcott, 1975; Schlafer, 2004; Pozor, 2016). There is a significant variation in the length of UC: a large study on 145 Thoroughbred mares found a mean length of 55 cm across a broad range of 32–90 cm (Withwell and Jeffcott, 1975). In human medicine, the helical pattern, or coiling of the UC (left spiral, counter clockwise), is well studied and several authors have addressed the correlations between abnormal cord coiling and adverse pregnancy outcome (Machin et al., 2000; De Laat et al., 2006). The origin of the umbilical coiling is still poorly understood: the hypotheses include the foetal activity, asymmetric blood flow, foetal hemodynamic forces (Ferguson and Dodson, 2009). The coiling makes the umbilical cord a structure both flexible and strong, and provides resistance to external forces, which could compromise blood flow. Also in equine species, chirality or natural coiling of the vessels is common. Schlafer (2004) reported as normal four to five coils

over the length of UC. In human clinical practice, determining the “umbilical coiling index” (number of complete coils divided by the length of the cord; average 0.24 coils per centimeter) may identify the fetus at risk (van Dijk et al., 2002; Chitra et al., 2012; Ernst et al., 2013; Ohno et al., 2016).

Mesenchymal stem cells (MSCs), also known as multipotent stromal cells or mesenchymal progenitor cells (Dominici et al., 2006) are of increasing interest in the regenerative medicine field. They represent a heterogeneous population of highly proliferative cells, with a characteristic of self-renewal and in vitro multilineage differentiation capacity (Pittenger et al., 1999; Fortier, 2005). They can differentiate into lineages of mesenchymal tissues, such as bone, cartilage, adipose tissue (AT), muscles, and tendon (Tuan et al., 2003). Although it was originally believed that they participate in tissue homeostasis by replacing damaged or senescent cells, it is now postulated that they contribute to healing by playing a trophic role, producing cytokines and growth factors (Caplan, 2009).

Placental tissues and foetal fluids represent a source of cells for regenerative medicine. They are readily available and easily procured without invasive procedures. Mesenchymal Stem Cells (MSCs) from foetal fluids and adnexa are defined as an intermediate between embryonic and adult stem cells, due to the preservation of some characteristics typical of the primitive native layers. The UC, as discarded material after delivery, represents an excellent alternative non-invasive source of MSCs. In fact, MSCs could be derived from WJ or umbilical cord blood (UCB). Other sources of foetal MSCs are amniotic fluid (AF) and amniotic membrane (AM). However, for practical reasons, the most common harvest method employed clinically is from bone marrow (BM) or adipose tissue (AT), although umbilical cord blood banks are rapidly expanding. BM-MSCs are easy to harvest, isolate and expand but pneumopericardium is a potential severe, but rarely reported, complication (Durando et

al., 2006). AT-MSCs are also easy to harvest but require a more invasive standing surgical procedure. AT yields a greater quantity of MSCs per volume without expansion when compared to BM, but their osteogenic and chondrogenic differentiation capacity has been reported to be lower and they are less studied than BM-MSCs (Vidal et al. 2007, 2008; Kisiday et al. 2008; Colleoni et al. 2009). Studies in large animal models are particularly important in orthopedic diseases, as regeneration and function of the load-bearing musculoskeletal tissues can be assessed best when the size of the anatomical structure and the load it is subjected to are of similar dimensions as in humans. Furthermore, the most reliable results are obtained when the disease model best possibly reflects the conditions encountered in humans (Brehm et al., 2012; Cook et al., 2014). Only recently it has been demonstrated a high level of analogy between human and equine cells, providing a reliable basis for translational studies on MSC therapies in the equine large animal model (Hillmann et al., 2016).

The purpose of this PhD thesis is to perform a dissertation about the equine umbilical cord, with particular attention to its macroscopic characteristics moving into its microscopic features.

The first section collects studies about macroscopic and histological features of equine umbilical cord; the second one includes studies on equine Mesenchymal Stem Cells derived from foetal tissues: their characterization and immunophenotype, their comparison with MSCs derived from equine adult tissues and the comparison between equine and human foetal MSCs. Finally, the third section includes the clinical application of MSCs derived from AF and WJ on cutaneous wounds of foals of different ages.

References

- Brehm W., Burk J., Delling U., Gittel C., Ribitsch I., (2012). *Stem cell-based tissue engineering in veterinary orthopaedics*. Cell Tissue Res; 347 (3), 677–688.
- Caplan A.I., (2009). *Why are MSCs therapeutic? New data: new insight*. J Pathol; 217, 318-324.
- Chitra T., Sushanth Y.S., Raghavan S., (2012). *Umbilical coiling index as a marker of perinatal outcome: an analytical study*. Obstet Gynecol Int; 213689, 1-6.
- Colleoni S., Bottani E., Tessaro I., Mari G., Merlo B., Romagnoli N., Spadari A., Galli C., Lazzari G., (2009). *Isolation, growth and differentiation of equine mesenchymal stem cells: effect of donor, source, amount of tissue and supplementation with basic fibroblast growth factor*. Vet Res Commun; 33, 811- 821.
- Cook J.L., Hung C.T., Kuroki K., Stoker A.M., Cook C.R., Pfeiffer F.M., Sherman S.L., Stannard J.P., (2014). *Animal models of cartilage repair*. Bone Joint Res; 3 (4), 89–94.
- de Laat M.W., Franx A., van Alderen E.D., Nikkels P.G., Visser G.H., (2005). *The umbilical coiling index, a review of the literature*. J Matern Fetal Neonatal Med; 17(2): 93-100.
- Dominici M., Le Blanc K., Mueller I., Slaper-Cortenbach I., Marini F., Krause D., Deans R., Keating A., Prockop D., Horwitz E. (2006). *Minimal criteria for defining multipotent mesenchymal stromal cells. The International Society for Cellular Therapy position statement*. Cytotherapy; 8(4), 315-317.
- Durando M.M., Zarucco L., Schaer T.P., Ross M., Reef V.B., (2006). *Pneumopericardium in a horse secondary to sternal bone marrow aspiration*. Equine vet Educ; 18(2), 75-79.

Ernst L.M., Minturn L., Huang M.H., Curry E., Su E.J., (2013). *Gross patterns of umbilical cord coiling: correlations with placental histology and stillbirth*. *Placenta*; 34(7): 583-588.

Ferguson W.L., Dodson R.B., (2009). *Bioengineering aspects of the umbilical cord*. *Eur J Obstet Gynecol Reprod Biol*; 144(S1): S108-S113.

Fortier L.A., (2005). *Stem cells: classifications, controversies and clinical applications*. *Vet Surg*; 34(5), 415-423.

Ghezzi F., Raio L., Di Naro E., Franchi M., Balestreri D., D'Addario V., (2001). *Normogram of Wharton's jelly as depicted in the sonographic cross section of the umbilical cord*. *Ultrasound Obstet Gynecol*; 18(2): 121-125.

Kisiday J.D., Kopesky P.W., Evans C.H., Grodzinsky A.J., McIlwraith C.W., Frisbie D.D., (2008). *Evaluation of adult equine bone marrow and adipose derived progenitor cell chondrogenesis in hydrogel cultures*. *J Orthop Res*; 26(3), 322-331.

Kulkarni M.L., Matadh S.P., Ashok C., Pradeep N., Avinash T., Kulkarni M.A., (2007). *Absence of Wharton's Jelly around the umbilical arteries*. *Indian J Pediatr*; 74(8): 787-789.

Labarrere C., Sebastiani M., Siminovich M., Torassa E., Althabe O., (1985). *Absence of Wharton's jelly around the umbilical arteries: an unusual cause of perinatal mortality*. *Placenta* 6(6) : 555-559.

Machin G.A., Hackerman J., Gilbert-Barness E., (2000). *Abnormal umbilical cord coiling is associated with adverse perinatal outcomes*. *Pediatr Dev Pathol*; 3(5): 462-71.

Ohno Y., Terauchi M., Tamakoshi K., (2016). *Perinatal outcomes of abnormal umbilical coiling according to a modified umbilical coiling index*. *J Obstet Gynecol Res.* ; 42(11): 1457-1463.

Pittenger M.F., Mackay A.M., Beck S.C., Jaiswal R.K., Douglas R., Mosca J.D., Moorman M.A., Simonetti D.W., Craig S., Marshak D., (1999). *Multilineage potential of adult human mesenchymal stem cells*. Science; 284(5411): 143-147.

Schlafer D.H., (2004). *The umbilical cord-lifeline to the outside world: structure, function and pathology of the equine umbilical cord*. In: Proceedings of a workshop on the equine placenta. Eds: Powell D., Furry D., Hale G. Kentucky Agricultural Experimental Station, Lexington, pp 92-99.

Tuan R.S., Boland G., Tuli R., (2003). *Adult mesenchymal stem cells and cell based tissue engineering*. Arthritis Res Ther; 5(1): 32-45.

Vidal M.A., Kilroy G.E., Lopez M.J., Johnson J.R., Moore R.M., Gimble J.M., (2007). *Characterization of equine adipose tissue-derived stromal cells: adipogenic and osteogenic capacity and comparison with bone marrow-derived mesenchymal stromal cells*. Vet Surg; 36(7), 613-622.

Whitwell K.E., Jeffcott L.B., (1975). *Morphological studies on the fetal membranes of the normal singleton foal at term*. Res Vet Sci; 19(1): 44-55.

SECTION I- Studies on equine umbilical cord

CHAPTER 1

STUDY OF UMBILICAL CORD IN THE EQUINE SPECIES

Abstract: Oral presentation

XXI International SIVE Congress (Società Italiana Veterinari per Equini), February 6th-8th 2015, Pisa, Italy

Lanci A.¹, Iacono E.¹, Palermo C.², Grandis A.¹, Pirrone A.³, Merlo B.¹, Castagnetti C.¹

¹Department of Veterinary Medical Sciences, University of Bologna, Ozzano Emilia, Bologna, Italy; ² Practitioner, Modena; ³Practitioner, Bologna



XXI SIVE INTERNATIONAL CONGRESS

Pisa, Palazzo dei Congressi • 6-8 Febbraio 2015 • February 6th-8th 2015

STUDY OF UMBILICAL CORD IN THE EQUINE SPECIES

A. Lanci, DVM, PhD Student¹, E. Iacono, DVM, PhD, Professor¹, C. Palermo, DVM^{1,2},
 A. Grandis, DVM, PhD, Professor¹, A. Pirrone, DVM, PhD^{1,3}, B. Merlo, DVM, PhD, Professor¹,
 C. Castagnetti, DVM, PhD, Professor, DECAR¹

¹ Department of Veterinary Medical Sciences, University of Bologna, Ozzano Emilia (BO), Italy

² Practitioner, Modena, Italy

³ Practitioner, Bologna, Italy

Work type: **Original Research**

Topic: **Reproduction**

Purpose of the work. The umbilical cord (UC) plays an essential role in the exchange between the mother and the foetus, allowing the latter to receive oxygen and nutrients necessary for survival and development. The UC intervacular stroma consists of mucous connective tissue, also called Wharton's jelly (WJ). It develops from extraembryonic mesoderm, binds and encases the umbilical vessels, protecting them from twisting and compression during pregnancy. WJ also has angiogenic and metabolic roles for the umbilical circulation. Some authors demonstrated that in human, an alteration of its composition could be related to fetal pathologic condition (Ferguson et al 2009). The aims of the study were to macroscopically describe the equine UC, and, for the first time in the horse, to evaluate the weight and the microscopic composition of WJ.

Materials and used methods. Twenty-four mares with normal pregnancy and parturition have been enrolled. The following data were registered for each mare: age, parity, length of pregnancy, total length of UC, length of UC amniotic and allantoic portion, total number of UC coils and their number in each segment, sex and weight of the foal at birth. There was no control of mare breeding. The Kolmogorov-Smirnov test was used to evaluate the distribution of continuous variables; the presence of differences in the UC macroscopic structure between gender was evaluated by T Student, considering significant a P value <0.05. Pearson's correlation test was used to assess the presence of correlations between the data registered. Immediately after breaking the UC, the part closest to the foal (~15 cm), characterized by an abundant amount of WJ, was severed and transported to the lab, where WJ was separated from vessels, weighted, and fixed in 4% paraformaldehyde for microscopic examinations. Fixed tissue sections were labelled with antibodies anti-type I, IV and V collagen, and anti-fibrillin. Furthermore fibroblast cells were highlighted using Masson's trichrome staining. To verify the presence of elastic, reticular and nervous fibers, orcein staining and silver impregnation were used.

Outcomes. The mean total length of UC was 58.3 ±17 cm; the mean length of amniotic portion was 33.2 ±10.6 cm, while the allantoic segment was 27.0 ±10.5 cm. These data confirmed those previously reported (Whitwell et al., 1975). The total UC length and the allantoic portion length resulted statistically higher in males (n=10) than in females (n=14; P<0.05). As in humans, this could be due to the higher weight at birth in males (Naeye, 1985). The mean total number of UC coils was 5.1 ±2.8, with 2.7 ±0.9 coils in the amniotic portion and 3.0 ±1.8 coils in the allantoic portion, respectively. Our study revealed that total number of coils (R=0.43, P<0.05) and coils number of the allantoic portion (R=0.67, P<0.05) were positively related with parity. A positive correlation was also observed between the length of the allantoic portion and its coils (R=0.58, P<0.05). Coils formation is the result of rotations given by the foetus. Since in the horse from the eighth month of gestation foetal movements occur only along the longitudinal axis, the number of coils observed is lo-

wer than that reported in human. This could also be related to the mean UCI value registered in the present study (0.10 ± 0.04), lower than that reported in babies (van Dick et al., 2002). Different from humans, we did not observe any correlation between UCI and age of the mare, length of pregnancy, sex and weight of the foal, but UCI was positively related with the total number of coils ($R=0.448$, $P<0.05$) and with their number in the amniotic portion ($R=0.699$, $P<0.05$). On the contrary, the UCI resulted negatively related to the total UC length ($R=-0.526$, $P<0.05$) and to the amniotic portion UC length ($R=-0.499$, $P<0.05$). From each UC sample, 4.5 ± 3.45 g of WJ were isolated. As in humans (Takeki, 1993), the immunohistochemical analysis revealed the presence of fibroblast cells positive for antibodies anti-type II, IV and V collagen, anti-fibrillin, surrounded by a dense network of reticular fibers. Given their abundance, we could not confirm the presence of nervous fibers. Different from humans, in the horse UC, elastic fibers are less concentrated, with an uneven pattern around the vessels.

Conclusions. In this study we highlighted similarities and differences between equine and human macroscopic and microscopic characteristics of the umbilical cord. Given the presence in human species of a strong correlation between these and specific pathological conditions of newborn and mother, further studies are needed, both on normal and high risk pregnancies, to verify the presence of these correlations also in the equine species.

Bibliography

1. Ferguson VL, Dodson RB. Bioengineering aspects of the umbilical cord. Eur J Obstet Gynecol Reprod Biol 2009; 144S: S108-S113.
2. Naeye RL. Umbilical cord length: Clinical significance. J Pediatr 1985; 107: 278-81.
3. Takechi K, Kuwabara Y, Mizuno M. Ultrastructural and immunohistochemical studies of Wharton's jelly umbilical cord cells. Placenta 1993; 14: 235-45.
4. van Dijk CC, Franx A, de Laat MWM, Bruinse HW, Visser GHA, Nikkels PGJ. Manual of pathology of the human placenta. Springer, NY 2002.
5. Whitwell KE, Jeffcott LB. Morphological studies on the foetal membranes of the foal at term. Res Vet Sci 1975; 19: 44-55.

Corresponding address

Dott.ssa Aliai Lanci - Università di Medicina Veterinaria di Bologna Dimevet
Via Tolara di Sopra, 50 - 40064 Ozzano dell'Emilia (BO), Italia - E-mail: aliai.lanci2@unibo.it

MACROSCOPIC CHARACTERISTICS OF THE UMBILICAL CORD IN STANDARD BRED, THOROUGHBRED AND SADDLEBRED HORSES

Article in preparation (Journal: Theriogenology)

Mariella J.¹, Iacono E.¹, **Lanci A.**¹, Merlo B.¹, Palermo C.³, Morris L.², Castagnetti C.¹

¹*Department of Veterinary Medical Sciences, University of Bologna, via Tolara di Sopra 50, 40064, Ozzano Emilia, Bologna, Italy*

²*Equibreed NZ, 99 Parklands Rd, RD 1, Te Awamutu 3879, New Zealand*

³*Practitioner, France*

Introduction

The umbilical cord (UC) is an important connection between mother and fetus allowing the latter to receive oxygen and nutrients necessary for survival and development. The equine UC develops from the convergence of the two foetal sacs, the amnion and allantois around the remnants of the yolk sac and the vitelline duct to form a cord-like structure by Day 50 (Whitwell, 1975; Latshaw, 1987). The equine UC division into an intra-amniotic and intra-allantoic portion was illustrated since 1753 (Steven, 1982). The intra-amniotic portion is proximal, covered by amnion and attached to the fetus at the umbilicus; it contains two umbilical arteries and one umbilical vein, the urachus, and the vitelline vein remnant (Whitwell and Jeffcott 1975; Schlafer, 2004b). The distal intra-allantoic portion is covered by the allantois and it is attached to the allantoic sac (Whitwell and Jeffcott 1975; Schlafer, 2004a). In this portion, the two major umbilical arteries become divergent and multibranched towards the chorion and the two umbilical veins remain close to these arteries. The two major veins unite at the proximal end of the allantoic portion or just inside the amniotic cavity (Whitwell and Jeffcott 1975, Schlafer, 2004a). The normal attachment side to the

allantochorion is between the two horns (Schlafer, 2004b). The urachus connects the fetal urinary bladder to the allantoic cavity within loose stromal tissue in the amniotic portion.

Few studies described the equine umbilical cord, mainly in the Thoroughbred (Whitwell and Jeffcott 1975; Schlafer, 2004a). On the contrary, in human medicine the gross features of the UC has been intensively studied and one of its peculiar characteristics, the helical structure, focused the attention of bioengineers and physical scientists (Ferguson and Dodson, 2009). Strong et al., (1994) devised an Umbilical Coiling Index (UCI) calculated by dividing the total number of umbilical coils by the umbilical cord length (cm) for use during ultrasonographic assessment of the UC. In more recent studies (Chitra et al., 2012; Ohno et al., 2016) found that the UCI is an effective indicator of perinatal outcome. A hypocoiled cord was strongly associated with preeclampsia in woman (Chitra et al., 2012; Ezimokahai et al., 2001).

Machin et al., (2000) reported frequency and clinical correlations of abnormally coiled cords in 1329 newborn. Principal clinical correlations found in ipercoiled and hypocoiled cords were foetal demise, foetal intolerance to labor, intrauterine growth retardation, and chorioamnionitis. Abnormal cord coiling was associated with thrombosis of chorionic plate vessels, umbilical venous thrombosis, and cord stenosis. The authors concluded that an abnormal cord coiling is a chronic state, established in early gestation, that may have chronic (growth retardation) and acute (foetal intolerance to labor and foetal demise) effects on foetal well-being. The cause of abnormal cord coiling is until now unknown. In human medicine, an antenatal detection of abnormal UCI by ultrasound could lead to elective delivery of fetuses at risk, thereby reducing the foetal death rate and it is recommend that the UCI become part of the routine placental pathology examination.

In equine reproductive medicine, despite the macroscopic examination of the placenta after delivery is a fundamental feature of post-partum examination, the UCI has never been investigated.

The present study aimed to describe the macroscopic features of equine umbilical cord, such as length and number of coils of each portion, to calculate the umbilical coiling index in normal pregnancy and healthy foals. These features were compared between three different breeds and in relation to the foal's gender. This study also aimed to verify if there is a correlation between the macroscopic UC characteristics and mare and perinatal features.

Materials and Methods

Animals and data collection

One hundred twenty four healthy mares with normal pregnancy were enrolled in the study. Eighty/124 were housed for attending delivery at the Equine Perinatology Unit (EPU) "Stefano Belluzzi" - Department of Veterinary Medical Sciences - University of Bologna, during six breeding seasons (2011-2016); 44/124 were housed at EquiBreed - New Zealand, during the breeding season 2013. The mares were divided into three groups according to the breed: 70 Standardbreds (STB), 38 Thoroughbreds (THB) and 16 Saddlebreds (SAD).

Information about mare's age and parity were recorded at admission. At delivery, the following data were registered: length of pregnancy, placental weight, presence of foetal membranes alterations, UC length and number of coils of both portions. The Umbilical Coiling Index (UCI), which is the ratio between total coils and total UC length, was then determined. Placental weight was measured weighing the entire placenta along with the amnion and umbilical cord, as suggested by Elliott et al., 2009. Furthermore, immediately after foaling, APGAR score (Vaala, 2006), foal's weight and sex were recorded. Only healthy mares with normal delivery and healthy foal were enrolled. The foals were classified as

healthy when they had a normal clinical evaluation during the course of hospitalization, including a complete blood count and serum biochemistry at birth and an IgG serum concentration ≥ 800 mg/dL at 18 h of life.

Statistical analysis

All parameters were tested for normal distribution by using Kolmogorov–Smirnov test. Because the data showed non normal distribution, the variables were analyzed with nonparametric methods. Spearman's rank correlation coefficients were used to test the hypothesis that the anatomical features of the UC and the descriptive data related to mares and foals were correlated.

Kruskal–Wallis test was performed to compare anatomical characteristics of the UC, placental weight and data relative to foals and mares between the 3 groups. When a statistically significant difference was found, the Bonferroni post-hoc procedure for all pair-wise comparisons was applied. To tests the hypothesis that anatomical features of the UC, placental and foal's weight were related to foal's gender, the Wilcoxon's test was performed. The Mann-Whitney test was used to compare the length of the allantoic and amniotic portion of the cord in each breed.

Descriptive statistics, including mean \pm SD and range (min/max values) were calculated. A P value less than 0.05 was considered statistically significant. All analyses were carried out using the commercial software Analyse-it, version 2.03 (Analyse-it Software Ltd., Leeds, West Yorkshire, England).

Results

Data were collected in the three different breeds and significant differences are reported in *Table 1.1*.

Correlations were investigated within each breed. In STB, the mare's age was correlated with parity ($P < 0.0001$; $r_s = 0.80$) and foal's weight at birth ($P = 0.034$; $r_s = 0.26$); the foal's weight was correlated with parity ($P = 0.037$; $r_s = 0.26$), gestational length ($P = 0.030$; $r_s = 0.27$), placental weight ($P < 0.0001$; $r_s = 0.59$) and UC allantoic length ($P = 0.013$; $r_s = -0.32$). Gestational length was correlated with placental weight ($P = 0.025$; $r_s = 0.28$).

In THB, the gestational length was correlated with placental weight ($P = 0.012$, $r_s = -0.42$), the foal's weight was correlated with placental weight ($P < 0.0001$, $r_s = 0.59$). No other correlations were found.

In SAD, mare's age was correlated with allantoic length ($P = 0.03$; $r_s = 0.56$); gestational length was correlated with placental weight ($P = 0.025$; $r_s = -0.54$); foal's weight at birth was correlated with placental weight ($P = 0.005$; $r_s = 0.69$), number of total coils ($P = 0.04$; $r_s = 0.60$), and allantoic coils ($P = 0.002$; $r_s = 0.74$).

About the UC, in each breed, total length was correlated with number of total coils; UC's amniotic length was correlated with the number of amniotic coils as the allantoic length with the number of allantoic coils. The UCI was similar in all breeds: in STB was 0.09 ± 0.03 , in THB was 0.09 ± 0.02 and in SAD was 0.1 ± 0.03 .

The significant gender-based differences within each breed are summarized in *Table 1.2*.



Figure 1.1. Amniotic coils at the end of the stage II labour in STB mares (a, b, c, d). There is more coils in a, b, than in c, d.

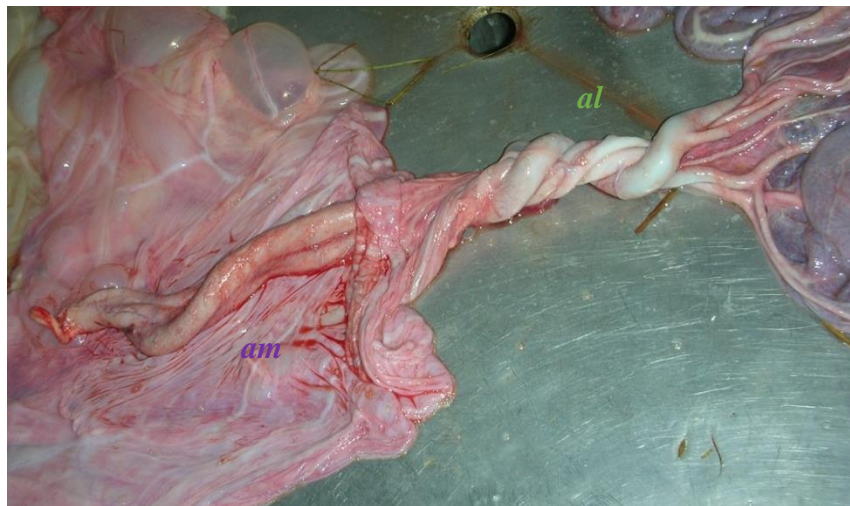


Figure 1.2. Amniotic portion (am) and allantoic portion (al) with coils.

	STB (n=70)	THB (n=38)	SAD (n=16)
Mare's age (y)	10.1 ± 4.5 ^a (4-22)	8.4 ± 2.8 ^a (4-16)	16.3 ± 4.1 ^{bs} (7-24)
Parity (n)	4 ± 3 (1-13)	3 ± 1 (1-6)	2 ± 1 (1-3)
Gestational length (d)	343 ± 14 ^{a*} (322-389)	352 ± 16 ^b (330-396)	344 ± 14 ^{ab} (320-363)
Foal's sex	27 M 43 F	18 M 20 F	7 M 9 F
Foal's weight (kg)	49.1 ± 9.4 ^a (31-64)	65 ± 8.7 ^{bs} (48-85)	48.5 ± 8.3 ^a (27-59)
Placenta's weight (kg)	5.5 ± 1.3 ^a (2.8-6.3)	6.6 ± 1.1 ^{bs} (4-8)	4.8 ± 0.4 ^a (4.5-5)
UC total length (cm)	56 ± 12.5 (37-95)	56.1 ± 10.6 (34-81)	60.3 ± 18.2 (34-100)
UC total coils(n)	5 ± 1	5 ± 1	6 ± 1
UC allantoic length (cm)	25.8 ± 8.9 (11-53)	22.9 ± 6.9 (10-42)	29.9 ± 12.5 (12-53)
UC allantoic coils (n)	2 ± 1	2 ± 1	3 ± 1
UC amniotic length (cm)	30.1 ± 8.2 ^{a*} (18-60)	33.2 ± 7.4 ^b (16-51)	30.3 ± 13.2 ^{ab} (15-65)
UC amniotic coils (n)	3 ± 1	3 ± 1	3 ± 1
UCI	0.09 ± 0.03	0.09 ± 0.02	0.1 ± 0.03

*Table 1.1. Data collected in the three different breeds. Continuous variables are expressed as mean ± SD and minimum and maximum value (range). Different letters in rows indicate significant differences (*P < 0.05, #P < 0.001 and \$P < 0.0001, respectively) between groups.*

	Male	Female	Breed, P value
Foal's weight (kg)	68.1 ± 7.7 (56-85)	62.3 ± 8.9 (50-79)	THB, P = 0.03
Placenta's weight (kg)	6.9 ± 1.2 (4-8)	6.2 ± 1 (4.6-7.3)	THB, P = 0.03
UC total length (cm)	60.3 ± 11.6 (37-85)	53.1 ± 12.4 (37-95)	STB, P = 0.008
UC allantoic length (cm)	29.3 ± 9.9 (14-53)	23.5 ± 7.5 (11-42)	STB, P = 0.03

Table 1.2. Significant gender-based differences within breeds. Continuous variables are expressed as mean ± SD and minimum and maximum value (range).

Discussion

Many authors described the characteristics of the normal equine placenta but only few data were provided on the umbilical cord. Most of them are related to Thoroughbreds or to mixed group of breeds. To our knowledge, there are no studies that compare placenta and UC features between equine breeds.

In the present study, emerged that mare's age was higher in SAD than in THB and STB. This probably reflects the different attitude and management of the breeds: STB and THB begin their reproductive career early, while SAD begin the agonistic activity when they are older than THB and STB. Only in STB, mare's age was correlated with parity. This probably reflects the stud farm management that caused an increased use of the mare for reproduction purpose and less use of reproductive biotechnologies.

As recently reported (Rosales et al., 2017), normal gestational length in THB ranged between 330 and 396 days, with a mean of 352. In the mare, gestational length is influenced by daylight (Hodge et al., 1982; Sharp, 1988). All THB included in the present study were housed near Auckland, New Zealand, where the hour of daylight ranged from 11.20 to 14.30, while in Bologna, Italy, daylight ranged from 11 to 15.25 (<http://www.timeanddate.com/sun/new-zealand/auckland>). This is probably the reason because STB, all housed in Italy, had a lower gestational length than THB; it is worth noting that the STB gestational length reported in the present study is comparable to THB gestational length reported in studies from the United Kingdom (Davies Morel et al., 2002).

As regard the foal weight, it was correlated with the placental weight in all breeds. Normal placental weight at term is approximately 11% of the foal weight (Pascoe and Knottenbelt, 2003; Schlafer, 2004), as further confirmed in the present study. Only in THB, foal's weight and subsequently the placental weight is higher in colt than in filly and probably this is due to a more pronounced sexual dimorphism as reported by Hintz et al (1979). It is worth noting

that in STB, which had a higher number of foaling than the other breeds, foal's weight was related to parity and gestational length. The hypothesis suggested by Elliott et al. (2009) and Wilsher and Allen (2002, 2003) is that the equine uterus needs to be in some way primed by a first pregnancy before it can achieve its full potential in terms of facilitating foetal growth. Wilsher and Allen (2003) suggested that the primiparous placentas have reduced microcotyledon surface densities coupled with reduced corionic volumes resulting in less total available area for haemotrophic exchange of nutrients and gases.

The correlation between gestational length and foal's weight is not in accordance with the current knowledge about the equine pregnancy length. Foals born after a prolonged pregnancy are defined postmature and they usually show weak suckle reflex, poor thermoregulation and glucose regulation, poor postural reflexes, fully erupted incisors and are thin with poor muscle development (Palmer, 1998). Since the gestational length ranges reported in the present study in healthy mares with healthy foals are particularly wide, in the authors' opinion, it is difficult to define what a prolonged pregnancy is in the equine species. Also Palmer (1998) reported that normal gestational length may vary from 315 days to more than 390 days.

As regard the mean total UC length, data reported in the present study are comparable to the previous reported in Thoroughbred (Whitwell and Jeffcott, 1975; Whitehead et al., 2003), Standardbred (Oulton et al., 2003), and Warmblood (Govaere et al., 2014). What is surprising from the data is the wide range of length and that the human UC has the same length of the equine one. A preliminary study in infants with a short umbilical cord showed that they had lower tibia speed of sound (SOS) measurements compared with infants with a longer cord. The authors postulated that this difference might be due to the restricted activity of the fetus with the short cord (Wright and Chan, 2009). In human newborns, decreased foetal movements and activity have been associated with decreased infant bone mineralization

(Miller, 2005). This field of research was never been investigated in the equine neonates. From the first studies in the 60's in human medicine, it is known that the cord's length is not correlated to maternal and foetal factors such as parity, age, weight, sex and presentation and that there is little growth of the cord during the last trimester (Walker and Pye, 1960). Also Malpas (1964) found no correlation of cord length with placental or birth weight. Miller et al. (1981) noted that cord length was related to the stretching placed on the cord by the developing embryo and fetus; the tension is determined by the availability of intrauterine space and the occurrence of foetal movement. In a more recent study (Sheiner et al., 2004), the authors found that cord problems such as true cord knots and nuchal cords were significantly associated with male gender; they hypothesized that it is due to the longer cords and suggested that further studies should investigate umbilical cord length differences between male and female fetuses. Also in veterinary medicine, this aspect has never been investigated. The length of the two portions of the cord is statistically different in STB and THB, where the amniotic portion is longer than the allantoic one. The amniotic portion is longer in THB than in STB, probably because of the higher foetal weight. In the present study, only in STB the length of the UC and the allantoic portion are longer in colt than in filly. Since there is not weight difference between male and female in STB, the hypothesis is that the difference in the allantoic length could be due to other factors as described in human medicine. We can speculate that the amniotic portion is longer than the allantoic because is more affected by the stretching during the foetal movement. In human medicine, the helical pattern, or coiling, of the umbilical cord is well studied and several studies have addressed the correlations between abnormal cord coiling and adverse pregnancy outcome (Machin et al., 2000; de Laat et al., 2006). The origin of the umbilical coiling is still poorly understood: the hypotheses include foetal activity, asymmetric blood flow, foetal and hemodynamic forces

(Ferguson and Dodson, 2009). The umbilical coil is defined as one complete spiral of 360° of the umbilical vessels around each other. The coiling makes the umbilical cord a structure both flexible and strong, and provides resistance to external forces which could compromise blood flow. To the authors knowledge, the number of coils and the UCI was never been investigated in veterinary medicine. In the equine species, this is the first study that investigated these features and it seems that the number of the coils (total, allantoic and amniotic coils) is the same in each breed studied. Only in SAD, there is a positive correlation with the foals' weight at birth and it cannot be excluded that the foetal weight is one of the item that contribute to the origin of the umbilical coiling. Data obtained from the present study could be considered as a normal range of number of coils and UCI in the equine physiological pregnancies.

Currently, there are no data about the correlation between the number of coils and the adverse pregnancy outcome in the equine, whereas in human medicine it is well known: undercoiling may give way to kinking and compression, whereas overcoiling may give way to occlusion. This may help to explain the association with low Apgar Score in undercoiled cords and with low arterial pH and asphyxia with overcoiled cords (Machin et al., 2000; de Laat et al., 2006). What is worth noting is that it is the normal characteristic of the equine umbilical cord and that it should be considered during the evaluation of equine placenta immediately after foaling and placental expulsion, as it is well known by the equine specialist (Pozor, 2016).

References

Chitra T., Sushanth Y.S., Raghavan S., (2012). *Umbilical coiling index as a marker of perinatal outcome: an analytical study*. *Obstet Gynecol Int*; 2012:213689.

Davies Morel M.C., Newcombe J.R., Holland S.J., (2002). *Factors affecting gestation length in the Thoroughbred mare*. *Anim Reprod Sci*; 74(3-4):175-185.

de Laat M.W., Franx A., Bots M.L., Visser G.H., Nikkels P.G., (2006). *Umbilical coiling index in normal and complicated pregnancies*. *Obstet Gynecol*; 107(5):1049-55.

Elliott C., Morton J., Chopin J., (2009). *Factors affecting foal birth weight in Thoroughbred horses*. *Theriogenology*; 71(4):683-689.

Ezimokhai M., Rizk D.E., Thomas L., (2000). *Maternal risk factors for abnormal vascular coiling of the umbilical cord*. *Am J Perinatol*; 17(8):441-445.

Ferguson W.L., Dodson R.B., (2009). *Bioengineering aspects of the umbilical cord*. *European J Obstet Gynecol Reprod Biol*; 144S: S108-S1139.

Govaere J., Hoogewijs C., De Schawer C., Roels K., Vanhaesebrouck E., De Lange V., Ververs C., Piepers S., (2014). *Placenta evaluation in Warmblood horses*. *Journal of Equine veterinary Science*; 34, 237.

Hintz R.L., Hintz H.F., Van Vleck L.D., (1979). *Growth rate of Thoroughbred. Effects of age of dam, year and month of birth, and sex of foal*. *J Anim Sci*; 48(3), 480-487.

Hodge S.L., Kreider J.L., Potter G.D., Harms P.G., Fleeger J.L., (1982). *Influence of photoperiod on the pregnant and postpartum mare*. *Am J Vet Res*; 43(10), 1752-1755.

Latshaw W.K., (1987). *Embryonic membranes and placentation*. In: Veterinary Developmental Anatomy: a clinically orientated approach, Ed: Latshaw W.K., Decker B.C., Philadelphia, 49-74.

Machin G.A., Hackerman J., Gilbert-Barness E., (2000). *Abnormal umbilical cord coiling is associated with adverse perinatal outcomes*. *Pediatr Dev Pathol*; 3(5): 462-471.

Malpas P., (1964). *Length of the umbilical cord at term*. *Br Med J*; 1(5384): 673-674.

Miller M.E., (2005). *Hypothesis: fetal movement influences fetal and infant bone strength*. *Med Hypotheses*; 65(5): 880–886.

Ohno Y., Terauchi M., Tamakoshi K., (2016). *Perinatal outcomes of abnormal umbilical coiling according to a modified umbilical coiling index*. *J Obstet Gynaecol Res*; 42(11):1457-1463.

Oulton R.A., Fallon L.H., Meyer H., Zent W.W., (2003). *Observations of the foaling data from two central Kentucky thoroughbred operations during the spring of 2003*. In: Powell DG, Furry D, Hale G (eds) *Proceedings of the workshop on the equine placenta*. Lexington, KY: University of Kentucky, 68–71.

Palmer J.E., (1998). *Prematurity, dismaturity, postmaturity*. *Proceedings of the IVECCS VI*; 722-723

Pascoe R.R., Knottenbelt D.C., (2003). *The placenta*. In: *Equine Stud Farm Medicine and Surgery*, Eds: D.C. Knottenbelt, M. LeBlanc, C. Lopate and R.R. Pascoe, W.B. Saunders, New York; 325-342

Pozor M., (2016). Equine placenta - A clinician's perspective. Part 1: Normal placenta - Physiology and evaluation. *Equine Vet Educ*; 28(6): 327-334.

Rosales C., Krekeler N., Tennent-Brown B., Stevenson M.A., Hanlon D., (2017). *Periparturient characteristics of mares and their foals on a New Zealand Thoroughbred stud farm*. *N Z Vet J*; 65(1): 24-29.

Schlafer D.H., (2004a). *The umbilical cord-lifeline to the outside world: structure, function and pathology of the equine umbilical cord*. In: Proceedings of a workshop on the equine placenta. Eds: Powell D., Furry D., Hale G., Kentucky Agricultural Experimental Station, Lexington, 92-99.

Schlafer D.H., (2004b). *Postmortem examination of the equine placenta, fetus and neonate, methods and interpretation of findings*. *Proc Am Assoc Equine Pract*; 50, 144-161.

Sharp D.C., (1988). *Transition into the breeding season: clues to the mechanism of seasonality*. *Equine Vet J*; 20(3): 159-161.

Sheiner E., Levy A., Katz M., Hershkovitz R., Leron E., Mazor M., (2004). *Gender does matter in perinatal medicine*. *Fetal Diagn Ther*; 19(4):366-369.

Steven DH., (1982). *Placentation in the mare*. *J Reprod Fertil Suppl*; 31: 41-55.

Strong T.H., Jarles D.L., Vega J.S., Feldman D.B., (1994). *The umbilical coiling index*. *Am J Obstet Gynecol*; 170(1 Pt 1):29-32.

Vaala W.E., (2006). *Perinatology*. In: Higgins AJ, Snyder JR, editors. *The Equine Manual*. 2nd edition, W.B. Saunders; 803-804.

Walker C.W., Pye B.G., (1960). *The length of the human umbilical cord. A statistical report.* Br Med J 1(5172): 546-548.

Whitehead A.E., Foster R., Chenier T., (2003). *Placental characteristics of Standardbred mares.* In: Powell DG, Furry D, Hale G (eds) Proceedings of the workshop on the equine placenta. Lexington, KY: University of Kentucky; 71–76.

Whitwell K.E., (1975); *Morphology and pathology of the equine umbilical cord.* J Reprod Fert, Suppl; 23: 599-603.

Whitwell K.E., Jeffcott L.B., (1975). *Morphological studies on the fetal membranes of the normal singleton foal at term.* Res Vet Sci; 19(1), 44-55.

Wilsher S., Allen W.R., (2002). *The influences of maternal size, age and parity on placental and fetal development in the horse.* Theriogenology; 58(2-4): 833-835.

Wilsher S., Allen W.R., (2003). *The effects of maternal age and parity on placental and fetal development in the mare.* Equine Vet J; 35(5): 476-83.

Wright D., Chan G.M., (2009). *Fetal bone strength and umbilical cord length.* J Perinatol; 29(9): 603-605.

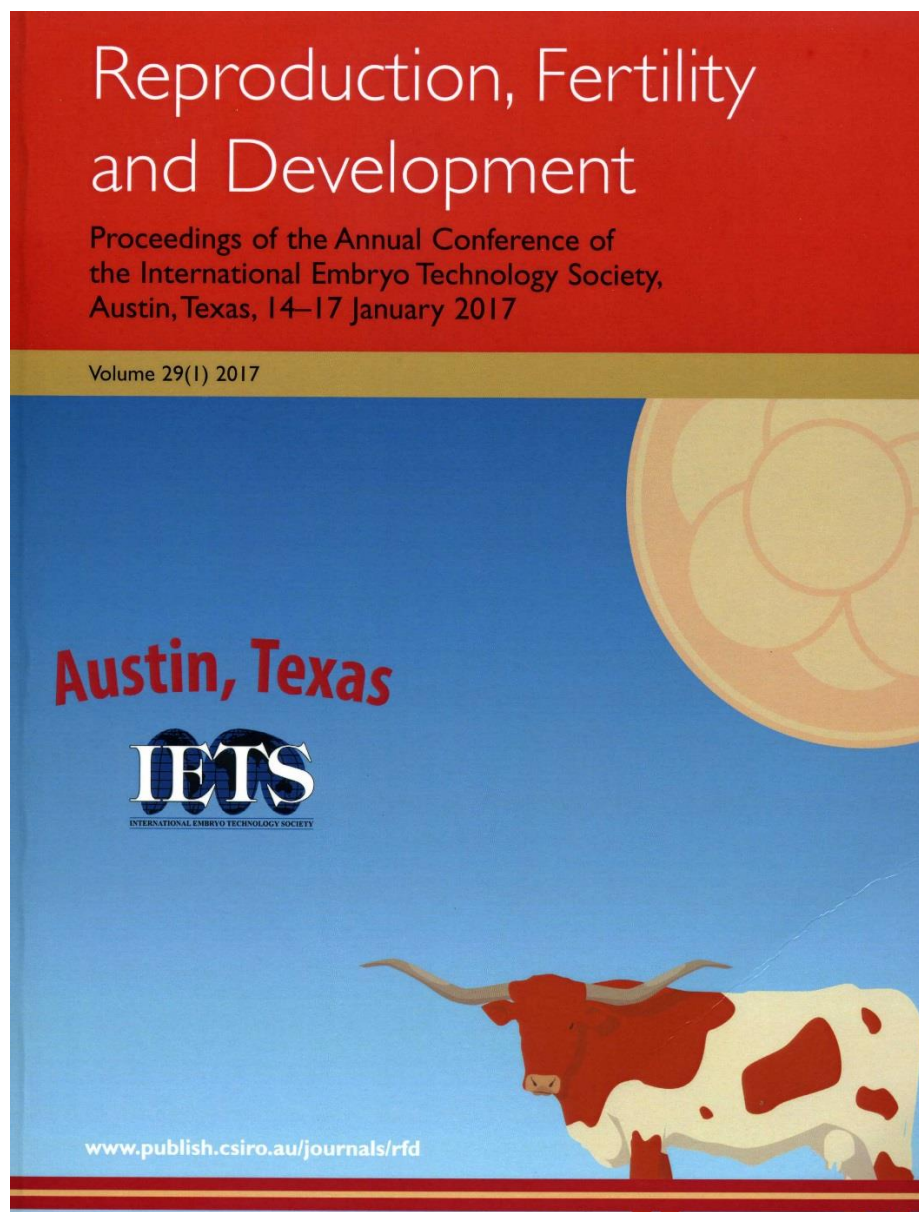
PRELIMINARY DESCRIPTIVE STUDY OF EQUINE PLACENTA GENERATED AFTER TRANSFER OF IN VIVO AND IN VITRO PRODUCED EMBRYOS

Abstract: Poster presentation

43rd Annual IETS Conference (International Embryo-Transfer Symposium), January 14th-17th 2017, Austin, Texas. *Reprod Fertil Dev.* 2016; 29 (1):156

Lanci A.¹, Mariella J.¹, Merlo B.¹, Castagnetti C.¹, Iacono E.¹

¹Department of Veterinary Medical Sciences, University of Bologna, Ozzano Emilia, Bologna, Italy



97 PRELIMINARY DESCRIPTIVE STUDY OF EQUINE PLACENTA GENERATED AFTER TRANSFER OF *IN VIVO*- AND *IN VITRO*-PRODUCED EMBRYOS

A. Lanci, J. Mariella, B. Merlo, C. Castagnetti, and E. Iacono

Department of Veterinary Medical Sciences, Ozzano dell'Emilia, Bologna, Italy

Placental changes associated with artificial reproductive technologies have been described in several species, but little information is available in horses. Joy *et al.* (2012) reported that human placentas from intracytoplasmic sperm injection derived embryos were heavier and thicker than those produced after natural conception. Despite the most growing interest and efficiency of artificial reproductive technologies in equine species, only recently, Pozor *et al.* (2016) described placental abnormalities in pregnancies generated by somatic cell NT, but there are no studies on equine placenta generated by intracytoplasmic sperm injection and traditional embryo transfer. In the present preliminary study, macroscopic differences of placentas generated after transfer of *in vitro*- or *in vivo*-produced embryos were registered. Twelve Standardbred recipient mares with pregnancy generated after transfer of *in vivo*-derived (Group 1) and *in vitro*-derived (Group 2) embryos were enrolled; 10 Standardbred mares with pregnancy derived by traditional AI were included as control (Group 3). All pregnancies were physiological, and newborn foals were healthy. Mare age, parity, length of pregnancy, gross evaluation and weight of placenta, total length of umbilical cord (UC), length of UC, number of UC coils, foal sex, and weight at birth were registered. Collected data are listed in Table 1 and are expressed as mean \pm standard deviation. Differences between groups were evaluated by 1-way ANOVA, and the difference in proportion of overweight placentas was evaluated with the Fisher test. The gross evaluation of placenta revealed 8/12 placentas (2/4 Group 1; 6/8 Group 2) were heavier than 11% (Madigan, 1997) due to oedema of the chorioallantois. No overweight placentas were registered in Group 3. In Group 1, 1/4 placentas had villous hypoplasia, and in Group 2, 1/8 placentas had cystic pouches on the UC. There were no significant differences among groups. However, the proportion of overweight placentas between Group 2 (6/8) and Group 3 (0/10) approached significance ($P = 0.06$). Although preliminary, the results of the present study suggest that production of equine embryos *in vitro* may lead to alterations in placental development. Several studies in cattle and sheep have suggested that alterations in the placentas of pregnancies derived from *in vitro*-produced embryos are related to effects of culture on epigenetic regulation. Less is known in the horse about the effects of *in vitro* embryo production on placental development; thus, further research in this area is necessary.

Table 1. Characteristics of full-term placentas derived from AI or embryo transfer with *in vivo*- and *in vitro*-produced embryos

Item	Group 1, n = 4	Group 2, n = 8	Group 3, n = 10
Mare's age (y)	9.5 \pm 3.1	4.6 \pm 0.9	11.2 \pm 4.9
Parity (no.)	1.3 \pm 0.5	1.0 \pm 0.0	4.5 \pm 3.7
Gestational length (d)	342.3 \pm 1.5	343.9 \pm 9.9	340.6 \pm 6.4
Foal sex	2 female; 2 male	4 female; 4 male	7 female; 3 male
Foal weight (kg)	49.3 \pm 7.8	44.3 \pm 4.2	49.4 \pm 6.0
Placenta weight (kg)	6.3 \pm 0.7	5.2 \pm 0.5	5.1 \pm 1.4
Total UC ¹ length (cm)	53.5 \pm 13.7	52.8 \pm 10.2	56.1 \pm 16.3
Total UC coils (no.)	4.5 \pm 1.7	4.6 \pm 1.5	5.9 \pm 1.4
Allantoic UC length (cm)	29.5 \pm 13.8	21.8 \pm 7.5	20.9 \pm 8.9
Allantoic UC coils (no.)	2.3 \pm 1.0	1.8 \pm 1.0	2.2 \pm 0.9
Amniotic UC length (cm)	24.0 \pm 4.2	31.0 \pm 7.2	35.2 \pm 42.3
Amniotic UC coils (no.)	2.3 \pm 1.0	2.9 \pm 0.8	3.7 \pm 1.3
UC insertion	4/4 between 2 horns	6/8 between 2 horns, 2/8 base of pregnant horn	5/10 between 2 horns, 3/10 base of nonpregnant horn, 2/10 base of pregnant horn

¹UC = umbilical cord.



Preliminary descriptive study of equine placenta generated after transfer of in vivo and in vitro produced embryos



Lanci A.* Mariella J., Merlo B., Castagnetti C. and Iacono E.

Department of Veterinary Medical Sciences, University of Bologna, Ozzano Emilia (BO), Italy



alailanci2@unibo.it



INTRODUCTION

Placental changes associated with artificial reproductive technologies have been described in several species, but little information is available in horses. Joy et al. (2012) reported that human placentas from intracytoplasmic sperm injection derived embryos were heavier and thicker than those produced after natural conception. Despite the most growing interest and efficiency of artificial reproductive technologies in equine species, only recently, Pozor et al. (2016) described placental abnormalities in pregnancies generated by somatic cell NT, but there are no studies on equine placenta generated by intracytoplasmic sperm injection and traditional embryo transfer.

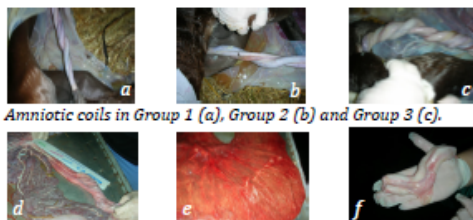
EXPERIMENTAL METHODS

In the present preliminary study, macroscopic differences of placentas generated after transfer of in vitro- or in vivo-produced embryos were registered. Twelve Standardbred recipient mares with pregnancy generated after transfer of in vivo-derived (Group 1) and in vitro-derived (Group 2) embryos were enrolled; 10 Standardbred mares with pregnancy derived by traditional AI were included as control (Group 3). All pregnancies were normal, and newborn foals were healthy. Mare's age and parity, length of pregnancy, placenta gross evaluation and weight, total length of umbilical cord (UC), length of UC, number of UC coils, foal's sex, and weight at birth were registered.

RESULTS

Collected data are listed in Table 1 and are expressed as mean \pm standard deviation. Differences between groups were evaluated by 1-way ANOVA, and the difference in proportion of overweight placentas was evaluated with the Fisher test. The gross evaluation of placenta revealed 8/12 placentas (2/4 Group 1; 6/8 Group 2) heavier than 11% (Madigan, 1997) due to edema of the chorioallantois. No overweight placentas were registered in Group 3. In Group 1, 1/4 placentas had villous hypoplasia, and in Group 2, 1/8 placentas had cystic pouches on the UC.

There were no significant differences among groups. However, the proportion of overweight placentas between Group 2 (6/8) and Group 3 (0/10) approached significance ($P = 0.06$).



Amniotic coils in Group 1 (a), Group 2 (b) and Group 3 (c).

Collection of allantoic UC length (d), villous hypoplasia in Group 1 (e) and cystic pouches in Group 2 (f).

	Group 1 n=4	Group 2 n=8	Group 3 n=10
Mare's age (y)	9.5 \pm 3.1	4.6 \pm 0.9	11.2 \pm 4.9
Mare's parity (n)	1.3 \pm 0.5	1.0 \pm 0.0	4.5 \pm 3.7
Gestational length (d)	342.3 \pm 1.5	343.9 \pm 9.9	340.6 \pm 6.4
Foal's sex	2 F; 2 M	4 F; 4 M	7 F; 3 M
Foal's weight (kg)	49.3 \pm 7.8	44.3 \pm 4.2	49.4 \pm 6.0
Placental weight (kg)	6.3 \pm 0.7	5.2 \pm 0.5	5.1 \pm 1.4
Total UC length (cm)	53.5 \pm 13.7	52.8 \pm 10.2	56.1 \pm 16.3
Total UC coils (n)	4.5 \pm 1.7	4.6 \pm 1.5	5.9 \pm 1.4
Allantoic UC length (cm)	29.5 \pm 13.8	21.8 \pm 7.5	20.9 \pm 8.9
Allantoic UC coils (n)	2.3 \pm 1.0	1.8 \pm 1.0	2.2 \pm 0.9
Amniotic UC length (cm)	24.0 \pm 4.2	31.0 \pm 7.2	35.2 \pm 12.3
Amniotic UC coils (n)	2.3 \pm 1.0	2.9 \pm 0.8	3.7 \pm 1.3
UC insertion	4/4*	6/8* 2/8*	5/10* 3/10* 2/10*

Table 1. Data registered at delivery



* basis of pregnant horn
* between two horns (g)
* basis of nonpregnant horn (h)



CONCLUSIONS

Although preliminary, the results of the present study suggest that production of equine embryos in vitro may lead to alterations in placental development. Several studies in cattle and sheep have suggested that alterations in the placentas of pregnancies derived from in vitro-produced embryos are related to effects of culture on epigenetic regulation. Less is known in the horse about the effects of in vitro embryo production on placental development; thus, further research in this area is necessary.

REFERENCES

- ✓ Joy J, Gannon C, McClure N, Cooke I. Is assisted reproduction associated with abnormal placentation? *Pediatr Dev Pathol*, 2012; 15(4):306-14.
- ✓ Pozor MA, Sheppard B, Hinrichs K, Kelleman AA, Macpherson ML, Runcan E, Choi YH, Diaw M, Mathews PM. Placental abnormalities in equine pregnancies generated by SCNT from one donor horse. *Theriogenology*, 2016; 86(6):1573-82.

CHAPTER 2

MICROSCOPIC CHARACTERISTICS OF THE UMBILICAL CORD IN THE EQUINE SPECIES

Article in preparation

Department of Veterinary Medical Sciences, University of Bologna, Ozzano Emilia, Bologna, Italy

Introduction

The umbilical cord (UC) is an important connection between mother and fetus and is designed to protect blood flow to the fetus during pregnancy (Ferguson and Dodson, 2009). In human medicine, the microscopic aspects of the UC has been intensively studied, whereas in equine medicine, only few studies described UC microscopically. Both human and equine umbilical cords are composed of a vascular component and a gelatinous substance, Wharton's jelly (WJ). This is made of fibroblasts, collagen fibres and an amorphous ground substance composed mainly of hyaluronic acid (Schoenberg et al., 1960; Takechi et al., 1993; Franc et al., 1998).

In a recent study, Kumar et al. (2013) described gross anatomy and microscopic features at different sites of six normal equine UCs. However, the Wharton's jelly of healthy and ill foals was never microscopically investigated.

The aim of this preliminary study was to describe the equine umbilical cord microscopically and immunohistochemically.

Materials and Methods

Animals and UC sampling

Twenty-eight mares housed for attended delivery at the Equine Perinatology Unit of University of Bologna, during two breeding seasons (2014-2015) were included in the study. The mares were hospitalized at about 310 days of pregnancy because the owners requested an attended parturition, and remained under observation for at least 7 days postpartum. They were housed in wide straw bedding boxes and fed with hay ad libitum and concentrates twice a day. During the day, the mares were allowed to go to pasture. At admission, a complete clinical evaluation, including complete blood count, serum biochemistry and transrectal ultrasonography, was performed. During hospitalization, mares were clinically evaluated twice a day and by transrectal ultrasonography every 10 days, until parturition. Information about mare's age and parity were recorded at admission. At delivery, the following data were recorded: gestational length, days of pregnancy, length of stage II labour (minutes), placental weight and presence of foetal membranes alterations. Macroscopic evaluation of umbilical cords was performed to identify any abnormality and for the evaluation of WJ's distribution. Furthermore, immediately after foaling, APGAR score within 5 min from birth (Vaala, 2006), foal's weight, sex and outcome were recorded. For microscopic evaluation, immediately after breaking the umbilical cord, the UC intramniotic portion closest to the foal (about 15 cm), characterized by a more amount of WJ, was collected.

All the mares were healthy and delivered healthy foals after a normal pregnancy. The foals were classified as healthy when they had an Apgar score ≥ 8 and a normal clinical evaluation during the course of hospitalization, including a complete blood count and serum biochemistry at birth and an immunoglobulin G (IgG) serum concentration ≥ 800 mg/dL at 18 hs of life.

Wharton's jelly weight

At the Laboratory of Biotechnology and Animal Reproduction (LRBA) of the Department of Veterinary Medical Sciences (DIMEVET), UCs were disinfected by immersion in ethanol 70% for 10 minutes, and then they were rinsed by repeated immersion in DPBS, under a laminar flow hood. For each UC, Wharton's jelly was isolated and weighed.

Microscopic and immunohistochemical analysis

At the Laboratory of Normal Anatomy (LNA), after rinsing in PBS (pH 7.4) for 12 hours at 4°C, samples were stored in a PBS solution containing 0.1% sodium-azide, and 30% sucrose solution and they were stored at 4°C.

Microscopic description

Ten sections of 15 µm for each sample were obtained at the cryostat and they were mounted in gelatin-coated glass slides. Umbilical cord's sections were stained with Masson's trichrome stain. For an accurate analysis of WJ the section were stained also with Orcein technique to identify elastic fibres and with Silver Impregnation technique to identify reticular fibres.

Immunohistochemical analysis of WJ

The immunohistochemical analysis was conducted giving particular attention at WJ.

After three washings for 10 mins in PBS, sections were incubated with 1% H₂O₂ in PBS for 30 mins at room temperature to eliminate endogenous peroxidase activity. Sections were rinsed in PBS three times for 10 mins and incubated in a solution containing 10% normal goat serum (Colorado Serum, Denver, CO, #CS 0922) and 0.5% Triton X-100 (Merck, Darmstadt) in PBS for 2 hours at room temperature. Thereafter, the sections of each sample were incubated for 48 hours at 4°C in a solution containing:

- ✓ Rabbit anti-bovine collagen type I polyclonal antibody dilution 1:80 (Chemicon, Temecula, CA-USA, lotto NG1804950);
- ✓ Rabbit anti-human collagen type V polyclonal antibody dilution 1:40 (Chemicon, Temecula, CA-USA, lotto 0604027824);
- ✓ Rabbit anti-collagen type VI polyclonal antibody dilution 1:10-1:40 (Chemicon, Temecula, CA-USA, lotto NG 1833210);
- ✓ Anti-fibrillin clone 689 purified mouse monoclonal antibody dilution 1:200 (Chemicon, Temecula, CA-USA, lotto NRG1758239).

The primary antibody was diluted in a solution (1.8% NaCl in 0.01 M PBS containing 0.1% sodium azide) containing 1% normal goat serum and 0.5% Triton X-100. After three washing in PBS, the sections were incubated in goat biotinylated anti- rabbit 10µg/ml (Vector Laboratories, Burlingame, CA, USA, BA-1000) or goat biotinylated anti- mouse 10µg/ml (Vector Laboratories, Burlingame, CA, USA, BA-9200) for 2 hours at room temperature. The secondary antibody was diluted in PBS containing 1% normal goat serum and 0.5% Triton X-100. The sections were transferred to avidin–biotin complex (ABC kit Vectastain, PK-6100, Vector Laboratories, Burlingame, CA) for 30 min and the immunoperoxidase reaction was developed by 3,30-diaminobenzidine (DAB kit, SK-4100, Vector Laboratories, Burlingame, CA). Slides were dried overnight, dehydrated in ethanol, cleared in xylene, and coverslipped with Entellan (Merck, Darmstadt, Germany). All the incubations were performed in a humid chamber. Masson trichrome staining was also performed to better highlight the fibroblasts. The Orcein Technique and the Silver Impregnation Technique were performed.

Sections were observed with a Zeiss Axioplan microscope (Carl Zeiss, Oberkochen, Germany). Images were recorded by using a Polaroid DMC digital photcamera (Polaroid Corporation, Cambridge, MA, USA) and DMC 2 software.

Statistical analysis

Data were analysed for normality using a Shapiro-Wilk test. Pearson's test was performed to compare weight of WJ and data relative to foals and mares.

Data are expressed as mean \pm SD. All analyses were carried out using the software IBM SPSS Statistics 23 (IBM Corporation, Milan, Italy). Significance was assessed for $P < 0.05$.

Results

Information about mares, foals and weight of WJ were reported in *Table 2.1*.

The WJ was found just in the intramniotic portion of UC, closest to the foal, while it was absent in the allantoic portion (*Figure 2.1* and *Figure 2.2*).

Mare's age (years)	11 \pm 5
Parity	3 \pm 3
Gestational length (days)	340 \pm 8
Foal's weight (kg)	48.7 \pm 13.8
Foal's sex	14M; 14 F
WJ (g)	5.1 \pm 3.2

Table 2.1. Information about mares, foals and weight of WJ.

The amount of WJ (g) was negatively correlated with the mare's age ($P < 0.05$; $r = -0.387$). No others correlations were found.



Figure 2.1. Allantoic portion of UC: absence of WJ (a); amniotic portion (b) with WJ (white arrow).



Figure 2.2. Equine intramniotic portion of UC with Wharton's jelly (white arrow).

Microscopic description

All the vessels (two umbilical arteries and one umbilical vein) showed the three typical layers: tunica intima, tunica media and tunica adventitia (*Figure 2.5*). The endothelium of tunica intima was regular and well developed having a single layer of cells (*Figure 2.3*) resting on a basement membrane. The subendothelial layer was composed of connective tissue with some smooth muscle fibres between the collagen fibres (*Figure 2.3, 2.4*). The tunica media was thicker than tunica intima and it had multiple concentric smooth muscle and few collagen fibres (*Figure 2.4, 2.5*). The tunica adventitia was the thickest layer and the collagen fibres

progressively increased going towards the periphery, while smooth muscle fibres decreased (*Figure 2.5, 2.6*). A perivascular tissue, composed by dense collagen fibres arranged concentrically, surrounded the tunica adventitia (*Figure 2.6, 2.7*). This tight tissue was composed by dense and well organized connective tissue. On the contrary, the Wharton's jelly was made of loose connective tissue: collagen fibres were arranged to create a loose reticular texture (*Figure 2.6, 2.8 and 2.9*). Other cells observed in WJ were fibroblasts (*Figure 2.8e*) and white blood cells (*Figure 2.9*). Finally, the UC were externally surrounded by amniotic membrane (*Figure 2.6, 2.7*), composed by two thin layers: amniotic epithelium and subamnion, an amniotic connective tissue with collagen fibres and fibroblasts (*Figure 2.7 insert*).

The Orcein staining showed the absence of elastic fibres in the Wharton's jelly. They were less concentrated with an uneven pattern around the vessels (*Figure 2.10*).

Finally, the silver impregnation staining revealed a dense network of reticular fibres in the entire section of the cord (*Figure 2.11*).

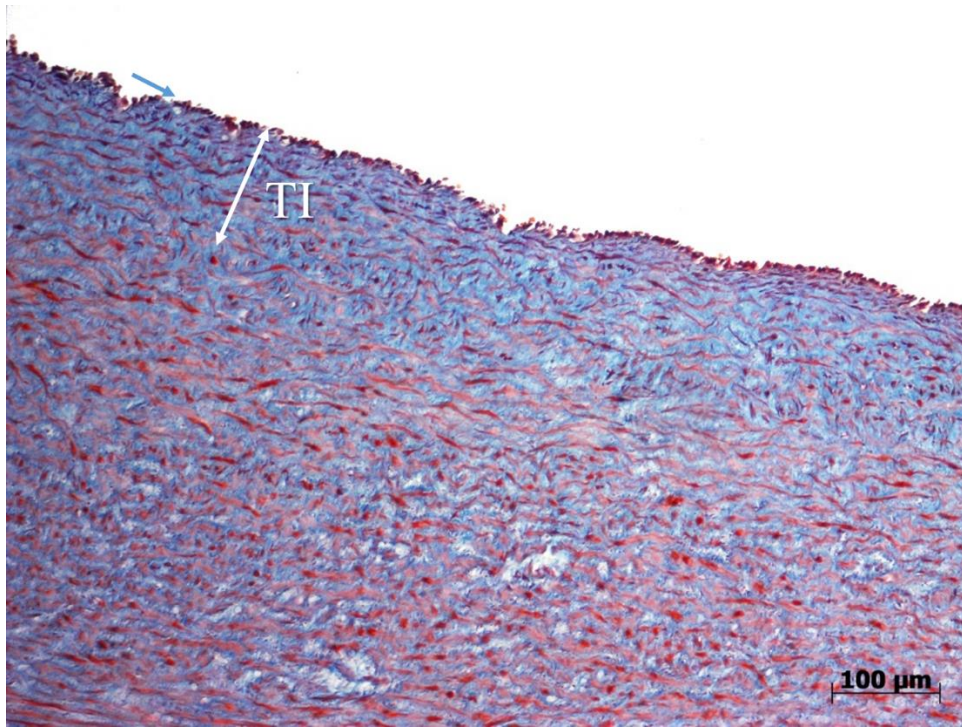


Figure 2.3. Tunica intima (TI) at 10x magnification, Masson's trichrome stain. The endothelium of tunica intima (blue arrow).

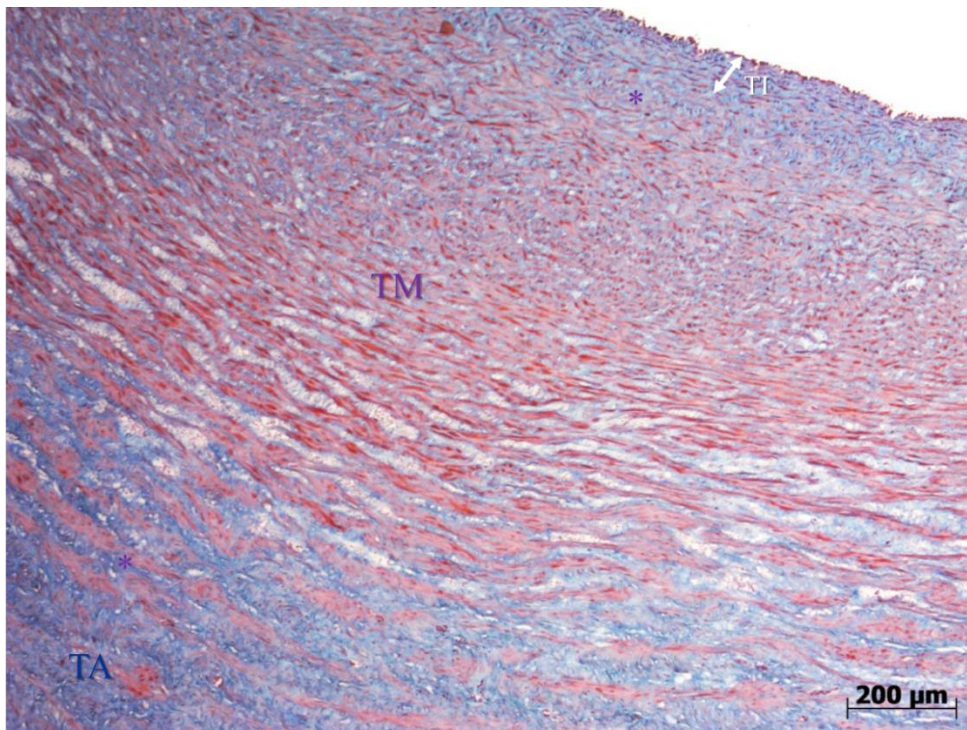


Figure 2.4. Tunica intima (TI), Tunica media (TM) is included between purple asterisks and tunica adventitia (TA). Magnification 5x and Masson's trichrome stain.

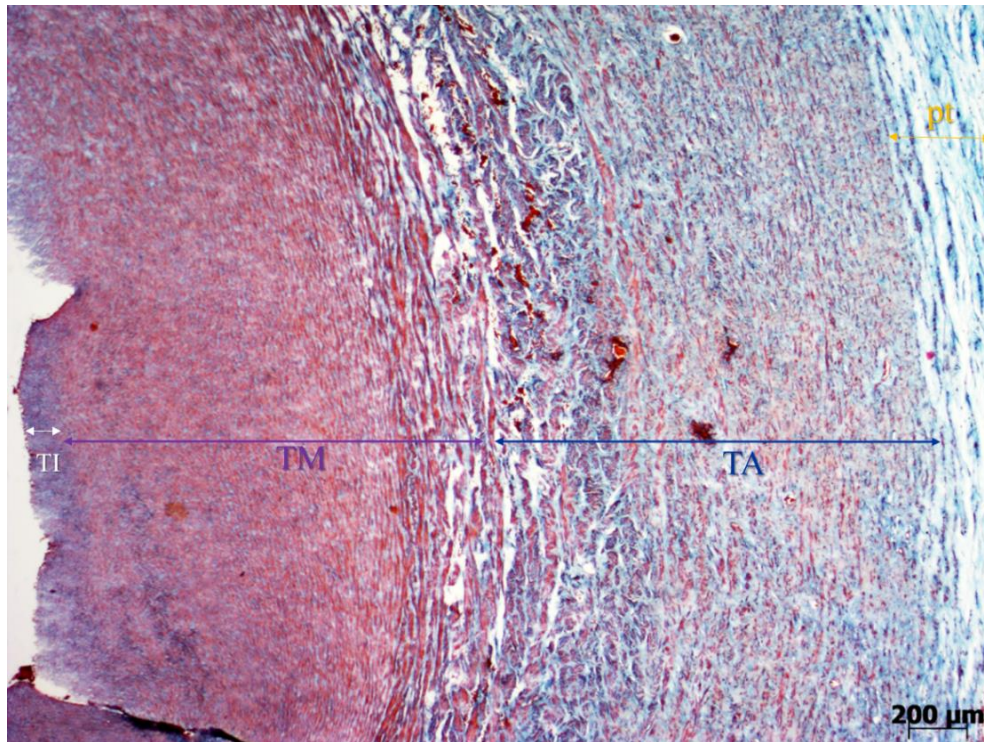


Figure 2.5. Umbilical vessel with the three layers: tunica intima (TI, white arrow), tunica media (TM, purple arrow), tunica adventitia (TM, blue arrow) and perivascular tissue (pt, orange arrow). Masson's trichrome stain.

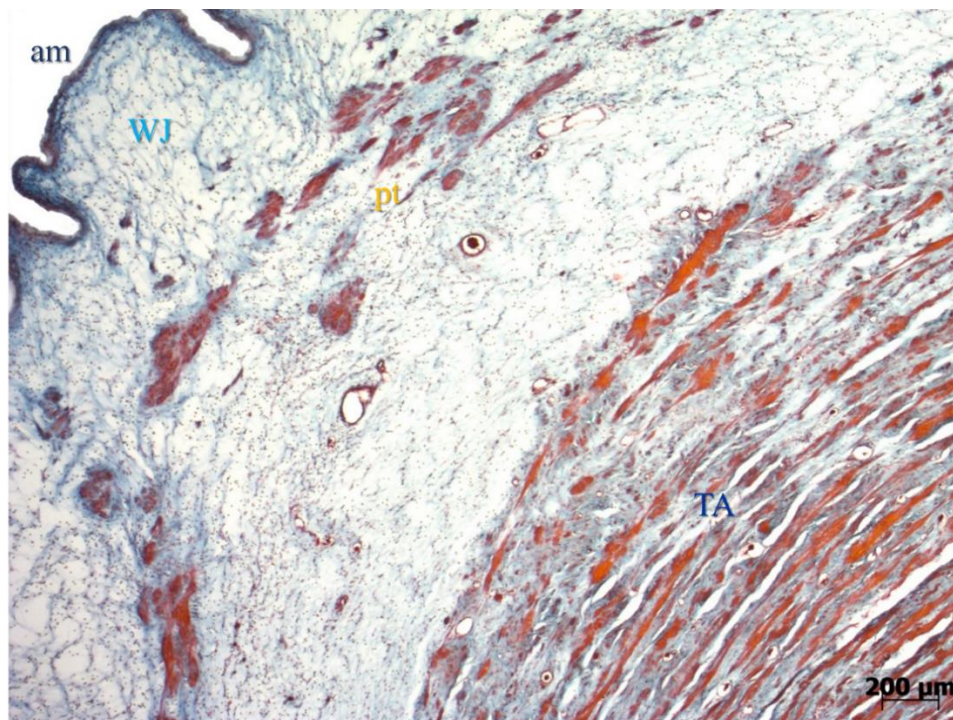


Figure 2.6. Umbilical section: tunica adventitia (TA), perivascular tissue (pt), Wharton's jelly (WJ) and amniotic membrane (am). Masson's trichrome stain.

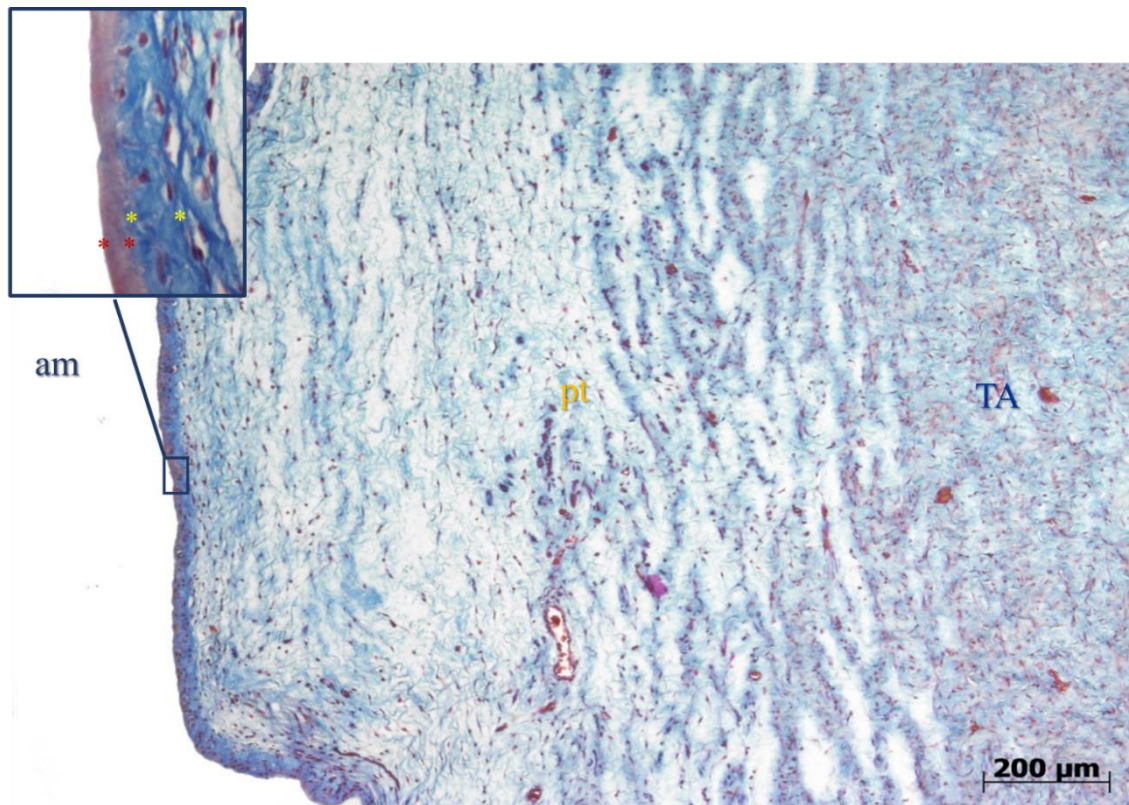


Figure 2.7. Umbilical section: tunica adventitia (TA), perivascular tissue (pt) and amniotic membrane (am). A particular of amniotic membrane is shown in the insert: it is composed by amniotic epithelium (included between red asterisks) and subamnion (included between yellow asterisks). Wharton's jelly is not present in this section. Masson's trichrome stain.

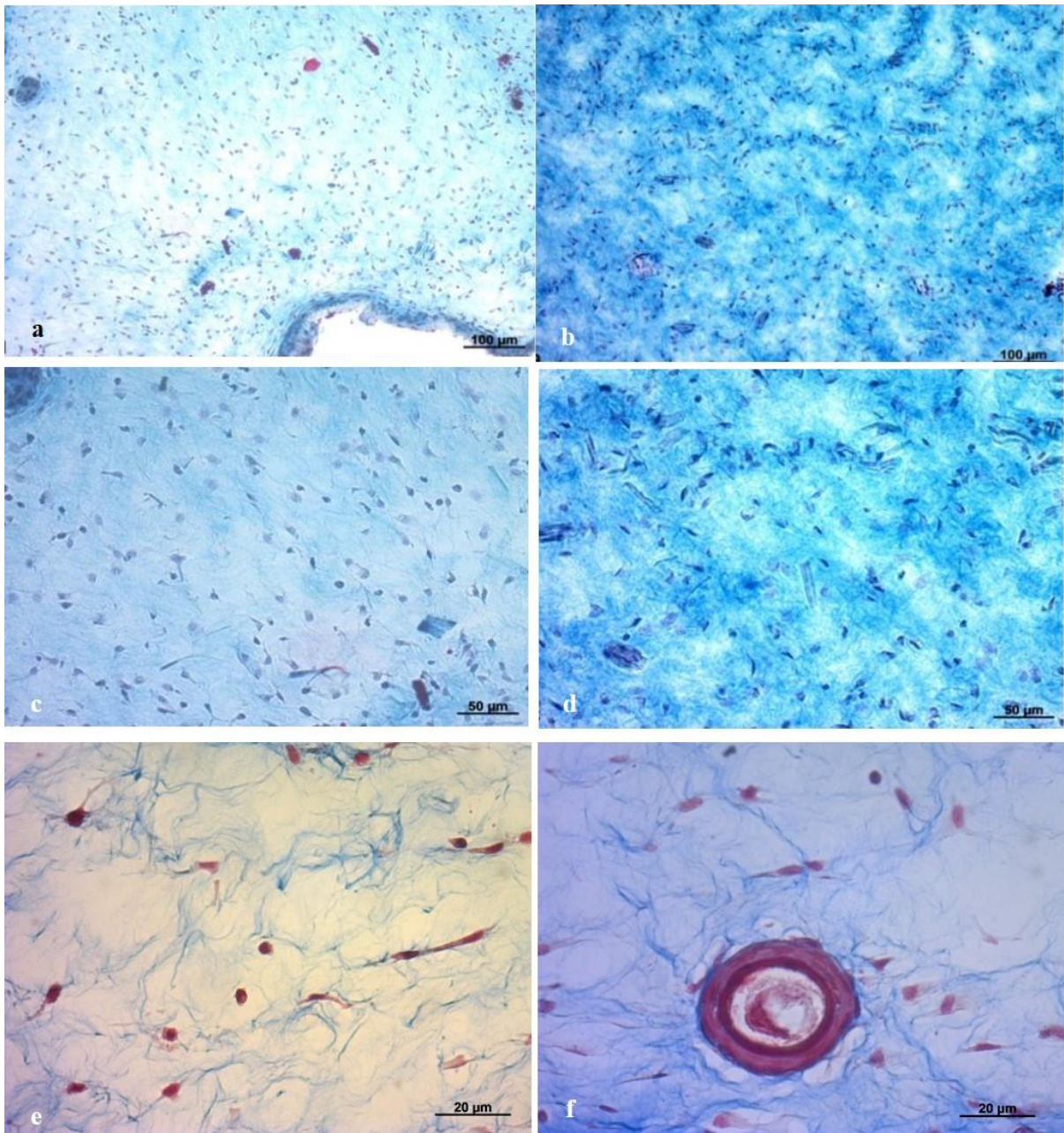


Figure 2.8. These photos represent contiguous sections of Wharton's jelly performed with Masson's trichrome at different magnifications (a. b. 10x; c. d. 20x; e. f. 40x). Elongated shape and cellular prolongations characterize fibroblasts. f. a section of capillary in WJ.

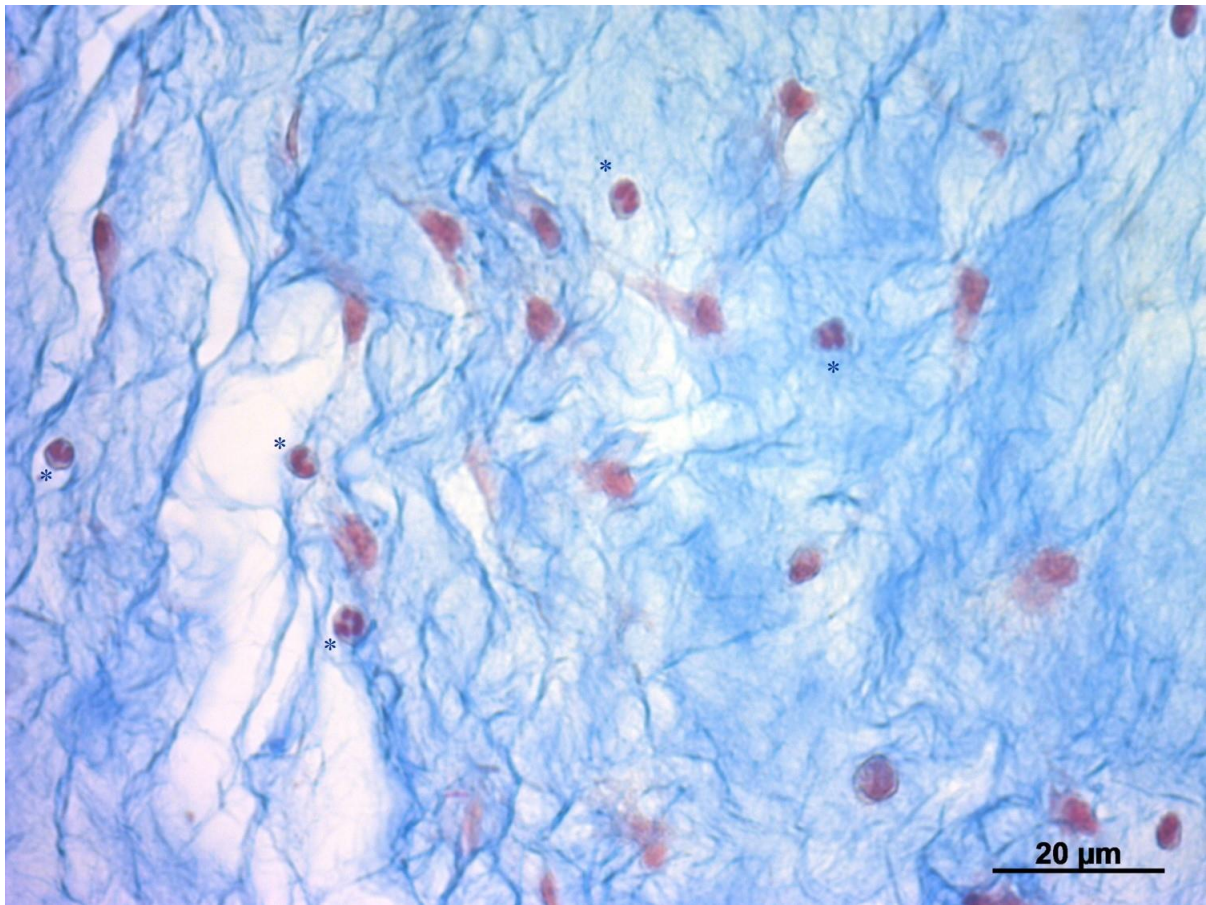


Figure 2.9. A particular of WJ: it contains white blood cells (blue asterisks).

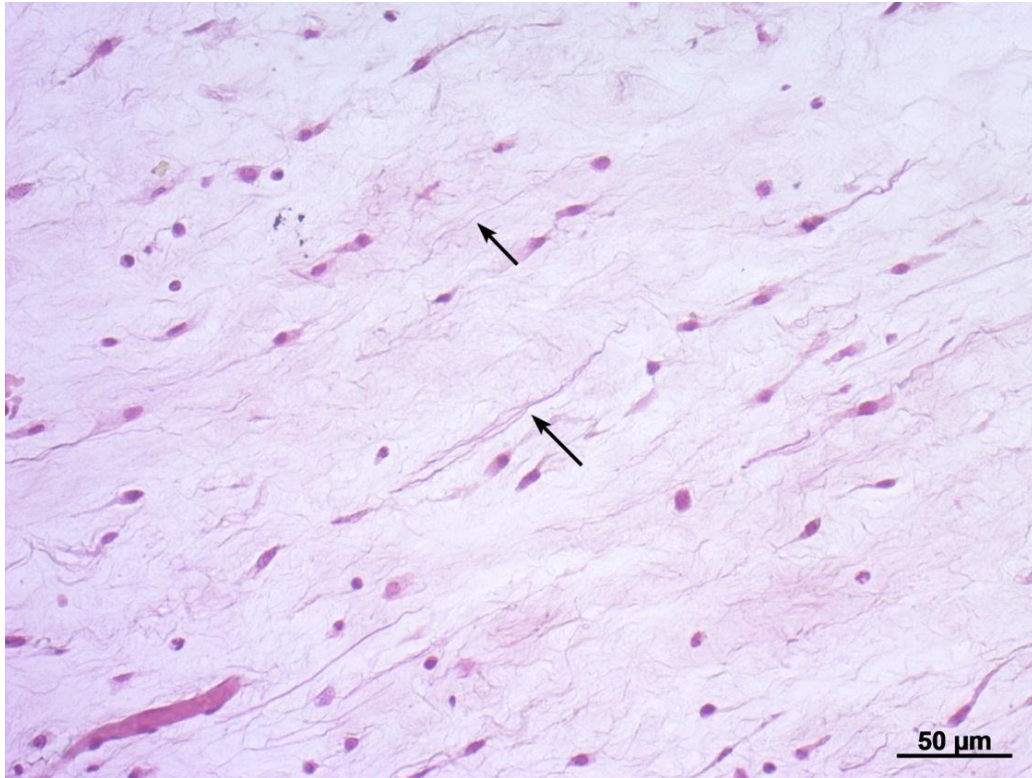


Figure 2.10. Orcein staining. Presence of uneven and less concentrated elastic fibres (black arrows).

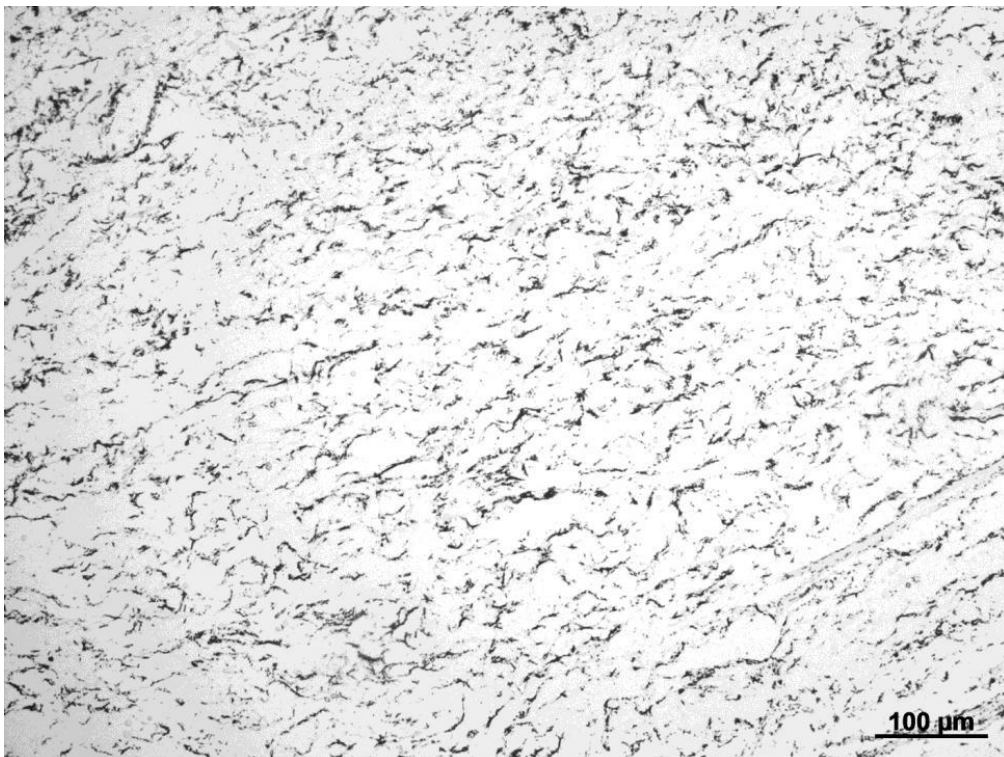


Figure 2.11. Silver impregnation. Presence of a dense network of reticular fibres.

Immunohistochemical analysis of WJ

The immunohistochemical analysis revealed the presence of fibroblast cells positive for antibodies anti-type I, V and VI collagen and anti-fibrillin (*Figure 4.12*).

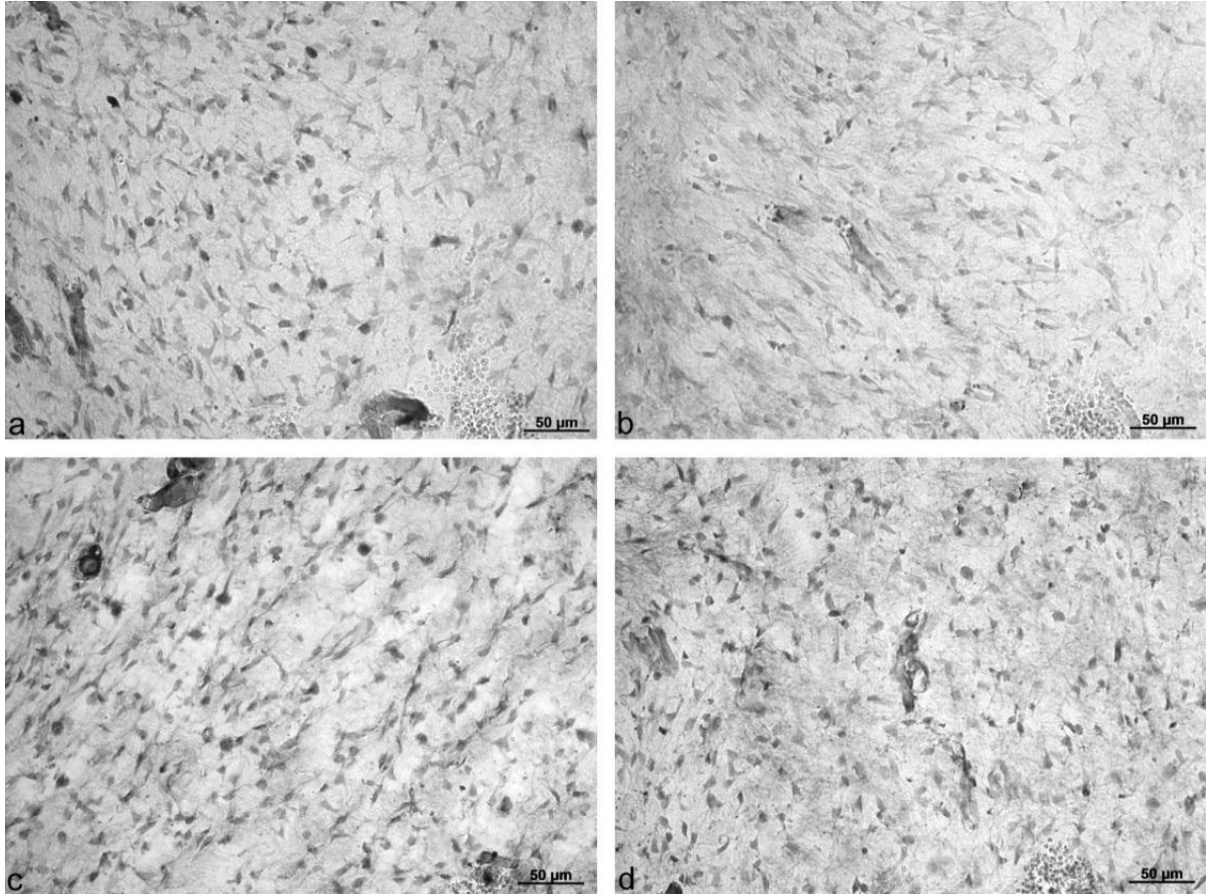


Figure 2.12. Immunohistochemical analysis at magnification 10x. The photos showed fibroblast reactive and positive to fibrillin (a), collagen type I (b), collagen type V (c) and collagen type VI (d).

Discussion

Wharton's jelly is fundamental for the well-being of the fetus because binds the umbilical vessels, protecting them from twisting and compression during pregnancy and delivery (Ferguson and Dodson, 2009). In human medicine, WJ is a well-defined structure: it is composed of collagen fibres, forming a network of interconnected cavities. The ground substance of the jelly is mainly composed by hyaluronic acid and proteoglycans dissolved in an aqueous solution of salts, metabolites and plasma proteins (Klein and Meyer 1983; Vizza et al., 1996; Ghezzi et al., 2001).

In the present study, we investigated the microscopic features of umbilical cords collected at delivery of healthy foals born from healthy mares after normal pregnancy. The microscopic description focused on the analysis of Wharton's jelly, a still poorly known tissue in the equine species. For the first time in equine medicine, we reported the physiological amount of Wharton's jelly in normal umbilical cord. In human medicine, in fact, a quantitative variation of WJ was associated with pathological conditions such as hypertensive disorders (Bankowski et al., 1996), foetal distress (Goodlin, 1987), gestational diabetes (Weissman and Jakobi, 1997) and foetal growth restriction (Bruch et al., 1997; Ghezzi et al., 2001; Ghezzi et al., 2004). Furthermore, the total absence of WJ has been associated with foetal death (Kulkarni et al., 2007). The reduction of WJ facilitates torsion, compression or stretching of UC that would adversely affect foetal blood flow (Ferguson and Dodson, 2009; Kurita et al., 2009). Moreover, Goodlin (1987) reported that male fetus had more WJ, but with connective more loose; then male and female fetuses had the same density of WJ. We found that the amount of WJ at term was negatively correlated with the mare's age. No differences were found in the amount of WJ between colts and fillies.

Furthermore, in human medicine, different authors measured the amount of WJ during pregnancy. Raio et al. (1999) reported that quantitative WJ variations occurred in normal

pregnancies: they measured ultrasonographically the Area of WJ (WJA) and reported that WJA increased up to 32 weeks of gestation and then remained at this plateau until the end of pregnancy. Ghezzi et al. (2001) found that the ratio of the WJA to the total umbilical cord area decreased significantly with advancing gestation. This is in agreement with Sloper et al. (1979) who reported that the water content of the umbilical cord is significantly lower in term than in preterm neonates with a progressive reduction from 30 weeks' gestation to term. Similarly, Bruch et al. (1997) reported that the proportion of WJ was higher in UCs of fetuses delivered before 32 weeks of gestation than in those delivered between 37 and 41 weeks. In our study, the microscopic aspect of WJ was similar to that described by Kumar et al. (2013) in 6 Thoroughbred foals. However, on the contrary, we found just few elastic fibres scattered in UC section. As in humans (Takechi et al., 1993), the immunohistochemical analysis in normal umbilical cords revealed the presence of fibroblast cells positive for antibodies anti-type II, IV and V collagen, anti-fibrillin, surrounded by a dense network of reticular fibres. Given their abundance, we could not confirm the presence of nervous fibres. Different from humans, in the equine UC, elastic fibres are less concentrated with an uneven pattern around the vessels. In this study, we highlighted similarities and differences between equine and human microscopic characteristics of the umbilical cord. Given the presence in human species of a strong correlation between these and specific pathological conditions of newborn and mother, further studies are needed, both on normal and high risk pregnancies to verify the presence of these correlations also in the equine species.

References

- Bańkowski E., Sobolewski K., Romanowicz L., Chyczewski L., Jaworski S., (1996). 6 *Collagen and glycosaminoglycans of Wharton's jelly and their alterations in EPH-gestosis.* Eur J Obstet Gynecol Reprod Biol; 66(2): 109-117.
- Bruch J.F., Sibony O., Benali K., Challer C., Blot P., Nessmann C., (1997). *Computerized microscope morphometry of umbilical vessels from pregnancies with intrauterine growth retardation and abnormal umbilical artery Doppler.* Hum Pathol; 28(10): 1139–1145.
- Ferguson V.L., Dodson R.B., (2009). *Bioengineering aspects of the umbilical cord.* Eur J Obstet Gynecol Reprod Biol; 144S: S108-S113.
- Franc S., Rousseau J.C., Garrone R., van der Rest M., Moradi-Améli M., (1998). *Microfibrillar composition of umbilical cord matrix: characterization of fibrillin collagen VI and intact collagen V.* Placenta; 19(1): 95-104.
- Ghezzi F., Raio L., Di Naro E., Franchi M., Balestreri D., D'Addario V., (2001). *Nomogram of Wharton's jelly as depicted in the sonographic cross section of the umbilical cord.* Ultrasound Obstet Gynecol; 18(2): 121-125.
- Ghezzi F., Raio L., Duwe D.G., Cromi A., Karousou E., Du`rig P., (2004). *Sonographic umbilical vessel morphometry and perinatal outcome of fetuses with a lean umbilical cord.* J Clin Ultrasound; 33(1): 18-23.
- Goodlin R.C., (1987). *Fetal dysmaturity, "lean cord," and fetal distress.* Am J Obstet Gynecol; 156(5): 1357.

Klein J., Meyer F.A., (1983). *Tissue structure and macromolecular diffusion in umbilical cord. Immobilization of endogenous hyaluronic acid.* Biochim Biophys Acta; 755(3): 400-411.

Kulkarni M.L., Matadh P.S., Ashok C., Pradeep N., Avinash T., Kulkarni A.M., (2007). *Absence of Wharton's jelly around the umbilical arteries.* Indian J Pediatr; 74(8): 787-9.

Kurita M., Hasegawa J., Mikoshiba T., Purwosunu Y., Matsuoka R., Ichizuka K., Sekizawa A., Okai T., (2009). *Ultrasound evaluation of the amount of Wharton's jelly and the umbilical coiling index.* Fetal Diagn Ther; 26(2): 85-89.

Naeye R.L., (1985). *Umbilical cord length: Clinical significance.* J Pediatr; 107: 278-281.

Raio L., Ghezzi F., Di Naro E., Gomez R., Mueller M.D., Maymon E., Mazor M., (1999). *Sonographic measurements of the umbilical cord and fetal anthropometric parameters.* Eur J Obstet Gynecol Reprod Biol; 83: 131–135.

Schlafer D.H., (2004). *The umbilical cord-lifeline to the outside world: structure, function and pathology of the equine umbilical cord.* In: Proceedings of a workshop on the equine placenta. Eds: Powell D., Furry D., Hale G, Kentucky Agricultural Experimental Station. Lexington; 92-99.

Schoenberg M.D., Hinman A., Moore R.D., (1960). *Studies on connective tissue. V. Fiber formation in Wharton's jelly.* Lab Invest; 9:350-5.

Sloper K.S., Brown R.S., Baum J.D., (1979). *The water content of the human umbilical cord.* Early Hum Dev; 3(2): 205–210.

Takechi K., Kuwabara Y., Mizuno M., (1993). *Ultrastructural and immunohistochemical studies of Wharton's jelly umbilical cord cells*. Placenta; 14(2): 235-245.

Vaala W.E., House J.K., Madigan J.E., (2002). *Initial management and physical examination of the neonate*. In: Smith. B.P. (Ed.). Large Animal Internal Medicine. Mosby Inc St Louis MO USA; 277-293.

Vizza E., Correr S., Goranova V., Heyn R., Angelucci P.A., Forleo R., Motta P.M., (1996). *The collagen skeleton of the human umbilical cord at term. A scanning electron microscopy study after 2N-NaOH maceration*. Reprod Fertil Dev; 8(5): 885-894.

Weissman A., Jakobi P., (1997). *Sonographic measurements of the umbilical cord in pregnancies complicated by gestational diabetes*. J.Ultrasound Med; 16(10): 691-694.

Whitwell K.E., Jeffcott L.B., (1975). *Morphological studies on the foetal membranes of the foal at term*. Res Vet Sci; 19(1): 44-55.

SECTION II- Studies on equine Mesenchymal Stem Cells

CHAPTER 3

EXPRESSION OF PROINFLAMMATORY CYTOKINES BY EQUINE MESENCHYMAL STEM CELLS FROM FOETAL ADNEXA: PRELIMINARY DATA

Abstract: Poster presentation

5th International Satellite Symposium AICC-GISM (Gruppo Italiano Staminali Mesenchimali), November 14th 2014, Verona, Italy

Iacono E.¹, Rossi B.¹, **Lanci A.**¹, Castagnetti C.¹, Merlo B.¹

¹Department of Veterinary Medical Sciences, University of Bologna, Ozzano Emilia, Bologna, Italy



P62 Posters

Expression of proinflammatory Cytokines by Equine Mesenchymal Stem Cells from foetal adnexa: preliminary data

Iacono Eleonora, Rossi Barbara, Lanci Aliai, Castagnetti Carolina, Merlo Barbara

University of Bologna, Department of Veterinary Medical Sciences, Ozzano Emilia (BO), Italy

MSCs regulate localization, self-renewal and differentiation of hematopoietic stem cells due to MSCs' secretion of cytokines. In the present study, we examined, for the first time in equine foetal MSCs, the expression of pro-inflammatory cytokines TNF- α , IL-1 β and IL-8, by RT-PCR analysis. Furthermore, we monitored proliferation and examined CD expression of MSCs from equine amniotic membrane (AM), Wharton's jelly (WJ) and amniotic fluid (AF). Samples were recovered at labor from 3 mares. Undifferentiated cells, cultured in DMEM-TCM 199, plus 10% FBS, were passaged up to 3 times. Population-doubling times (DT) were calculated, and data were analyzed by ANOVA. No significant differences ($P>0.05$) were found between cell doublings of all passages. DT of AM (2.4 ± 1.0 d), AF (1.8 ± 0.2 d) and WJ (1.9 ± 0.1 d) resulted statistically similar ($P>0.05$). No lag phase was observed during in vitro culture. At P3, characterization was performed. GAPDH was employed as reference gene. Differently from previous studies, all cell lines resulted negative both for MHC-I and MHC-II, confirming the immunosuppressive function of MSCs. AM and AF cells did not express hematopoietic marker CD34 and CD45, but expressed mesenchymal marker, CD90. Differently, WJ cells resulted positive also for IL-8 and weakly positive for CD34. This was already observed in human WJMSCs. Recent reports indicate that CD34+ stem cells have the potential to secrete growth factors, cytokines, and chemokines. However, until now, little is known about direct immune-regulatory functions of CD34+ stem cells during inflammation. All isolated cells resulted negative for CD73. As postulated in a previous study, this could be related to the negative expression of TNF- α and IL-1 β in the isolated cells. Further studies are needed to verify if the expression of pro-inflammatory cytokines changes in different culture conditions and at different culture passages, and if their expression could interfere with cells differentiation potency.

EXPRESSION OF PRO-INFLAMMATORY CYTOKINES BY EQUINE MESENCHYMAL STEM CELLS FROM FOETAL ADNEXA: PRELIMINARY DATA



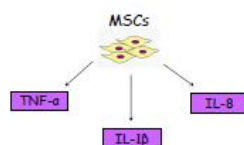
Iacono E., Rossi B., Lanci A., Castagnetti C., Merlo B.

Department of Veterinary Medical Sciences, University of Bologna, Ozzano Emilia (Bologna), Italy

eleonora.iacono2@unibo.it

Introduction

Mesenchymal Stem Cells regulate localization, self-renewal and differentiation of hematopoietic stem cells through secretion of cytokines.



Aim

- ✓ Study of proliferation, doubling times and cell doublings in equine foetal MSCs;
- ✓ Molecular characterization: Mesenchymal stem cells (MSC), Haematopoietic Stem Cells (HSC) and Major Histocompatibility Complexes (MHC) markers by RT-PCR analysis
- ✓ Evaluation of the expression of pro-inflammatory cytokines (TNF- α , IL-1 β and IL-8) by RT-PCR analysis \rightarrow first time in equine foetal MSCs!



Materials and Methods



Wharton's Jelly (WJ)

Amniotic Membrane (AM)

Amniotic Fluid (AF)

Samples recovered at labor from 3 mares

Culture in DMEM + 10% FBS until P5

Molecular characterization at P3 by RT-PCR:

- MSC markers
- HSC markers
- MHC markers

Evaluation of the expression of pro-inflammatory cytokines at P3 by RT-PCR

	Forward (5' \rightarrow 3')	Reverse (3' \rightarrow 5')	References
CD73	GGGATTTTGGGATGACCTCAAAAAG	GCTGCAACGGCAATGATTTCA	Mohenty et al. 2014
CD90	TGGGAACCTCGGCTCTCT	GCTTATGCGCTGGACATGG	Mohenty et al. 2014
CD34	CACCTAAACCTCTACATCTTTCTCTCA	GGCAGATACCTTGAGTCAATTCA	Mohenty et al. 2014
CD45	TGATTCGGAGAAATGACCATGTA	AGATTTGGGCTTCTCTGTAAAC	Mohenty et al. 2014
MHC I	GGAGAGGAGCAGAGATACA	CTGTCACTGTTTGGAGTCT	Corradetti et al. 2011
MHC II	TCTACACTGGCCAAATGG	CCACCATGCGCTTCTCTG	Corradetti et al. 2011
IL-8	CGGTCCAGTGCATCAAG	TGGCGACTCTCAATCACTCT	Jirku et al. 2007
IL-1 β	TGAAGGGCAGCTTCCAAAGAC	GGAGAAATGSAAGCTGGATGC	Jirku et al. 2007
TNF- α	GCTCCAGACGGTGGCTGTGG	GGCAGTCCACCAAAATGG	Jirku et al. 2007
GAPDH	GTCCATGGCATCACTGGCAC	CCTGCTTCACCACTTCTTG	Destanreis et al. 2011

Results

Cell culture, Doubling Times (DTs) and Cell Doublings (CDs)

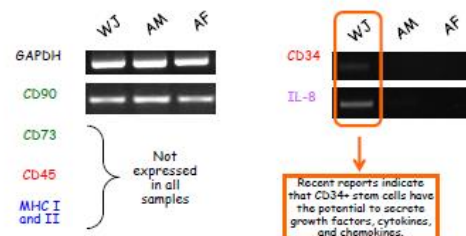


- No lag phase was observed during in vitro culture.
- DTs statistically similar ($P > 0.05$)

AM	AF	WJ
2.4 \pm 1.0 d	1.8 \pm 0.2 d	1.9 \pm 0.1 d

- CDs: No significant differences ($P > 0.05$) were found between CDs of all passages.

Gene expression profile



Conclusions

Further studies are needed to verify if the expression of pro-inflammatory cytokines changes in different culture conditions and at different culture passages, and if their expression could interfere with cells differentiation potency.

ULTRASTRUCTURAL CHARACTERISTICS AND IMMUNE PROFILE OF MESENCHYMAL STEM CELLS DERIVED FROM EQUINE FOETAL ADNEXA

Article under review (Reproduction)

Iacono E.¹, Pascucci L.², Rossi B.¹, **Lanci A.**¹, Ceccoli M.¹, Merlo B.¹.

¹Department of Veterinary Medical Sciences, University of Bologna, Ozzano Emilia, Bologna, Italy

² Department of Veterinary Medicine, University of Perugia, Perugia, Italy

Introduction

Both in human and equine species, mesenchymal stem cells (MSCs) from perinatal tissue, primarily amniotic membrane (AM) and Wharton's jelly (WJ) may be particularly useful in the clinic for autologous transplantation for newborns and after banking in later stages of life. Even though they were originally clinically utilized for their differentiation and proliferation potential, MSCs are increasingly thought to improve tissue regeneration through paracrine actions, involving extracellular microvesicles or secreted factors (Liang et al., 2014). Despite a lot of data have been reported on these features of human MSCs, only two reports are present on the ultrastructural characteristics and immunophenotype of adult and amniotic derived MSCs in equine species (Pascucci et al., 2014; Lange-Consiglio et al., 2016) . Given the increasing interest in using MSCs for regenerative medicine in horses, in the present study, for the first time in equine species, MSCs derived from AM and WJ were compared. Because MSCs may modulate the immune response, angiogenesis, apoptosis, oxidation level, migration, and themselves differentiation (Liang et al., 2014), migration, expression of stemness markers, immunophenotype, and ultrastructural features were analyzed. Furthermore, spheroids formation and differentiation potential were determined.

Materials and Methods

Unless otherwise indicated, chemicals were purchased from Sigma-Aldrich, and laboratory plastics from Sarstedt Inc.

Animals

Samples were recovered from 13 Standardbred mares, housed at the Department of Veterinary Medical Sciences, University of Bologna, for attended delivery. Experimental procedures were approved by the Ethics Committee, University of Bologna. The written consent was given by the owners to allow tissues recovery for research purposes.

Cell isolation and Doubling method

Samples, recovered immediately after delivery, were washed under flowing water for removing straw or feces debris and stored in D-PBS (Dulbecco's Phosphatase Buffered Solution) added with antibiotics (100 iu/ml penicillin and 100 µg/ml streptomycin), at 4°C, until processing. In the lab, cells were isolated as previously described (Iacono et al., 2012). Primary cells were plated in a 25 cm² flask in Dulbecco's Modified Essential Medium (D-MEM) F12 Glutamax® (Gibco) supplemented with 10% FBS (Gibco) and antibiotics and incubated in a 5% CO₂ humidified atmosphere at 38.5°C. At ~80-90% of confluence, cells were dissociated by 0.25% trypsin, counted and plated at the concentration of 5x10³ cells/cm² as "Passage 1" (P1), and so on for the following passages. Calculation of cell-doubling time (DT) and cell-doubling numbers (CD) was carried out according to the formulae of Rainaldi et al. (1991).

Adhesion and Migration Assays

In order to define differences between WJ and AM-MSCs, spheroid formation and migration test were performed. For adhesion assay, cells were cultured in 'hanging drops' (5.000 cells/drop) for 24 h. Images were acquired by a Nikon Eclipse TE 2000-U microscope.

Spheroid areas were determined using ImageJ software Version 1.6 (imagej.nih.gov/ij/). Starting from the binary masks obtained by ImageJ, the volume of each spheroid was computed using ReViSP (sourceforge.net/projects/revisp/; Bellotti et al., 2016), a software specifically designed to accurately estimate the volume of spheroids and to render an image of their 3D surface.

To assess cell migration potential, a scratch assay was carried out, as previously described (Liang et al., 2007). The distances of each scratch closure were calculated by ImageJ, and the migration percentages were calculated as previously reported (Rossi et al., 2014).

In vitro differentiation

At P3, in vitro differentiation potential of cells towards osteogenic, adipogenic and chondrogenic lineages was studied. Cells (5×10^3 cells /cm²) were cultured under specific induction media (*Table 3.1*). As negative control, an equal number of cells was cultured in expansion medium. To cytologically evaluate differentiation, cells were fixed with 10% formalin at room temperature (RT) and stained with Oil Red O, Alcian Blue and Von Kossa for adipogenic, chondrogenic and osteogenic induction, respectively. Quantitative analysis of in vitro differentiation was performed by Image J.

Adipogenic medium (7 days) (Iacono et al., 2012)	Chondrogenic Medium (21 days) (Iacono et al., 2012)	Osteogenic Medium (21 days) (Mizuno and Hyakusoku, 2003)
- DMEM F12 - 15% Rabbit Serum - 0.5 mM IBMX ^a (removed after 3 days) - 1 μ M DXM ^b (removed after 6 days) - 10 μ g/mL insulin - 0.2 mM indomethacin	- DMEM/TCM199 - 1% FBS - 6.25 μ g/mL insulin - 50 nM AA2P ^c - 0.1 μ M DXM ^b -10 ng/mL hTGF β 1 ^d	- DMEM/TCM199 - 10% FBS - 50 μ M AA2P ^c - 0.1 μ M DXM ^b - 10 mM BGP ^e

Table 3.1. Specific induction media compositions.^aIBMX: isobutylmethylxanthine, ^bDXM: Dexamethasone, ^cAA2P: Ascorbic Acid 2-Phosphate, hTGF: ^d human Transforming Growth Factor, ^eBGP: Beta-Glycerophosphate.

Immunocytochemistry (ICC)

Cells at P3, cultured on ICC slides, were fixed with 4 % paraformaldehyde (20 min at RT), then washed in phosphate buffer (PB). Cells were blocked in goat serum (10 %) for 1 h and incubated overnight with primary antibodies (*Table 3.2*), then they were washed in PB2 (PB + 0.2 % BSA + 0.05 % saponin) and incubated with anti-mouse- or anti-rabbit- FITC conjugated secondary antibodies for 1 h. Nuclei were then labelled with Hoechst 33342. The excess of secondary antibody and Hoechst were removed by 3 washes with PB2. Images were obtained with a Nikon Eclipse E400 microscope, using the software Nikon NIS-Elements.

Primary Antibody	Dilution
α -SMA (α -smooth muscle actin) (Gene tex)	1:500
E-Cadherin (Cell Signaling Tech. #3195)	1:200
N-Cadherin (Biorbyt orb11100)	1:100
pan-Cytokeratin (Chemicon Inter.Millipore CBL234)	1:250

Table 3.2. Primary antibodies for ICC.

Molecular Characterization

One million cells were snap-frozen and RNA was extracted using Nucleo Spin® RNA kit (Macherey-Nagel) following the manufacturer's instructions. cDNAs were synthesized by RevertAid RT Kit (ThermoFisher Scientific) and used directly in PCR reactions, following the instructions of Maxima Hot Start PCR Master Mix (2X) (ThermoFisher Scientific). The primers used are listed in *Table 3.3*. PCR products were visualized with ethidium bromide on a 2% agarose gel.

Primers	References	Sequences (5'→3')	bp
MSC marker			
CD90	Mohanty et al., 2014	FW: TGCGAACTCCGCCTCTCT RW: GCTTATGCCCTCGCACTTG	93
CD73	Mohanty et al., 2014	FW: GGGATTGTTGGATACACTTCAAAG RW: GCTGCAACGCAGTGATTCA	90
Ematopoietic markers			
CD34	Mohanty et al., 2014	FW: CACTAAACCCTCTACATCATTTTCTCCTA RW: GGCAGATACCTTGAGTCAATTTCA	101
CD45	Mohanty et al., 2014	FW: TGATTCCCAGAAATGACCATGTA RW: ACATTTTGGGCTTGTCTGTAAAC	101
MHC markers			
MHC-I	Corradetti et al., 2011	FW: GGAGAGGAGCAGAGATACA RW: CTGTCACTGTTTGCAGTCT	218
MHC-II	Corradetti et al., 2011	FW: TCTACACCTGCCAAGTG RW: CCACCATGCCCTTTCTG	178
ILs			
TNF α	Jischa et al., 2008	FW: GCTCCAGACGGTGCTTGTG RW: GCCGATCACCCCAAAGTG	95
IL-8	Jischa et al., 2008	FW: CGGTGCCAGTGCATCAAG RW: TGGCCCACTCTCAATCACTCT	81
INF- γ	Castagnetti et al., 2012	FW: GTGTGCGATTTTGGGTTCTTCTA RW: TTGAATGACCTGGTTATCT	235
IL4	Castagnetti et al., 2012	FW: CAACTTCATCCAGGGATGCAA RW: CAGTCAGCTCCATGCACGAAT	107
IL- β 1	Castagnetti et al., 2012	FW: GAGGCAGCCATGGCAGCAGTA RW: TGTGAGCAGGGAACGGGTATCTT	257
IL-6	Visser and Pollitt, 2011	FW: AAACCACCTCAAATGGACCACTA RW: TTTTTCAGGGCAGAGATTTTGC	91
Pluripotency markers			
OCT4	Desmarais et al., 2011	FW: TCCCAGGACATCAAAGCTCTGCAGA RW: TCAGTTTGAATGCATGGGAGAAGCCAGA	679
NANOG	Desmarais et al., 2011	FW: GACAGCCCCGATTCATCCACCAG RW: GCACCAGGTCTGACTGTTCCAGG	492
SOX2	Desmarais et al., 2011	FW: GGCGGCAACCAGAAGAACAG RW: AGAAGAGGTAACCACGGGGG	663
Housekeeping			
GAPDH	Desmarais et al., 2011	FW: GTCCATGCCATCACTGCCAC RW: CCTGCTTACCACCTTCTTG	262

Table 3.3. Sequence of primers used for PCR analysis.

Transmission Electron Microscopy (TEM)

Ultrastructural examination was performed on AM and WJ-MSCs at P3. After detaching cells, obtained pellet was fixed with 2.5% glutaraldehyde in 0.1 M PB, pH 7.3, for 1 h, at RT. Cells were then washed twice in PB and post-fixed with buffered 2% osmium tetroxide for 1 h, at RT. They were finally dehydrated in a graded ethanol-propylene oxide series, pre-infiltrated and embedded in Epon 812. Ultrathin sections (90 nm) were mounted on 200-mesh copper grids, stained with uranyl acetate and lead citrate, and examined by a Philips EM 208 microscope (Center for Electron Microscopy, CUME, University of Perugia).

Statistical Analysis

Harvested WJ and AM (grams), CDs, DTs and percentages of migration are expressed as mean \pm standard deviation (SD). Statistical analyses were performed using IBM SPSS Statistics 21 (IBM Corporation). Data were analysed, for normal distribution, using a Shapiro-Wilk test, then using one-way ANOVA or a Student's t-test (CDs and DTs). The 3D spheroid volumes and mean gray intensity of differentiated cells were compared using Mann-Whitney's U-test, due to their non-normal distribution. Significance was assessed for $P < 0.05$.

Results

Cellular Growth

As soon as after foals' birth and immediately after foal detachment, UC (length ~15 cm) and AM samples were recovered. The mean weight of recovered jelly and AM were 5.22 ± 3.34 g and 15.60 ± 5.23 g, respectively. Adherent mononuclear cells, characterized by a homogeneous elongated fibroblast-like morphology were isolated from 13/13 (100%) WJ samples (*Figure 3.1 A*) and from 9/13 AM samples (69.2%) (*Figure 3.1 B*). Undifferentiated cells of both lines were passaged up to seven times; no changes in cell morphology was

observed throughout the culture period. DTs assay showed that AM and WJ-MSCs were able to divide for an extensive period in vitro. During P0 to P7, AM-MSCs showed a mean DT of 1.49 ± 0.34 days/CD, significantly lower than that recorded for WJ-MSCs (1.71 ± 0.65 days/CD; $P<0.05$). No statistically significant differences were found in DTs among earlier culture passages in both cell lines ($P>0.05$). However, AM-MSCs start to grow old by P6, while WJ-MSCs, despite an higher DT, get older later, starting from P7. In fact, at these passages, cells grew more slowly, as shown by significantly higher DTs compared to the earliest steps ($P<0.05$). By P7, total WJ and AM-MSCs cell doublings were similar (36.57 ± 0.76 vs 37.05 ± 0.59 ; $P>0.05$; *Figure 3.2*).

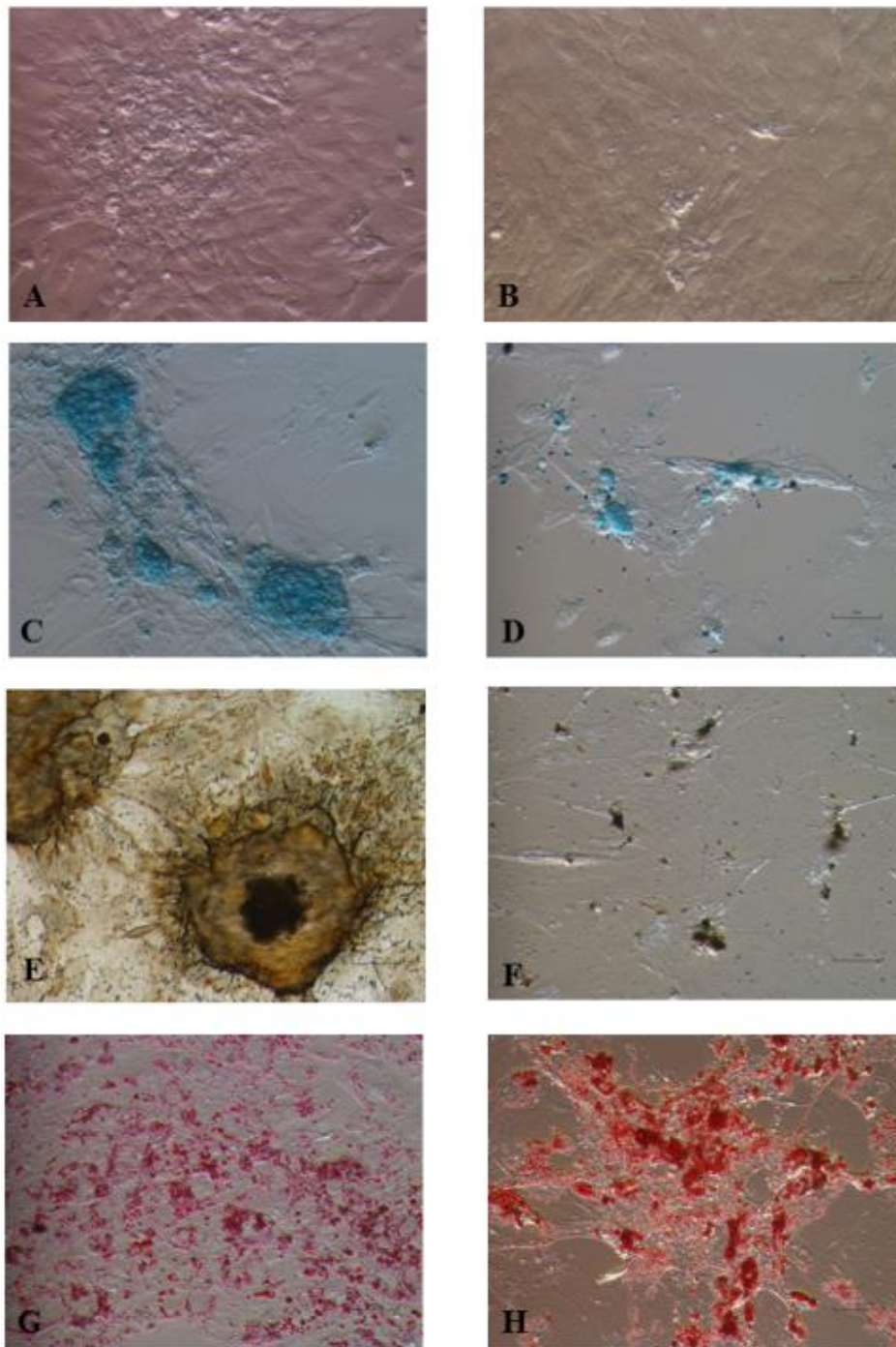


Figure 3.1. *A-B:* Monolayer of rapidly expanding adherent spindle-shaped fibroblastoid cells, isolated from WJ (**A**) and AM (**B**), compatible with undifferentiated mesenchymal stem cell. **C-H:** *In vitro* differentiation studies. **C-D:** Chondrogenic induction in WJ (**C**) and AM-MSCs (**D**) over three weeks: Alcian Blue staining of glycosaminoglycans in cartilage matrix. **E-F:** Osteogenic induction in WJ (**E**) and AM-MSCs (**F**) over three weeks: von Kossa staining of extensive extracellular calcium deposition. **G-H:** Adipogenic induction in WJ (**G**) and AM-MSCs (**H**) over one week: Oil red O staining of extensive intracellular lipid droplet accumulation.

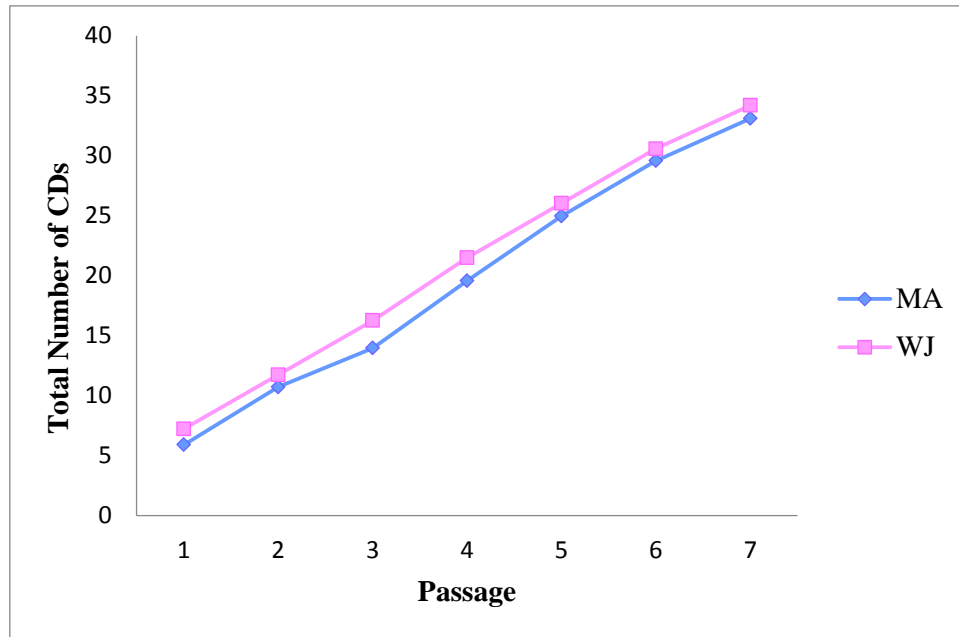


Figure 3.2. Number of cultured primary and passaged mesenchymal stem cells. All values reflect the mean \pm standard deviation.

Adhesion and Migration Assays

Both AM and WJ cells formed spheroids when cultured in hanging drops (*Figure 3.3 A*; *Figure 3.3 B*). Average areas and volume of the spheroids formed by WJ-MSCs were significantly smaller than from AM-MSCs ($P < 0.05$; *Figure 3.3*). Average percentage of migration, observed by scratch test, was statistically similar between cell lines (AM-MSCs vs WJ-MSCs: $34.14 \pm 4.51\%$ vs $38.20 \pm 2.88\%$; $P > 0.05$).

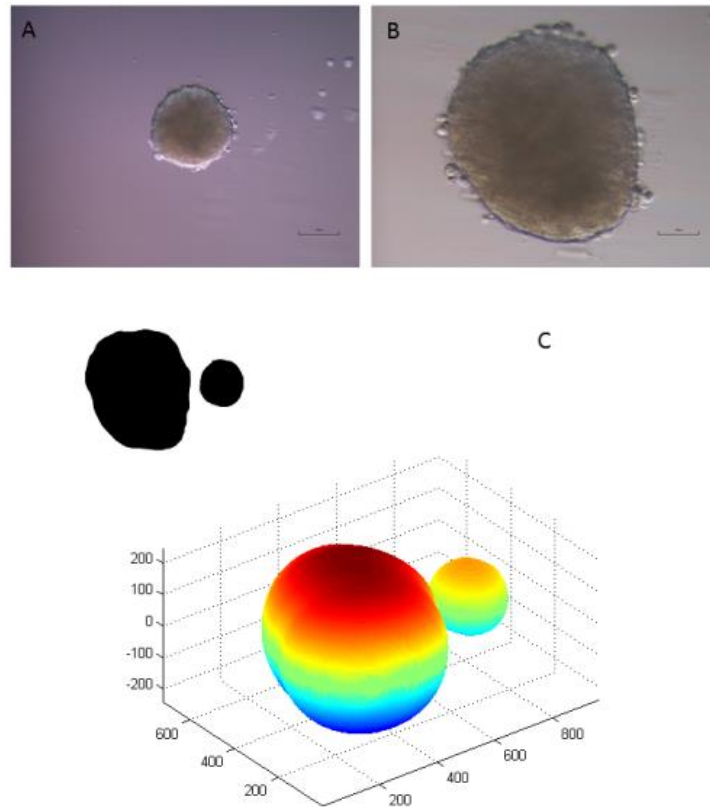


Figure 3.3. *A-B: Spheroid culture: Attachment of the spheroid 24 h after seeding of WJ-MSCs (A) and AM-MSCs (B). C: 3D Volume reconstruction: Starting from the 2D images acquired by imaging in bright field each spheroid, volume, and 3D mesh were obtained by ReViSP.*

In vitro Differentiation

Both cell lines were able to differentiate toward osteogenic, chondrogenic and adipogenic direction (Figure 3.1 C-H). However, WJ-MSCs showed a greater chondrogenic and osteogenic potential than AM-MSCs ($P < 0.05$), characterized by a greater accumulation of extra-cellular mucosubstances and calcium deposits, as showed by Alcian Blu (Figure 3.1 C-D) and Von Kossa stains respectively (Figure 3.1 E-F).

Phenotypic and Molecular Analysis by Immunocytochemistry and PCR

Data observed by immunocytochemical staining of AM and WJ-MSCs are showed in *Table 6.4*. Both cell lines clearly expressed mesenchymal marker, N-Cadherin (*Figure 6.4 A-B*) and the mesodermal marker alpha-SMA (*Figure 3.4 C-D*). On the contrary, WJ and AM- MSCs did not express pan-cytokeratin and E-Cadherin (*Figure 3.4 E-F*).

Data recorded by PCR were reported in *Table 3.5* and *Figure 3.5*.

Antibody	WJ-MSCs	AM-MSCs
α -SMA	+	+
E-Cadherin	-	-
N-Cadherin	+	+
pan-Cytokeratin	-	-

Table 3.4. Results obtained by ICC running on AM-MSCs and WJ-MSCs.

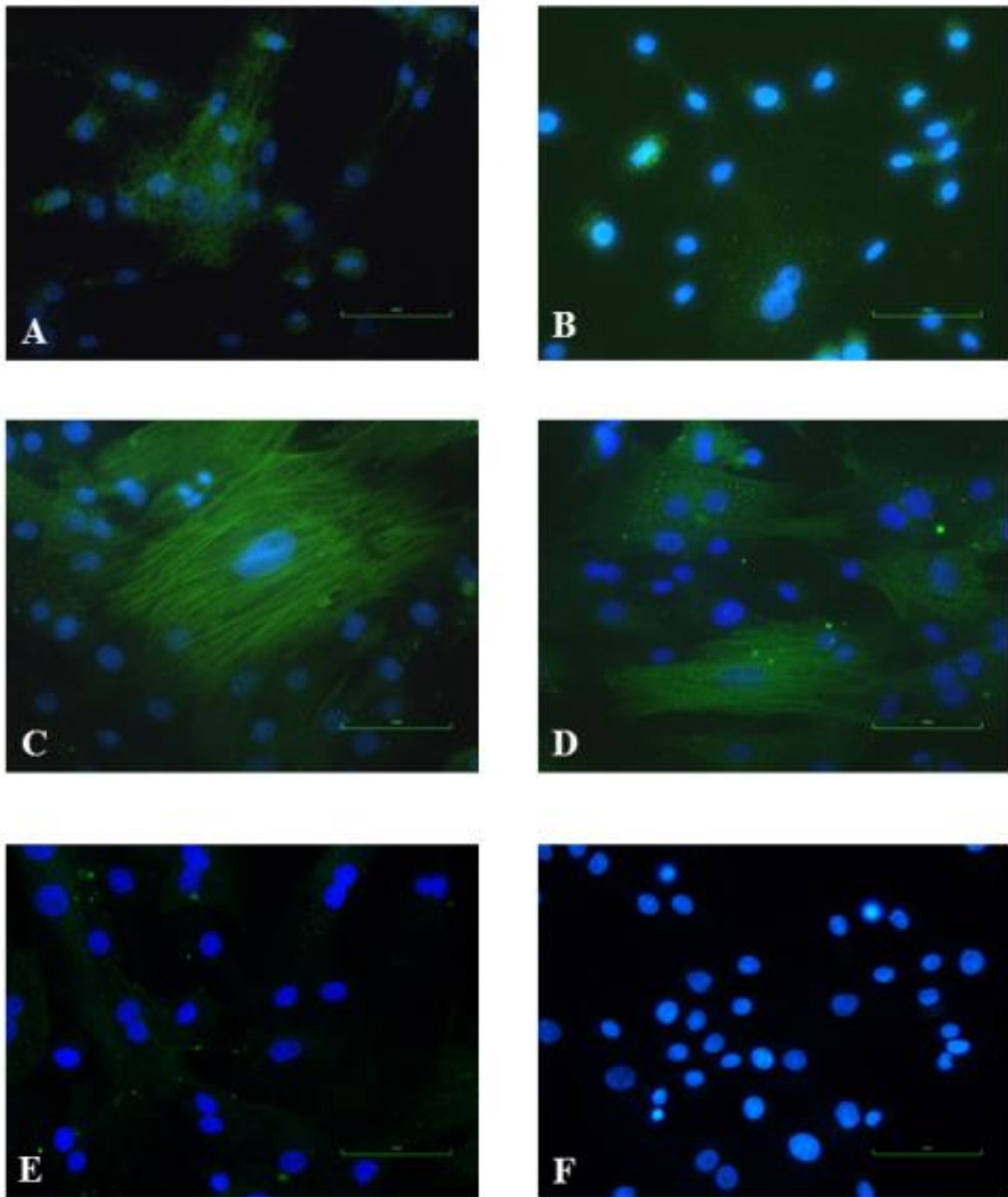


Figure 3.4. Photomicrographs of immunostaining of WJ and AM-MSCs. **A-B:** Expression of the mesenchymal marker N-Cadherin in the WJ (**A**) and AM-MSCs (**B**). **C-D:** Expression of the mesenchymal marker alpha-SMA in the WJ (**C**) and AM-MSCs (**D**). **E-F:** Absence of expression of the epithelial marker Cytokeratin in WJ-MSCs (**E**) and absence of expression of E-Cadherin in AM-MSCs (**F**). All images, represent the merge of Hoechst and antibody staining.

Primers	WJ-MSCs	AM-MSCs
MSC marker		
CD90	+	+
CD73	+	+
Ematopoietic markers		
CD34	+	+
CD45	-	-
MHC markers		
MHC-I	+	+
MHC-II	-	-
ILs		
TNF α	-	-
IL-8	+	+
INF- γ	-	-
IL4	-	-
IL- β 1	+	+
IL-6	+	+
Pluripotency markers		
OCT4	+	+
NANOG	-	-
SOX2	-	-

Table 3.5. Results obtained by PCR running on AM-MSCs and WJ-MSCs.

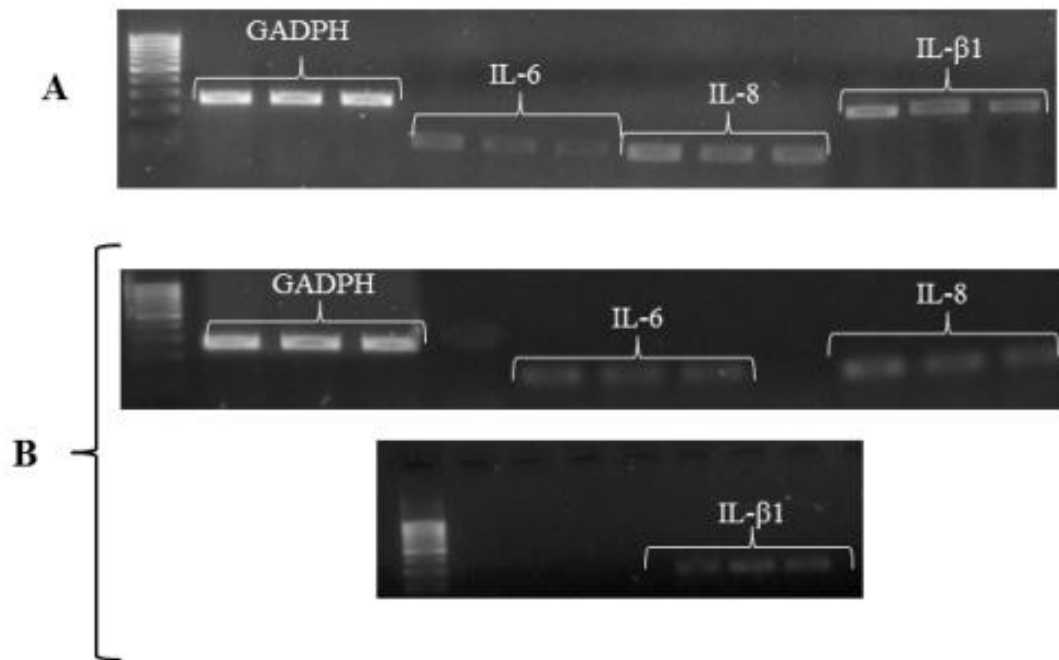


Figure 3.5. Reverse transcription-polymerase chain reaction analysis of immunomodulatory ($TNF-\alpha$, $IL-1\beta$, $IL-8$, $IL-6$, $IL-4$, $INF-\gamma$) specific gene expression on WJ-MSCs (A) and AMMSCs (B) at P3. GAPDH was used as the reference gene.

TEM

TEM images are reported as *Figure 3.6*, *3.7*, *3.8*, *3.9* and *3.10*. At low magnification, cells of both samples were quite small and uniform in size (diameter ranging from 10 to 15 μ m; *Figure 3.6 A*; *Figure 3.8 B*). AM-MSCs appeared generally well dissociated, while WJ-MSCs were frequently tightly adherent each other to form wide aggregates (*Figure 3.8 A*). Golgi complex was particularly well developed; it occupied a juxta-nuclear position and exhibited flattened cisternae, transport vesicles, and heterogeneous sized secreting granules. Some of them were very large and enclosed fine granular material (*Figure 3.6 C-D*; *Figure 3.8 C*). In both samples, the most relevant ultrastructural feature was represented by the very impressive number of large vacuolar bodies, up to 2 μ m in diameter, scattered throughout the cytoplasm. They showed a variety of appearances and ranged from multivesicular bodies (MVB) comprising intraluminal nanovesicles of different sizes (30-500 nm), to endolysosomes and

autophagic bodies. These vacuoles were present in both cell types, but were particularly abundant in WJ-MSCs (*Figure 3.7 A-C; Figure 3.8 A-B; Figure 3.9 A-C*). The occurrence of membrane vesicles shedding from cell surface was observed in both samples. They ranged in size from about 100 nm to 500 nm and included electron-lucent, as well as moderately electron-dense vesicles isolated or aggregated nearby the cells (*Figure 3.7 D; Figure 3.9 D*). Complex macro-vesicles measuring 500 nm to 1 μ m and containing packed nanovesicles, frequently budded from the cell surface or were detected in the intercellular space (*Figure 3.7 E; Figure 3.9 E*). Tunneling nanotubes were occasionally observed in both samples suggesting that this may be an additional mechanism of crosstalk between MSCs (*Figure 3.7 F; Figure 3.9 F*). The most noteworthy difference between AM-MSCs and WJ-MSCs was the presence of an abundant extracellular fibrillar matrix (EFM) located in the intercellular spaces among WJ-MSCs (*Figure 3.10 A-B*). It was composed of a finely granular and moderately electron-dense ground substance populated by a loosely arranged network of reticular fibrils. These were uniformly thin and tend to run parallel to the cell surface. Abundant vesicles were entrapped among the fibrils (*Figure 3.10 C*). The intercellular spaces were devoid of collagen fibrils. EFM was present in very poor quantities in AM-MSCs (*Figure 3.7 D*).

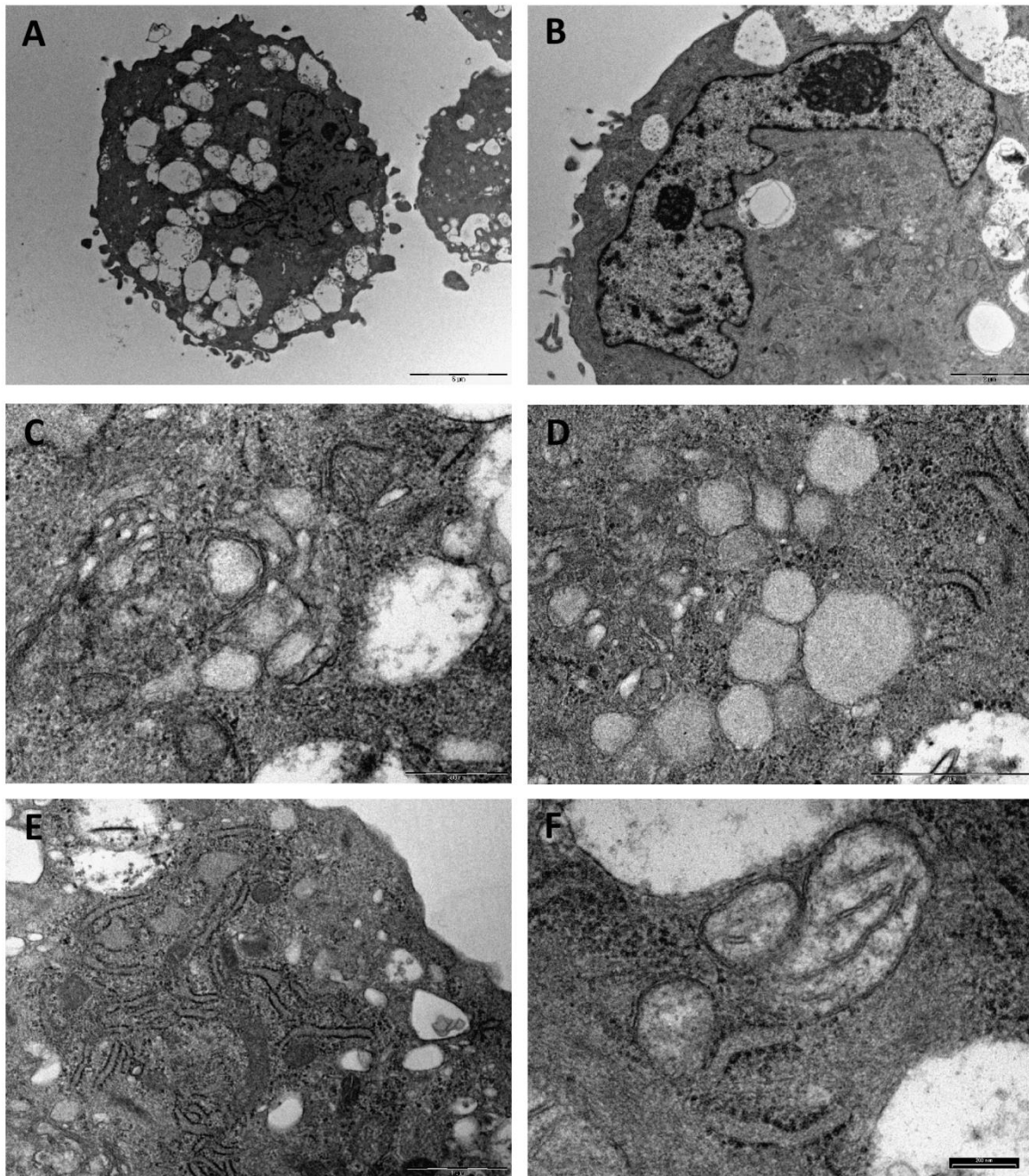


Figure 3.6. AM-MSCs ultrastructural features. **A:** The micrograph depicts a single AM-MSC showing a roundish shape and a unique euchromatic irregularly-profiled nucleus. Scale bar, 5 μ m. **B:** A particular of the nucleus containing two prominent nucleoli. Scale bar, 2 μ m. **C-D:** Well developed Golgi complex and a group of large secreting granules. Scale bar, 500 nm and 1 μ m. **E:** RER showing linear flat profiles and dilated cisternae. Scale bar, 1 μ m. **F:** A small group of typical mitochondria.

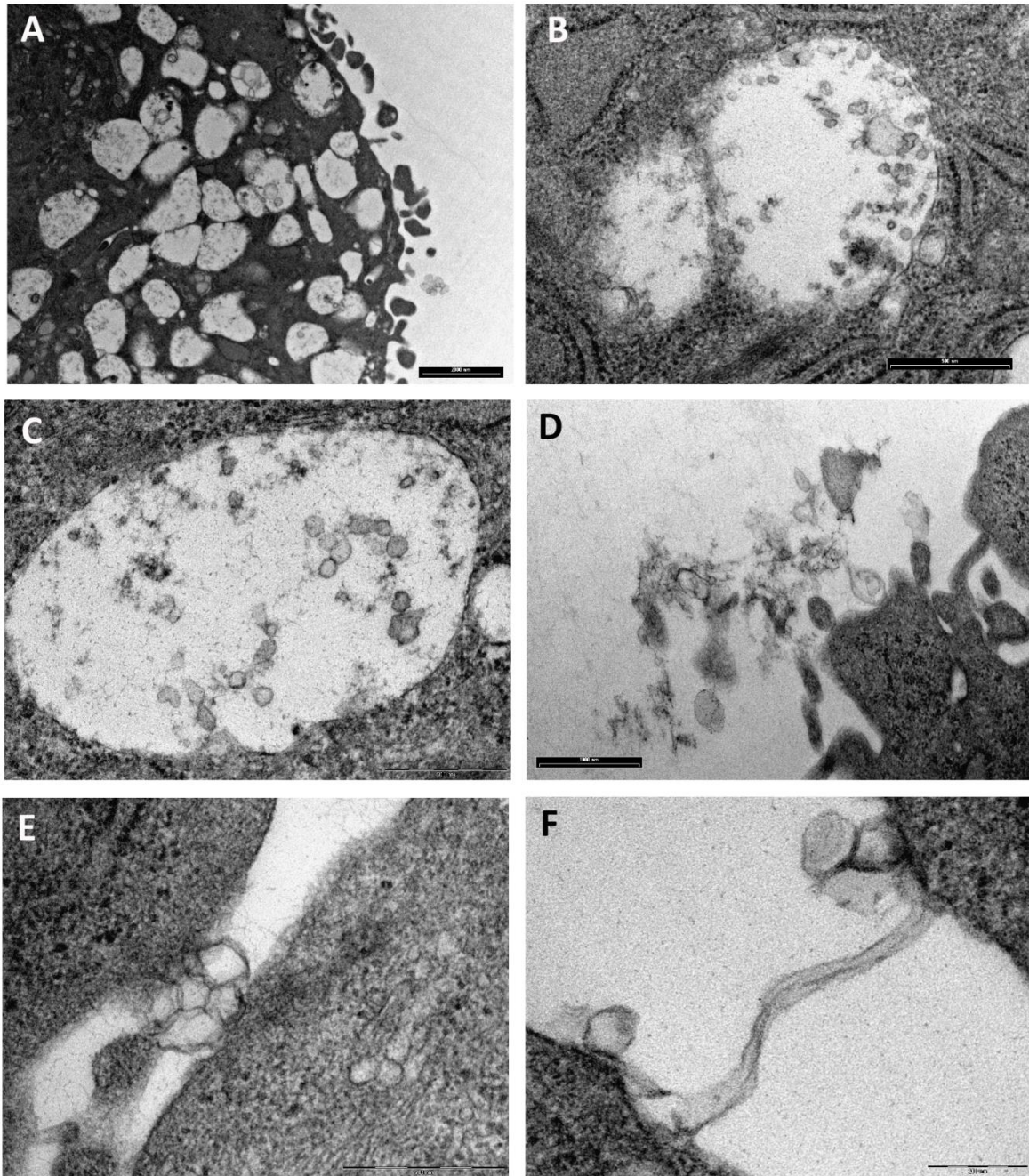


Figure 3.7. AM-MSCs ultrastructural features. **A:** Cell cytoplasm containing an enormous number of vacuolar elements, up to 2 μm in diameter. **B-C:** Maturing MVB containing endo-luminal vesicles. Scale bar, 500 nm. **D:** Membrane vesicles of heterogeneous sizes located in the peri-cellular space. Scale bar, 1 μm . **E:** A large vesicle (macro-vesicle) containing round-shaped smaller vesicles is placed in the intercellular space. Scale bar, 500 nm. **F:** A tunneling nanotube connecting two adjacent cells. Scale bar, 200 nm.

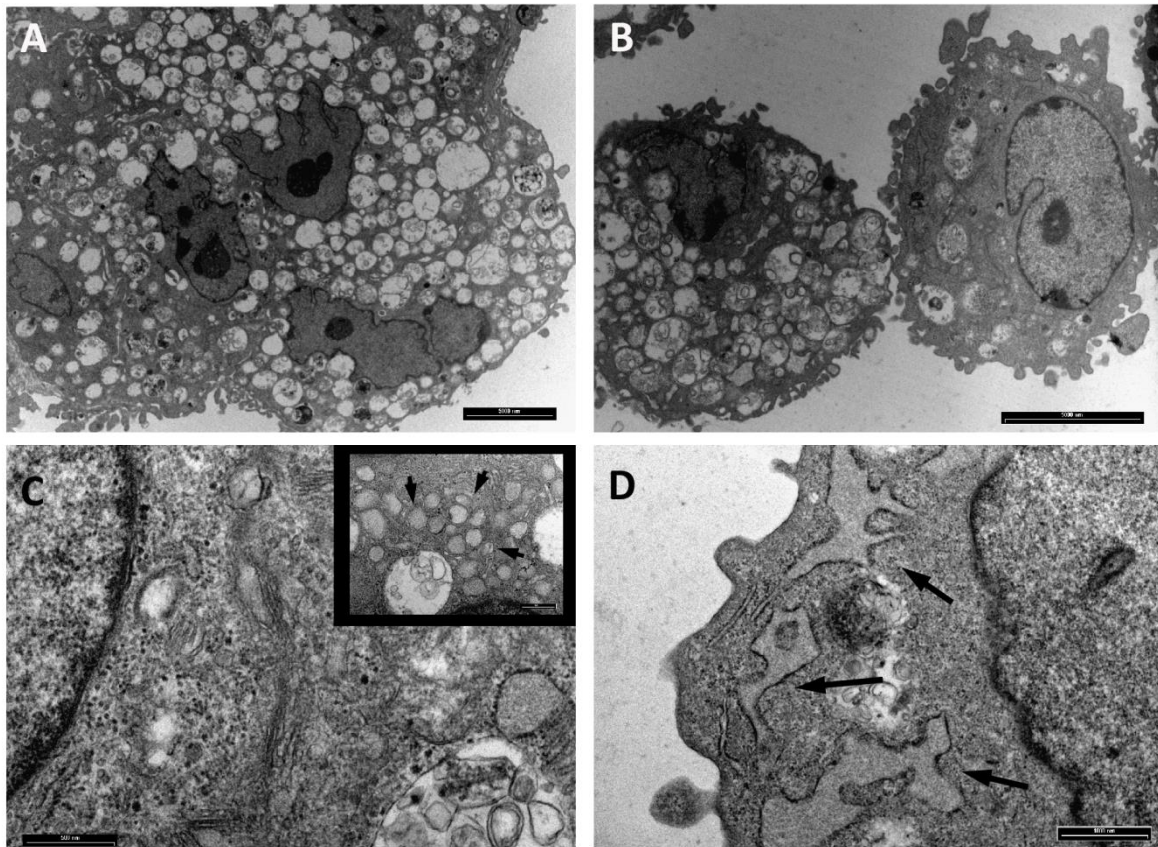


Figure 3.8. WJ-MSCs ultrastructural features. **A:** Low magnification image showing a group of reciprocally adherent WJ-MSCs with a single large euchromatic nucleus and a cytoplasm rich in vacuolar bodies. Scale bar, 5 μm . **B:** Electron micrograph of two WJ-MSCs showing a roundish shape and a unique euchromatic nucleus. The cell on the left is particularly rich of vacuolar bodies that are tightly packed inside its cytoplasm. Scale bar, 5 μm . **C:** Golgi apparatus in the juxta-nuclear area producing large secreting granules. Scale bar, 500 nm. **D:** Dilated cisternae of the RER. Scale bar, 1 μm .

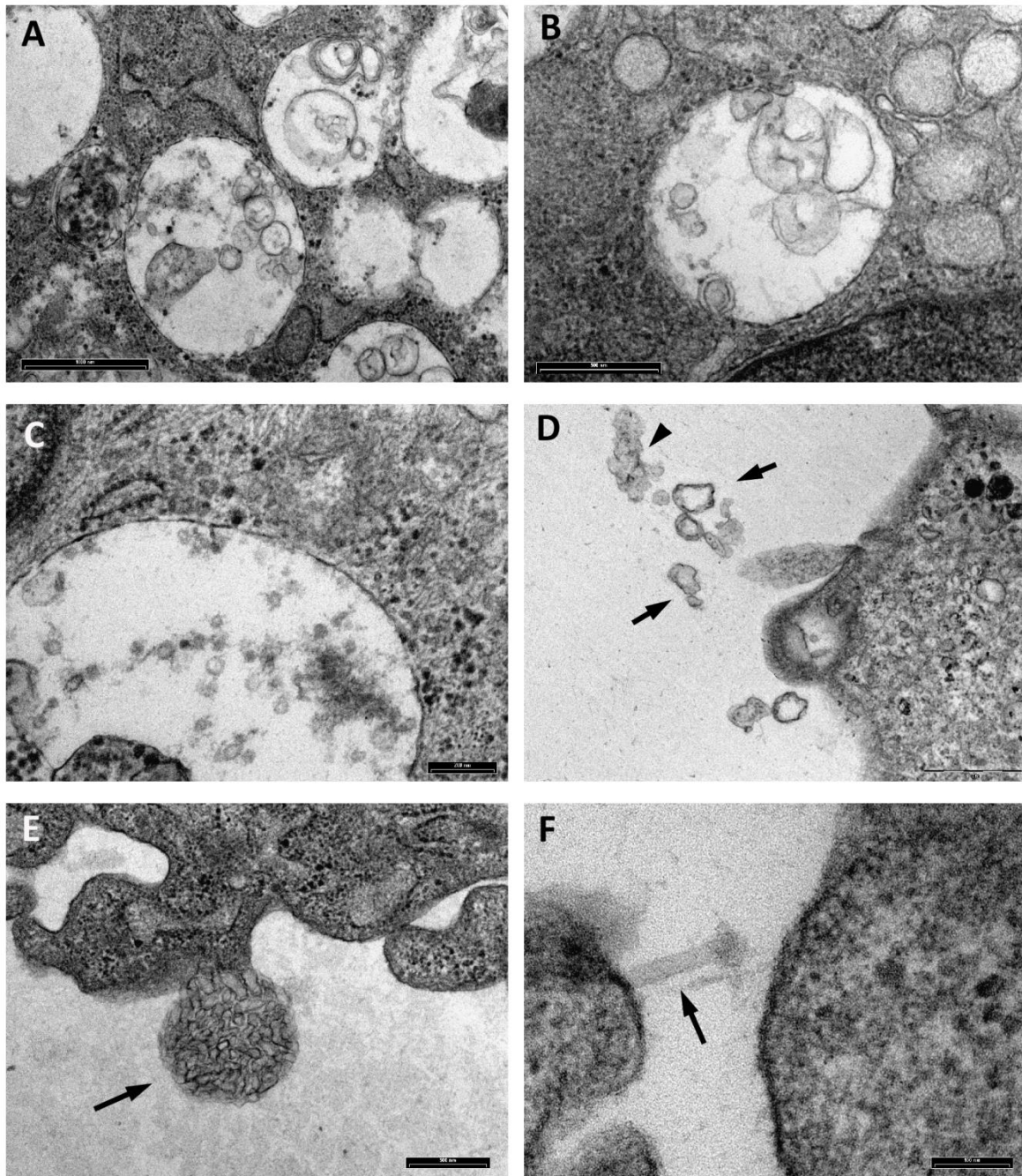


Figure 3.9. WJ-MSCs ultrastructural features. **A:** A particular of the cytoplasm containing a huge number of vacuolar structures, up to 2 μm in diameter. **B:** Vacuolar bodies characterized by endoluminal vesicles, very heterogeneous in size and morphology. Scale bar, 500 nm. **C:** A maturing MVB. Scale bar, 200 nm. **D:** Isolated (arrows) and aggregated (arrow head) extracellular vesicles located nearby the cell membrane. Scale bar, 500 nm. **E:** A large complex macro-vesicle budding from the cell surface. Scale bar, 500 nm. **F:** The image depicts a tunneling nanotube emerging from a cell. Scale bar, 100 nm.

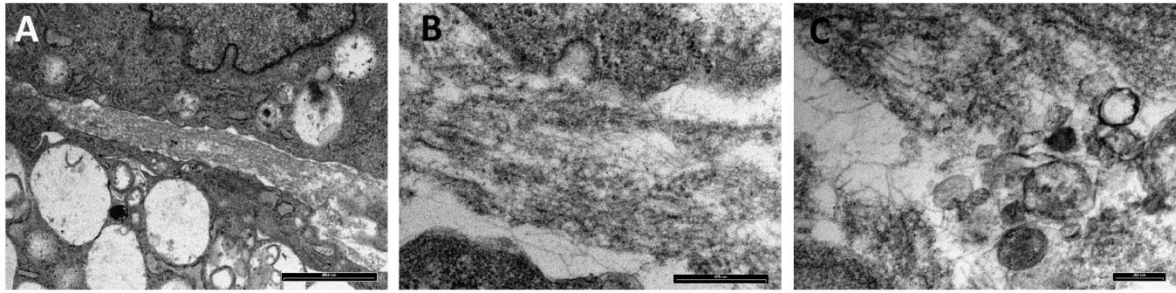


Figure 3.10. Extracellular fibrillar matrix (EFM) in WJ-MSCs. **A:** EFM fills the space between two cells. Scale bar, 2 μm . **B:** Note the finely granular appearance of the ground substance and the fibril network. Scale bar, 500 nm. **C:** Extracellular vesicles entrapped among the fibrils of EFM. Scale bar, 200 nm.

Discussion

In this study, for the first time in equine species, we compared proliferation, migration, spheroids formation, trilineage differentiation capacity, expression of stemness markers, immunophenotype and ultrastructural features of MSCs derived from WJ and AM. From both tissues, cells with mesenchymal morphology were isolated. However, in the present study, MSCs were isolated from all samples by collagenase digestion technique only for WJ. No other reports exist on the successful isolation rate from equine WJ and AM.

Despite the lower isolation rate, AM-MSCs showed a higher proliferation rate compared to WJ-MSCs. However, in both cell types, as in humans (Pasquinelli et al., 2007), TEM examination revealed an highly metabolic and synthetic nature, demonstrated by euchromatic nucleus, prominent nucleoli, abundant nuclear pores as well as by well developed RER and Golgi complex. Furthermore, the higher DTs did not correlate with total cell doubling number, because AM-MSCs began to grow old earlier, as registered by a higher DT at P6 of in vitro culture. These findings support previous observations by Vidal et al. (2012), which observed population doubling and senescence of different lines of equine MSCs, including umbilical cord matrix MSCs.

Beyond the growth curve, migration ability is an important feature of MSCs because of its fundamental significance for systemic application (Li et al., 2009; Burk et al., 2013). No differences were found between WJ-MSCs and AM-MSCs in migration ability.

Since the adhesion capability is related and enhanced to differentiation potential (Wang et al., 2009; Kavanagh et al., 2014; Sart et al., 2014), in the present study spheroid formation in vitro was assessed using the hanging drop method. Cell derived from WJ showed a higher adhesion ability, forming smaller spheroids, as determined by ReVisp. As recently observed for human WJ and AM-MSCs (Subramanian et al., 2015), also in horses the ability to form spheroids in vitro is related to an higher differentiation potential. In fact, in this study, the

analysis of differentiated cells by Image J, showed a higher WJ-MSCs chondrogenic and osteogenic potential.

The foetal adnexa derived MSCs demonstrate the characteristics defined by the International Society for Cellular Therapy criteria (Dominici et al., 2006), except for the CD34; these results confirmed that the lack of CD34 marker cannot be considered an essential requirement of a stem cell. Indeed its expression seems to depend on environment and in vitro culture passages (Lin et al., 2012). Furthermore, in the present study, anti-inflammatory and pro-inflammatory factors produced by foetal adnexa MSCs were investigated for the first time in the horse. As expected, at RT-PCR, these cells resulted negative for TNF- α , IL-4 and INF, cytokines produced only after in vitro stimulation (De Schauwer et al., 2014). On the contrary, both cell lines expressed, on their cDNA, IL-1 β , IL-6 and IL-8; this cytokines are important mediators of the inflammatory response, involved in a variety of cellular activities, including cell proliferation, differentiation, apoptosis, chemotaxis, angiogenesis and hematopoiesis (Lamalice et al., 2007). Data registered in this study confirmed those already reported in human WJ-MSCs (Fong et al., 2012; Choi et al., 2013) and AM-MSCs (Yazdanpanah et al., 2015). These factors are involved in the complex interaction between MSCs and the tissue microenvironment as well as production of membrane vesicles, containing molecules such as short peptides, proteins, lipids, and various forms of RNAs (György et al., 2011).

As previously observed in adult equine cells (Pascucci et al., 2014), the great number of vacuolar bodies that, actually, were not empty but contained small, medium and large intraluminal vesicles maturing from their internal membrane, may be interpreted as the ability of both cell types to produce a huge variety of “secreting” molecules. These are likely enclosed inside vesicles of different types with the aim to segregate and organize, in space

and time, the release of cell products in the extracellular milieu. Maybe we hypothesized, in addition, that the described structures represent a mechanism efficiently recycling cell constituents. The intense proliferating and metabolic activity, in fact, makes it necessary constantly renewing sub-cellular components, especially membrane fractions. The main difference between AM-MSCs and WJ-MSCs attained the presence of an abundant extracellular fibrillar matrix in the intercellular spaces among WJ-MSCs; it probably determines a tight intercellular adhesion even after trypsin treatment and is responsible of the observation of cell aggregates at TEM analysis. It is well known that these cells, in vivo, are immersed in a mucoid connective matrix. It seems evident that WJ-MSCs isolation and cultivation in vitro does not affect their ability to produce extracellular matrix.

It has emerged from the present study that cells isolated from different foetal origin matrices exhibit different morphological, molecular and differentiation potential. Equine WJ could be considered as a viable source for MSCs with reliable migration and differentiation capacities, and it is therefore a convenient cell source for autologous or allogeneic regenerative therapies. Although the molecular content and functional activities of MVs produced by WJ and AM-MSCs remain to be characterized, the results of the present study indicated that MSCs from equine foetal adnexa could be able to influence endogenous cells through paracrine action and constitutively produce MVs that may be partly responsible for their paracrine activity. However, further investigation is needed to find the best protocols for isolation and in vitro differentiation for AM-MSCs. Moreover, further in vivo studies will be required to substantiate our in vitro findings.

References

- Bellotti C., Duchi S., Bevilacqua A., Lucarelli E., Piccinini F., (2016). *Long term morphological characterization of mesenchymal stromal cells 3D spheroids built with a rapid method based on entry-level equipment*. Cytotechnology; 68(6): 2479-2490.
- Burk J., Ribitsch I., Gittel C., Juelke H., Kasper C., Staszyc C., Brehm W., (2013). *Growth and differentiation characteristics of equine mesenchymal stromal cells derived from different sources*. Vet J; 195(1): 98–106.
- Castagnetti C., Mariella J., Pirrone A., Cinotti S., Mari G., Peli A., (2012). *Expression of interleukin-1 β , interleukin-8, and interferon- γ in blood samples obtained from healthy and sick neonatal foals*. Am J Vet Res; 73(9): 1418–1427.
- Choi M., Lee H., Naidansaren P., Kim H., Cha J., Ahn H., Yang P., Shin J., Joe Y., (2013). *Proangiogenic features of Wharton's jelly-derived mesenchymal stromal/stem cells and their ability to form functional vessels*. Int J Biochem Cell Biol; 45(3); 560–570.
- Corradetti B., Lange-Consiglio A., Barucca M., Cremonesi F., Bizzarro D., (2011). *Size-sieved subpopulations of mesenchymal stem cells from intervacular and perivascular equine umbilical cord matrix*. Cell Prolif; 44(4): 330–342.
- De Schauwer C., Goossens K., Piepers S., Hoogewijs M., Govaere J., Smits K., Meyer E., Van Soom A., Van de Walle G., (2014). *Characterization and profiling of immunomodulatory genes of equine mesenchymal stromal cells from non-invasive sources*. Stem Cells Res Ther; 5(1); 6.
- Desmarais J., Demers S., Suzuki J.J., Laflamme S., Vincent P., Laverty S., Smith L., (2011). *Trophoblast stem cell marker gene expression in inner cell mass-derived cells from parthenogenetic equine embryos*. Reprod Camb Engl; 141(3), 321–332.

Dominici M., Le Blanc K., Mueller I., Slaper-Cortenbach I., Marini F., Krause D., Deans R., Keating A., Prockop D., Horwitz E., (2006). *Minimal criteria for defining multipotent mesenchymal stromal cells. The International Society for Cellular Therapy position statement.* *Cytotherapy*; 8(4): 315–317.

Fong C., Gauthaman K., Cheyyatraivendran S., Lin H., Biswas A., Bongso A., (2012). *Human umbilical cord Wharton's jelly stem cells and its conditioned medium support hematopoietic stem cell expansion ex vivo.* *J Cell Biochem*; 113(2), 658–668.

György B., Szabò T., Pásztoi M., Pál Z., Miják P., Aradi B., László V., Pállinger E., Pap E., Kittel A., Nagy G., Falus A., Buzás E., (2011). *Membrane vesicles, current state-of-the-art: emerging role of extracellular vesicles.* *Cell Mol Life Sci*; 68(16): 2667–2688.

Iacono E., Brunori L., Pirrone A., Pagliaro P.P., Ricci F., Tazzari P.L., Merlo B., (2012). *Isolation, characterization and differentiation of mesenchymal stem cells from amniotic fluid, umbilical cord blood and Wharton's jelly in the horse.* *Reprod Camb Engl*; 143(4), 455–468.

Jischa S., Walter I., Nowotny N., Palm F., Budik S., Kolodziejek J., Aurich C., (2008). *Uterine involution and endometrial function in postpartum pony mares.* *Am J Vet Res*; 69(11): 1525–1534.

Kavanagh D., Robinson J., Kalia N., (2014). *Mesenchymal stem cell priming: fine-tuning adhesion and function.* *Stem Cell Rev*; 10(4): 587–599.

Lamallice L., Le Boeuf F., Huot J., (2007). *Endothelial cell migration during angiogenesis.* *Circ Res*; 100(6): 782–794.

Lange-Consiglio A., Perrini C., Tasquier R., Deregibus M., Camussi G., Pascucci L., Marini M., Corradetti B., Bizzarro D., De Vita B., Romele P., Parolini O., Cremonesi F., (2016).

Equine amniotic microvesicles and their anti-inflammatory potential in a tenocyte model in vitro. Stem Cells Dev; 25(8): 610–621.

Li G., Zhang X., Wang H., Wang X., Meng C., Chan C., Yew D., Tsang K., Li K., Tsai S., Ngai S., Han Z., Lin M., He M., Kung H., (2009). *Comparative proteomic analysis of mesenchymal stem cells derived from human bone marrow, umbilical cord and placenta: implication in the migration.* Proteomics 9(1), 20–30.

Liang C.C., Park A.Y., Guan J.L., (2007). *In vitro scratch assay: a convenient and inexpensive method for analysis of cell migration in vitro.* Nat Protoc; 2(2): 329–333.

Liang X., Ding Y., Zhang Y., Tse H., Lian Q., (2014). *Paracrine mechanisms of mesenchymal stem cell-based therapy: current status and perspectives.* Cell Transplant; 23(9); 1045–1059.

Lin C., Ning H., Lin G., Lue T., (2012). *Is CD34 truly a negative marker for mesenchymal stromal cells?* Cytotherapy; 14(10): 1159–1163.

Mizuno H., Hyakusoku H., (2003). *Mesengenic potential and future clinical perspective of human processed lipoaspirate cells.* J Nippon Med Sch; 70(4), 300–306.

Mohanty N., Gulati B., Kumar R., Gera S., Kumar P., Somasundaram R., Kumar S., (2014). *Immunophenotypic characterization and tenogenic differentiation of mesenchymal stromal cells isolated from equine umbilical cord blood.* Vitro Cell Dev Biol–Anim; 50(6): 538–548.

Pascucci L., Alessandri G., Dall’Aglia C., Mercati F., Cloliolo P., Bazzucchi C., Dante S., Petrini S., Curina G., Ceccarelli P., (2014). *Membrane vesicles mediate pro-angiogenic activity of equine adipose-derived mesenchymal stromal cells.* Vet J; 202(2): 361–366.

Pasquinelli G., Tazzari P.L., Ricci F., Vaselli C., Buzzi M., Conte R., Orrico C., Foroni L., Stella A., Alviano F., Bagnara G., Lucarelli E., (2007). *Ultrastructural characteristics of human mesenchymal stromal (stem) cells derived from bone marrow and term placenta.* Ultrastruct Pathol; 31(1): 23–31.

Rainaldi G., Pinto B., Piras A., Vatteroni L., Simi S., Citti L., (1991). *Reduction of proliferative heterogeneity of CHEF18 Chinese hamster cell line during the progression toward tumorigenicity.* Vitro Cell Dev Biol; 27(12): 949–952.

Rossi B., Merlo B., Colleoni S., Iacono E., Tazzari P.L., Ricci F., Lazzari G., Galli C., (2014). *Isolation and in vitro characterization of bovine amniotic fluid derived stem cells at different trimesters of pregnancy.* Stem Cell Rev; 10(5), 712–724.

Sart S., Tsai A., Li Y., Ma T., (2014). *Three-dimensional aggregates of mesenchymal stem cells: cellular mechanisms, biological properties, and applications.* Tissue Eng Part B Rev; 20(5): 365–380.

Subramanian A., Fong C., Biswas A., Bongso A., (2015). *Comparative characterization of cells from the various compartments of the human umbilical cord shows that the Wharton's jelly compartment provides the best source of clinically utilizable Mesenchymal Stem Cells.* Plos One; 10(6): e0127992.

Vidal M., Walker N., Napoli E., Borjesson D., (2012). *Evaluation of senescence in mesenchymal stem cells isolated from equine bone marrow, adipose tissue, and umbilical cord tissue.* Stem Cells Dev; 21(2): 273–283.

Visser M., Pollitt C., (2011). *Lamellar leukocyte infiltration and involvement of IL-6 during oligofructose-induced equine laminitis development.* Vet Immunol Immunopathol; 144(1): 120–128.

Wang W., Itaka K., Ohba S., Nishiyama N., Chung U., Yamasaki Y., Kataoka K., (2009). *3D spheroid culture system on micropatterned substrates for improved differentiation efficiency of multipotent mesenchymal stem cells*. *Biomaterials*; 30(14): 2705–2715.

Yazdanpanah G., Paeini-Vayghan G., Asadi S., Niknejad H., (2015). *The effects of cryopreservation on angiogenesis modulation activity of human amniotic membrane*. *Cryobiology*; 71(3): 413–418.

CHAPTER 4

WHARTON'S JELLY DERIVED MESENCHYMAL STEM CELLS: COMPARING HUMAN AND HORSE

Article under review (Reproduction)

Merlo B.¹, Teti G.², Falconi M.², Ingrà L.², Salvatore V.², Buzzi M.³, Cerqueni G.⁴, Dicarlo M.⁴, **Lanci A.**¹, Castagnetti C.¹, Iacono E.¹

¹Department of Veterinary Medical Sciences, University of Bologna, Ozzano Emilia, Bologna, Italy

²Department for Biomedical and Neuromotor Sciences, University of Bologna, Italy

³Banca dei Tessuti, del Sangue cordonale e Biobanca Policlinico S.Orsola-Malpighi, Bologna, Italy

⁴Department of Clinical and Molecular Sciences, Polytechnic University of Marche, Ancona, Italy

Introduction

Mesenchymal stem cells (MSCs) are defined as a population of multipotent stem cells capable of plastic-adherence when maintained in standard culture conditions, expression of typical mesenchymal surface molecules (CD105, CD73 and CD90) and lacking hematopoietic ones (CD45, CD34, CD14 or CD11b, CD79 α or CD19 and HLA-DR), and able to differentiate into osteoblasts, adipocytes and chondroblasts in vitro (Dominici et al., 2006). Since these properties, MSCs offer a great chance for cell-based therapies and tissue engineering applications.

Placental tissues and foetal fluids represent a source of cells for regenerative medicine. They are readily available and easily procured without invasive procedures. MSCs from foetal fluids and adnexa are defined as an intermediate between embryonic and adult stem cells, due to the preservation of some characteristics typical of the primitive native layers.

Umbilical cord is routinely discarded at parturition and its extracorporeal nature facilitates isolation by eliminating the invasive and discomfort extraction procedures as well as patient risks that attend adult stem cells isolation. Most significantly, the comparatively large volume

of umbilical cord and ease of physical manipulation theoretically increase the number of stem cells that can be extracted, which makes it possible to get substantial number of cells in several passages without need of long term culture and extensive expansion *ex vivo*. Both in human and animals, multipotent stem cells are isolated from the mesenchyme-like cushioning material called Wharton's jelly (WJ) found between the vessels of the umbilical cord (Vangsness et al., 2015; Iacono et al., 2015). WJ cells represent a unique, easily accessible, and non-controversial source of early stem cells that can be readily manipulated. MSCs derived from Wharton's jelly (WJ-MSCs) are easier to isolate and expand than MSCs from other foetal and adult tissues, and impact fields such as regenerative medicine, biotechnology and agriculture (Troyer and Weiss, 2008).

The development of large animal experimental models, including horse, may open alternative strategies for investigating placental MSCs physiology and potential application for human and veterinary regenerative medicine. The objective of this study was to compare human and equine WJ-MSCs obtained following the same protocols in order to define similarities and differences, at ultrastructural level also, that can be useful in understanding specie-specific characteristics and in defining new animal models.

Materials and Methods

Chemicals were obtained from Sigma Aldrich (St. Louis, MO, USA) and laboratory plasticware was from Sarstedt Inc. (Newton, NC, USA) and Corning (Corning, NY, USA), unless otherwise stated.

Human and equine cells isolation and expansion

hWJ-MSCs and eWJ-MSCs were obtained from tissue of umbilical cords of respectively 7 and 10 full-term pregnancies. Informed consent was obtained from each patient according to

the guidelines of the National Bioethics Committee and the samples were treated following a protocol approved by the University of Bologna.

Wharton's jelly was cut in small fragments and digested with collagenase (Gibco, Thermo Fisher, Monza, Italy) 0.1% (w/v) in phosphate buffer saline (PBS) at 37°C approximately for 3 hours. Then, samples were washed in PBS with 10% (v/v) foetal bovine serum (FBS) (Gibco, Thermo Fisher, Monza, Italy) several times, centrifuged at 400 g for 50 minutes and finally re-suspended in DMEM/F12 Glutamax[®] medium (Gibco, Thermo Fisher, Monza, Italy) supplemented with 10% FBS (v/v), 1% (v/v) penicillin and streptomycin (Gibco, Thermo Fisher, Monza, Italy). Primary cells were plated in a 25 cm² flask, as "Passage 0" (P0), at a density of 5x10³ cell/cm² and incubated in 5% (v/v) CO₂ humidified atmosphere at 37°C (human) or 38.5°C (equine). The medium was completely replaced every 3 days until the adherent cell population reached about 80% confluence. At this point, the adherent primary MSCs were passaged by digestion with 0.25% trypsin-EDTA, counted with a haemocytometer, and reseeded as P1 at 5x10³ cells/cm². For the subsequent passages (P1-P6), cells were inoculated in 25 cm² flasks at 5x10³ cells/cm² and allowed to multiply to 90% confluence before trypsinization and successive passage. Cell-doubling time (DT) and cell-doubling numbers (CD) and cell culture time (CT) were calculated from haemocytometer counts for each passage according to the following two formulae (Rainaldi et al., 1991):

$$CD = \ln(N_f/N_i) / \ln(2)$$

$$DT = CT / CD$$

where N_f and N_i are the final and initial number of cells, respectively.

Cells at P3 were used for the subsequent determination and characterization.

Scratch assay

Cells (4.8×10^4) were seeded on 35 mm petri dishes and cultured until confluence in the same conditions as previously described. Scratches were made using 1 mL pipette tips, washed with medium and allowed to grow for additional 24 h. Immediately after the scratch and at the end of the culture, cells were observed under an inverted light microscope (Motic AE21, VWR International Srl, Milan, Italy; Eclipse TE 2000u, Nikon Instruments Spa, Florence, Italy) and photographed by CCD camera (Visicam 3.0, VWR International Srl, Milan, Italy; DS-Fi2, Nikon Instruments Spa, Florence, Italy). Gap distance of the wound was measured using Image J software (Version 1.48s; National Institutes of Health, USA). The migration percentages were calculated using the following formula:

$$[(\text{distance at time 0} - \text{distance at 24 h}) * 100] / \text{distance at time 0}$$

Adhesion test (hanging drop culture)

25 μ l drops of cell medium, containing approximately 5×10^3 cells each, were pipetted on the inner side of the lid of a 90 mm petri dish, which was gently inverted and allowed to grow for 48 h in the same cell culture conditions as previously described. Then, cells were observed under an inverted light microscope (Motic AE21, VWR International Srl, Milan, Italy; Eclipse TE 2000u, Nikon Instruments Spa, Florence, Italy) and photographed by CCD camera (Visicam 3.0, VWR International Srl, Milan, Italy; DS-Fi2, Nikon Instruments Spa, Florence, Italy). Area and volume of cell masses obtained were obtained by using Image J software and ReVisp software (Piccinini et al., 2015).

Immunophenotyping by flow cytometry

The cells obtained were checked for their staminal profile by FACSCalibur flow cytometry system (Becton Dickinson, CA, USA). 2.5×10^5 cells were removed with Dulbecco PBS and were then stained for 45 min with the following antibodies: fluorescein isothiocyanate-(FITC)-labeled mouse anti-human CD90 (StemCell Technologies, Milan, Italy), CD105, CD14, CD19, (Diacclone, France), R-phycoerythrin-(PE)-labeled mouse anti human CD34, CD45 (Diacclone, France), CD73 (Becton Dickinson, CA, USA), and anti HLA-DR (Diacclone, France). The control for FITC- or PE-coupled antibodies was isotypic mouse IgG1. The data were evaluated using CellQuest software (Becton Dickinson, CA, USA).

Transmission Electron Microscopy (TEM)

WJ-MSCs were fixed with 2.5% (v/v) glutaraldehyde in 0.1 mol/l cacodylate buffer for 2 h and post fixed with a solution of 1% (w/v) osmium tetroxide in 0.1 mol/l cacodylate buffer. The cells were then embedded in epoxy resins after a graded-ethanol serial dehydration step. The embedded cells were sectioned into ultrathin slices, stained by uranyl acetate solution and lead citrate, and then observed with transmission electron microscope CM10 Philips (FEI Company, Eindhoven, The Netherlands) at an accelerating voltage of 80 kV. Images were recorded by Megaview III digital camera (FEI Company, Eindhoven, The Netherlands). Cellular details were calculated on 20 different fields at 19000 magnification by Megaview software system (FEI Company, Eindhoven, The Netherlands).

Differentiation

WJ-MSCs were seeded in six-well culture plates at a density of 1.25×10^4 in the same culture condition as previously described. After 24 h, medium was completely replaced with adipogenic, chondrogenic and osteogenic induction medium consisting of DMEM/F12 medium supplemented as summarized in *Table 4.1*. To assess differentiation, cells were fixed with

10% (w/v) formalin for 1 h, and then stained. Oil Red O (0.3% (v/v) in 60% (v/v) isopropanol) was used to evaluate formation of neutral lipid vacuoles after 10 days of adipogenic differentiation. Chondrogenic and osteogenic differentiation were assessed after 21 days of culture in induction media by using 1% (w/v) Alcian Blue in 3% (v/v) acetic acid solution and 2% (w/v) Alizarin Red S (pH 4.1–4.3) solution, respectively. Cells were observed under an inverted light microscope (Motic AE21, VWR International Srl, Milan, Italy; Eclipse TE 2000u, Nikon Instruments Spa, Florence, Italy) and photographed by CCD camera (Visicam 3.0, VWR International Srl, Milan, Italy; DS-Fi2, Nikon Instruments Spa, Florence, Italy). Control samples consisted in WJ-MSCs cultured for the same period of time in DMEM/F12 plus 2% (v/v) FBS.

Images obtained after differentiation were analysed for colour intensity using Image J software (National Institutes of Health, USA) in order to compare the differentiation ability of human and equine WJ-MSCs.

Medium	Composition
<i>Adipogenic</i>	DMEM/F12 + 15% (v/v) rabbit serum + 1 $\mu\text{mol/l}$ DXM (removed after 6 days) + 0.5 mmol/l IBMX (removed after 3 days), 10 $\mu\text{g/ml}$ insulin, 0.2 mmol/l indomethacin
<i>Chondrogenic</i>	DMEM/F12 + 1% (v/v) FBS + 6.25 $\mu\text{g/ml}$ insulin + 50 nM AA2P, 0.1 $\mu\text{mol/l}$ DXM, 10 ng/ml hTGF β 1
<i>Osteogenic</i>	DMEM/F12 + 10% (v/v) FBS + 10 mmol/l BGP + 0.1 $\mu\text{mol/l}$ DXM + 50 $\mu\text{mol/l}$ AA2P

Table 4.1. Media used for tri-lineage differentiation of human and equine WJ-MSCs. DXM: dexamethasone ; IBMX: 3-isobutyl-1-methylxanthine; FBS: foetal bovine serum; AA2P: 2-phospho-L-ascorbic acid trisodium salt; hTGF β 1: human transforming growth factor; BGP. beta-glycerophosphate.

Statistical analysis

Growth curves were obtained from 3 samples per species. Tests and analysis were performed on P3 cells. Scratch and adhesion assays were done on 2 samples for each species, collecting data from 5 replicates per sample. FACS analysis, TEM and differentiation were performed on 3 sample for each species. Data are expressed as mean \pm SD. Data were analysed for normality using a Shapiro-Wilk test. Statistical differences were assessed by Student t Test or Mann-Whitney U test and by Friedman test using the software IBM SPSS Statistics 23 (IBM Corporation, Milan, Italy). Significance was assessed for $P < 0.05$.

Results

Primary culture of WJ-MSCs

Both human and equine cells obtained from each umbilical cord were adherent cells showing a fibroblast like morphology (*Figure 4.1 A,B*). Cells were cultured up to P6 and mean DT was higher ($P < 0.05$) for human (6.5 ± 4.3) than equine (3.5 ± 2.4) cells. No significant differences ($P > 0.05$) between all passages were observed for human cells (*Figure 4.2 A*) while eWJ-MSCs showed a trend to DT increasing starting from P4 ($P < 0.05$) (*Figure 4.2 B*). Total cell doublings after 44 days of culture were higher ($P < 0.05$) in the horse (20.3 ± 1.7) as compared to hWJ-MSCs (8.7 ± 2.4).

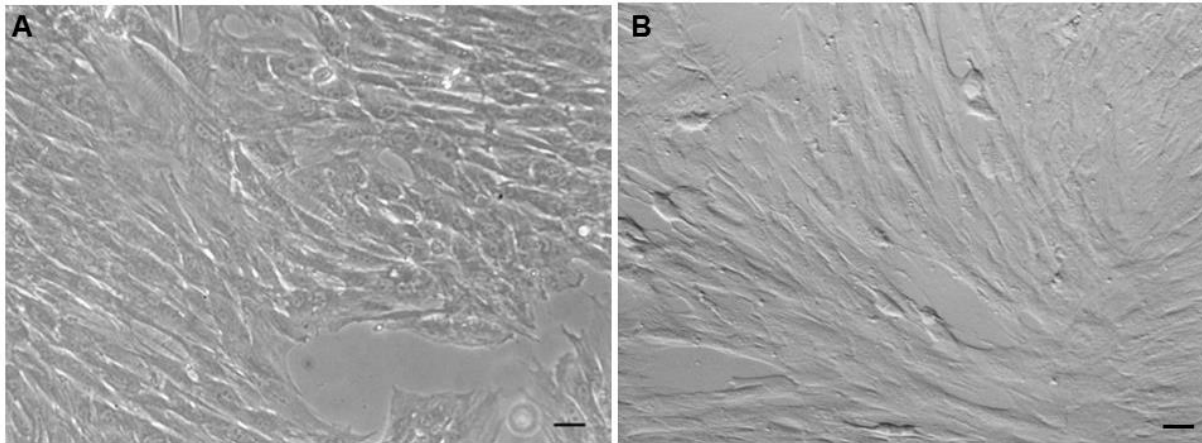


Figure 4.1. (A) Population of hWJ-MSCs (Ematossilin staining, phase contrast) after 5 days of cell culture and (B) of eWJ-MSCs after 9 days of culture. The adherent cells showed a spindle-shape morphology (scale bars 30 μ m).

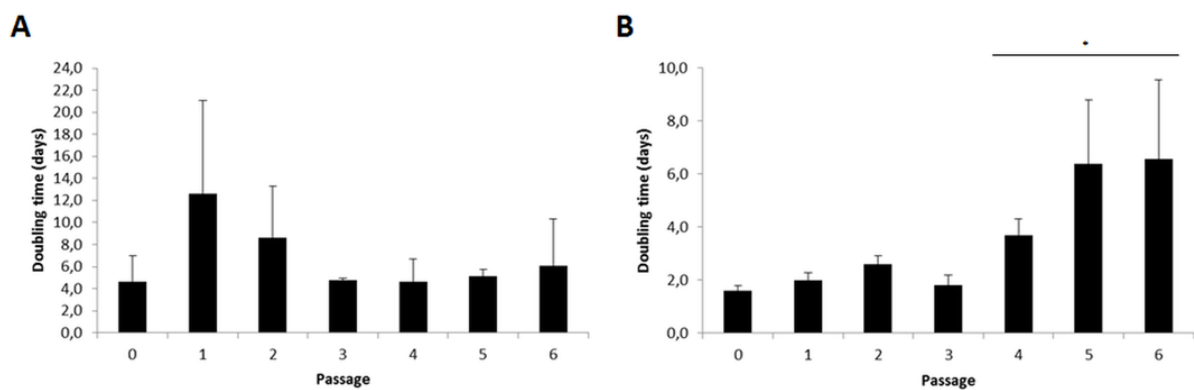


Figure 4.2. Doubling times of hWJ-MSCs (A) and eWJ-MSCs (B) over six passages of culture. * $P < 0.05$.

Scratch assay

In order to evaluate the ability of WJSCMs to migrate, a scratch assay was performed. Results showed, in both species, a good capacity of cells to proliferate and partially cover the cell free area after 24 h of culture (Figure 4.3 A-D), but hWJMSC reached a higher ($P < 0.05$) migration rate ($58.5 \pm 4.7\%$) as compared to eWJ-MSCs ($43.0 \pm 7.7\%$).

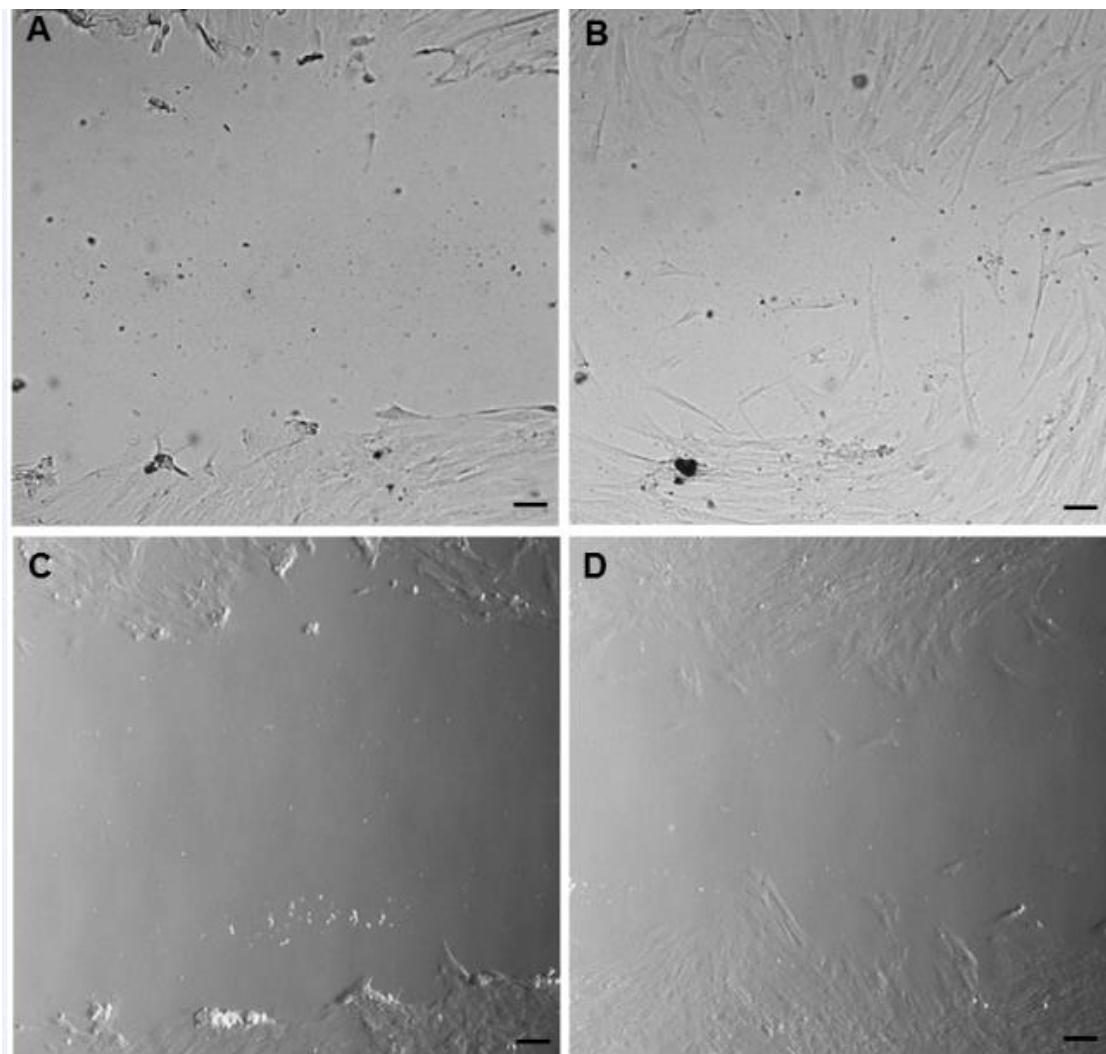


Figure 4.3. Scratch assay on hWJ-MSCs at t0 (A) and after 24 h (B) of cell growth. The same on eWJ-MSCs at t0 (C) and after 24h (D) (scale bar 90 μ m).

Adhesion assay

In order to evaluate the ability of WJ-MSCs to adhere each other, the adhesion assay was carried out. Results showed a higher ability for eWJ-MSCs than hWJ-MSCs to aggregate each other, as demonstrated by the lower ($P<0.05$) mean volume of the equine spheroids compared to human ones (*Figure 4.4 A*). Furthermore, the lower adhesion ability of hWJMSC was also observed since more frequently (about 50%) generating micro-masses (*Figure 4.4 B*).

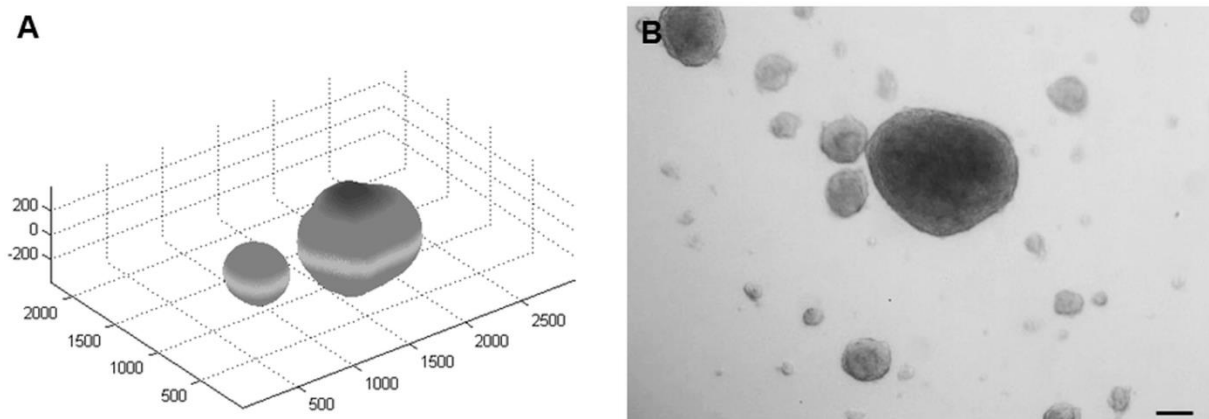


Figure 4.4. Adhesion assay. (A) Volume reconstruction and visualization of an equine (on the left) and a human (on the right) WJ-MSCs spheroid obtained after 48 h of hanging drop culture, as assessed by ReVisp (scale in pixels). (B) Low ability of hWJ-MSCs to aggregate each other making micro-masses (scale bar 90 μ m).

Immunophenotyping of WJ-MSCs by flow cytometry

In order to evaluate the mesenchymal phenotype, both human and equine WJ-MSCs obtained were characterized by flow cytometry. According to Domenici et al. (2006), the expression of the following markers was evaluated: CD105, CD73, CD90, CD14, CD19, CD34, CD45 and HLA-DR. hWJ-MSCs were highly positive for CD105, CD73 and CD90 and negative for CD34, CD19, CD45, CD14 and HLA-DR (*Table 4.2* and *Figure 4.5*). Using a pre-set antibody panel for human cells, most of the clones used were not suitable for equine cells, since cross-reactivity was lacking, as previously demonstrated (De Schauwer et al., 2012; Ibrahim and Steinbach, 2012; Iacono et al., 2015). As consequence, eWJ-MSCs were

evaluated only for the expression of CD90 (Table 4.2 and Figure 4.5). Furthermore, no cross-reactivity CD 19 (clone B-C3) was demonstrated, as it was not able to bind equine lymphocytes (positive control, data not shown).

Group	CD105 (%)	CD90 (%)	CD73 (%)	CD34 (%)	CD19 (%)	CD45 (%)	HLA-DR (%)
<i>hWJMSC</i>	99.98	100.00	99.98	1.53	1.76	1.35	0.87
<i>eWJMSC</i>	n/a	92.57	n/a	n/a	n/a	n/a	n/a

Table 4.2. Flow cytometry analysis of human and equine Wharton's jelly derived mesenchymal stem cells. *hWJMSC*: human Wharton's jelly derived mesenchymal stem cells; *eWJMSC*: equine Wharton's jelly derived mesenchymal stem cells; n/a: not applicable (no antibody cross-reactivity).

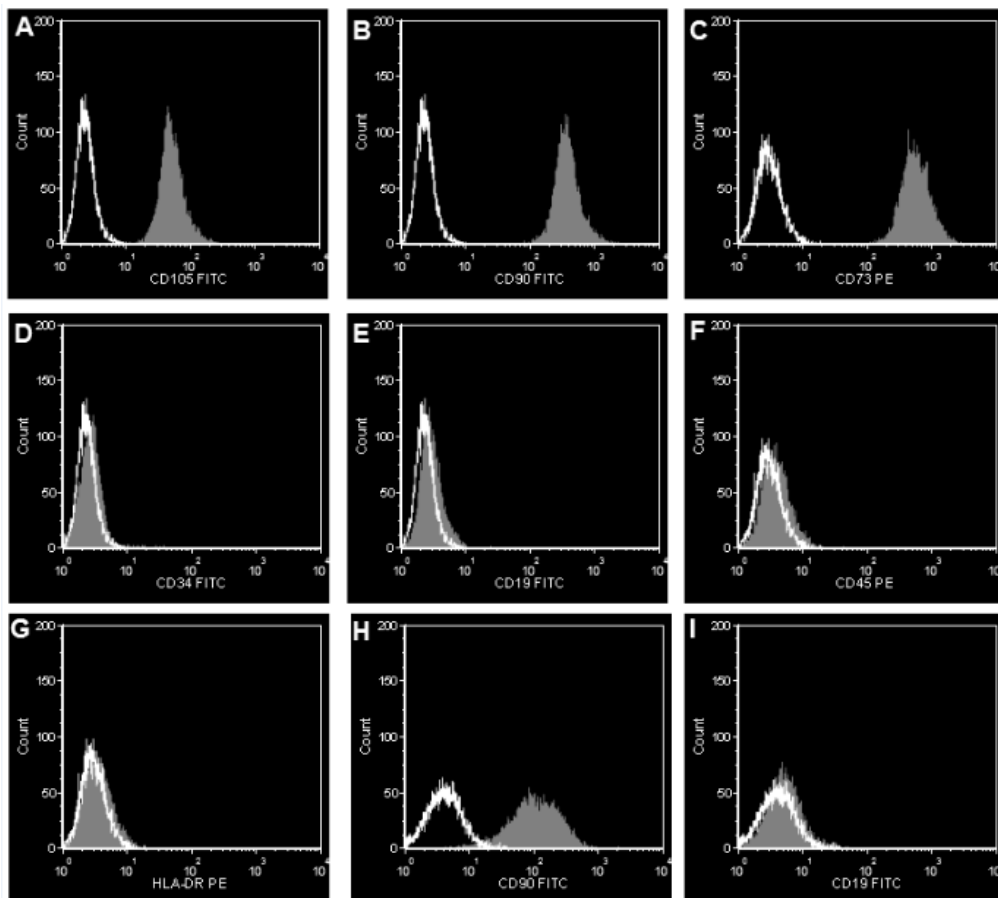


Figure 4.5. Flow cytometry analysis of hWJ-MSCs for (A) CD105, (B) CD90, (C) CD73, (D) CD34, (E) CD19, (F) CD45, (G) HLA-DR and of eWJ-MSCs for (H) CD90 and (I) CD19.

TEM analysis

TEM analysis was performed to evaluate ultrastructure of cells with the final goal to establish morphological parameters useful for the classification and comparison of human and equine WJ-MSCs.

hWJ-MSCs are spindle like shape (*Figure 4.6 A*) cells with an average area of $600 \mu\text{m}^2$, characterized by large euchromatic nucleus and one nucleolus each (*Figure 4.6 A*). At middle magnification, a widely developed Golgi apparatus (*Figure 4.6 B*) surrounded by several secretory vesicles with a diameter ranging from 70 to 200 nm, rough endoplasmic reticulum (RER) with cisternae showing moderately electron dense material and mitochondria with evident internal cristae were observed (*Figure 4.6 C*). An high number of free ribosomes, randomly distributed, characterized the cytoplasm. Several autophagic vesicles and autophagolysosomes with an average diameter of 600 nm, were observed in the cytoplasm of hWJ-MSCs (*Figure 4.6 D*). A few intercellular junctions were observed (*Figure 4.6 D* insert). EWJ-MSCs appear as large fibroblastic like cells, with an average diameter of $700 \mu\text{m}^2$, showing euchromatic nucleus and a variable number of nucleolus ranging from 2 to 6 each cell (*Figure 4.6 E*). At higher magnification, Golgi apparatus, often in more than one each cell, surrounded by several small vesicles with a diameter ranging from 50 to 250 nm, widespread in the cytoplasm (*Figure 4.6 F*). RER cisternae were numerous and partially enlarged, showing a moderately electron dense material. An high number of elongate mitochondria with evident internal cristae were also observed (*Figure 4.6 G*). Several autophagy vesicles and autophagolysosomes, with an average diameter of 700 nm characterized the cytoplasm (*Figure 4.6 H*). An high number of free ribosomes and a few

lipid droplets were randomly observed in the cytoplasm. Cell junctions were observed (*Figure 4.6 H insert*).

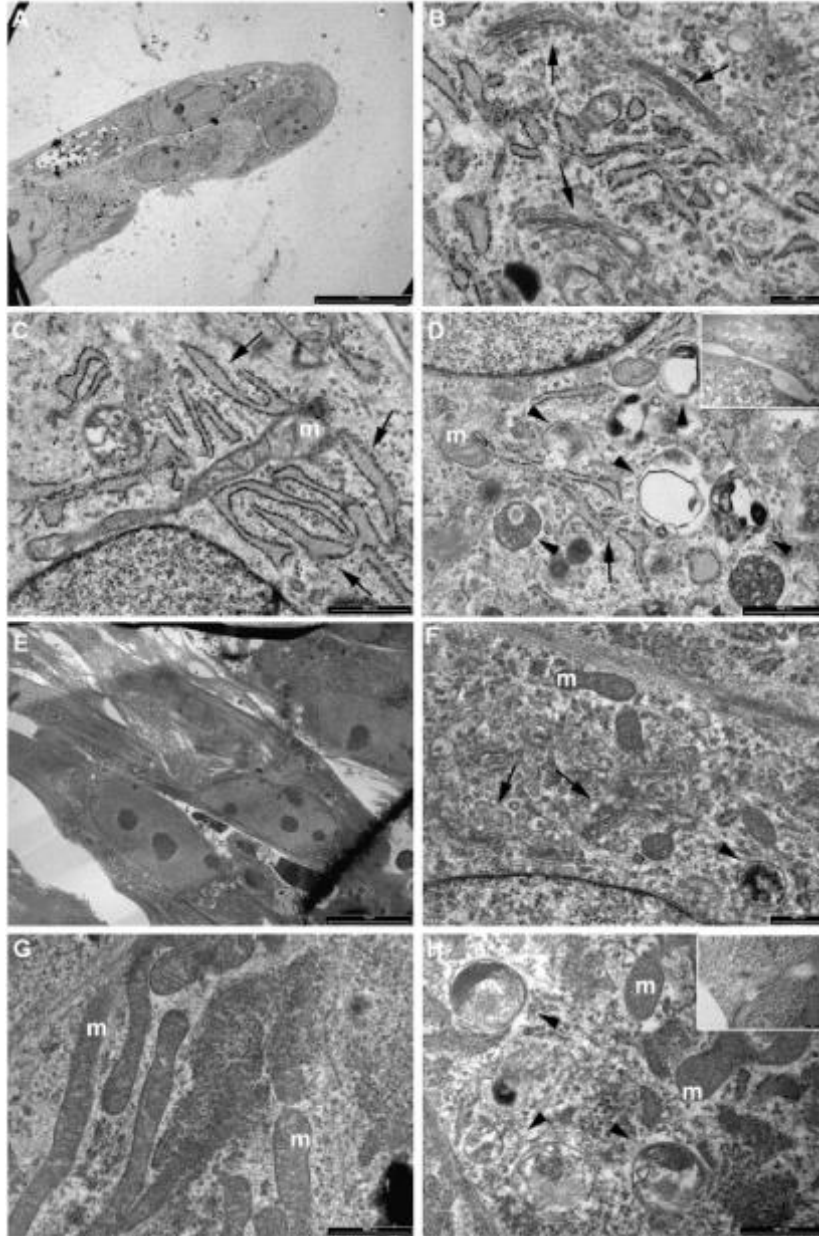


Figure 4.6. TEM analysis of hWJ-MSCs. (A) cluster of cells showing a spindle shape morphology (scale bar 20 μ m); (B) detail of Golgi apparatus (black arrow) (scale bar 500nm) (C) detail of RER (black arrow) and mitochondria (m) (scale bar 1000nm); (D) detail of cytoplasm showing autophagy vesicles and autophagolysosomes (black arrowhead), RER (black arrow) and mitochondria (m) (scale bar: 1000nm). Detail of a cell junction (insert; scale bar: 500nm). TEM analysis of eWJ-MSCs. (E) cluster of cells showing a spindle shape morphology (scale bar 10 μ m); (F) detail of Golgi (black arrows), mitochondria (m) and autophagy vesicle (black arrowhead) (scale bar 500 nm); (G) detail of

mitochondria (m) and free ribosomes (scale bar 1000 nm); (H) numerous autophagy vesicles and autophagolysosomes (black arrowhead) and some mitochondria (m) were detected in the cytoplasm (scale bar: 1000nm) Detail of a cell junction (insert; scale bar: 500nm).

Differentiation

Oil Red O showed the presence of several fat droplets in almost all cells after 10 days of differentiation both in human (Figure 4.7 A) and equine (Figure 4.8 A) cells, compared to control samples in which no fat droplets were detected (Figure 4.7 B, Figure 4.8 B).

Also for chondrogenic differentiation, control samples stained negative for Alcian Blue (Figure 4.7 D; Figure 4.8 D). while a strong blue colour in cells and extracellular matrix after 21 days of differentiation in both species (Figure 4.7 C human; Figure 4.8 C equine) suggested a gradual deposition of glycosaminoglycans.

A strong red colour in cells and extracellular matrix after 21 days of osteogenic differentiation in human (Figure 4.7 E) and equine (Figure 4.8 E) cells confirmed the deposition of calcium, and the presence of mineralized extracellular matrix, which was undetectable by alizarin red in control samples (Figure 4.7 F; Figure 4.8 F).

No differences ($P>0.05$) in the level of adipogenic differentiation were observed between human and equine WJ-MSCs, while eWJ-MSCs showed an higher ($P<0.05$) chondrogenic and osteogenic differentiation potential as compared to human counterparts, as demonstrated by the lower mean grey value observed after colour intensity analysis of differentiation images (Figure 4.9).

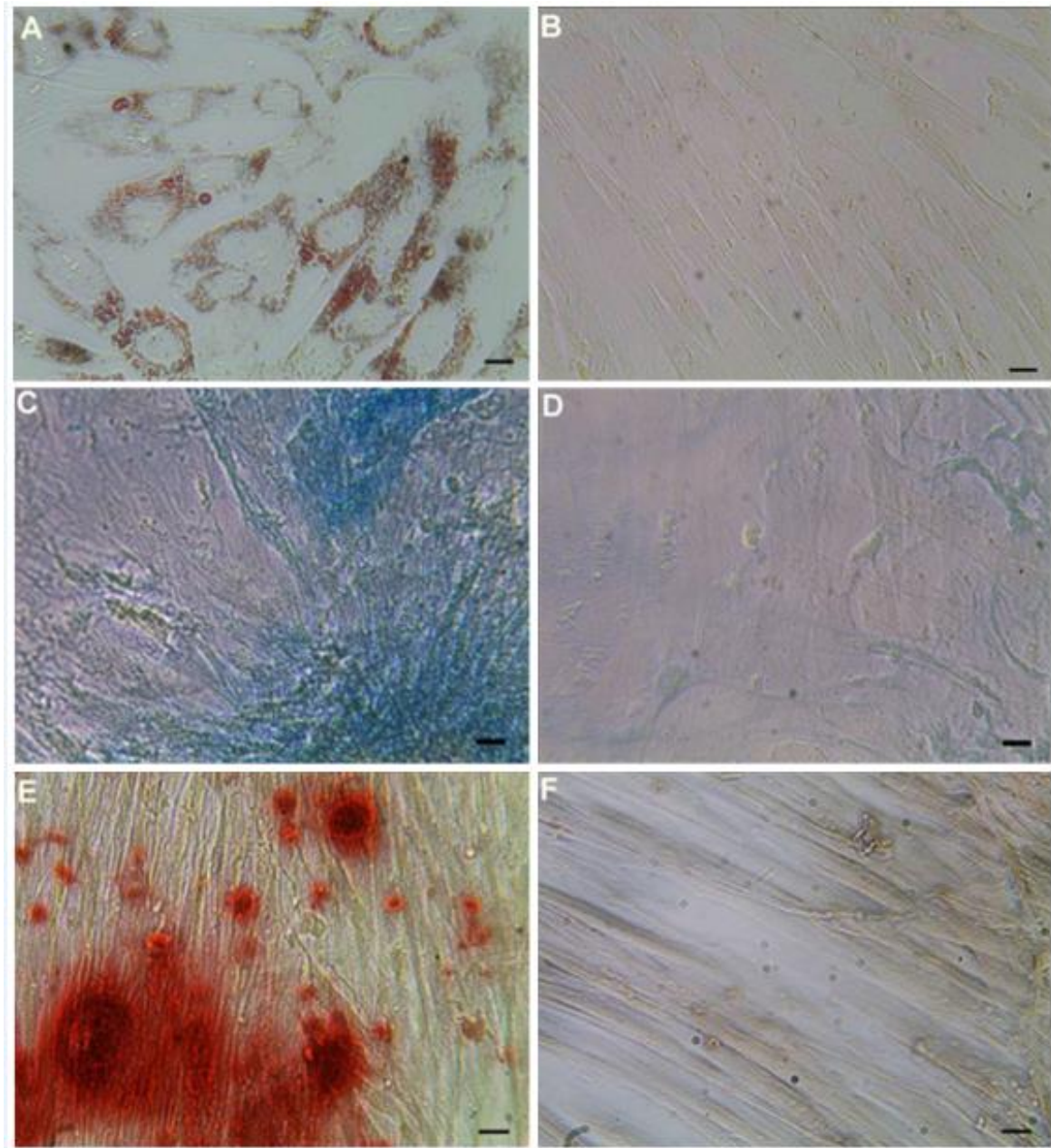


Figure 4.7. (A) adipogenic differentiation of hWJ-MSCs after 10 days of induction (Oil Red O staining , scale bar 20 μ m); (B) control samples consisting in hWJ-MSCs cultured with cell medium without any adipogenic factors (Oil Red O staining, scale bar 20 μ m); (C) chondrogenic differentiation of hWJUMSCs after 21 days of induction (Alcian Blue staining, scale bar 20 μ m); (D) control samples consisting in hWJ-MSCs cultured with cell medium without any chondrogenic factors (Alcian Blue staining, scale bar 20 μ m); (E) osteogenic differentiation of hWJ-MSCs after 21 days of induction (Alizarin Red staining, scale bar 20 μ m); (F) control samples consisting in hWJ-MSCs cultured with cell medium without any osteogenic factors (Alizarin Red staining, scale bar 20 μ m).

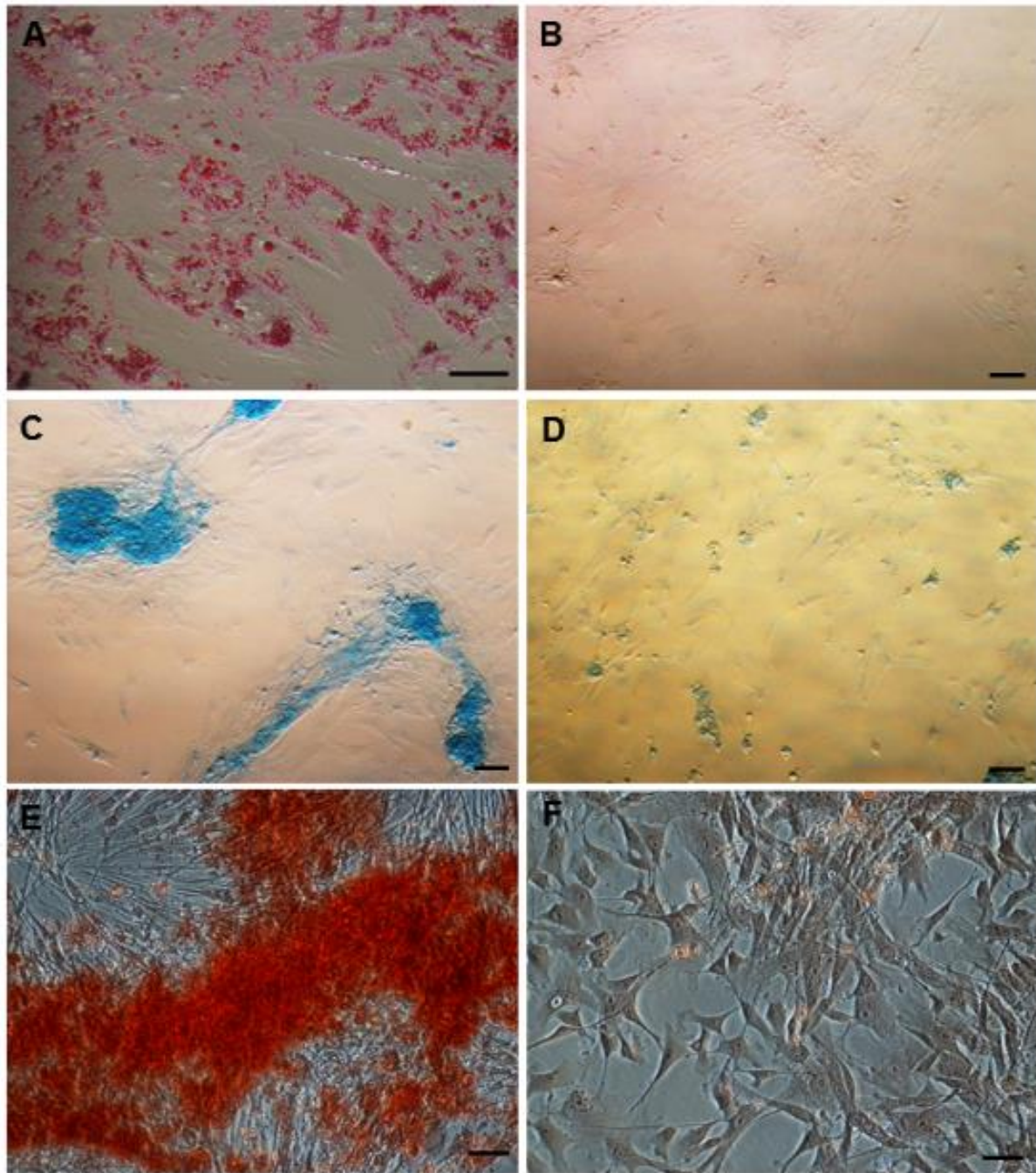


Figure 4.8. (A) adipogenic differentiation of eWJ-MSCs after 10 days of induction (Oil Red O staining, scale bar 50 μ m); (B) control samples consisting in eWJ-MSCs cultured with cell medium without any adipogenic factors (Oil Red O staining, scale bar 50 μ m); (C) chondrogenic differentiation of eWJ-MSCs after 21 days of induction (Alcian Blue staining, scale bar 50 μ m); (D) control samples consisting in eWJ-MSCs cultured with cell medium without any chondrogenic factors (Alcian Blue staining, scale bar 50 μ m); (E) osteogenic differentiation of eWJ-MSCs after 21 days of induction (Alizarin Red staining, scale bar 50 μ m); (F) control samples consisting in eWJ-MSCs cultured with cell medium without any osteogenic factors (Alizarin Red staining, scale bar 50 μ m).

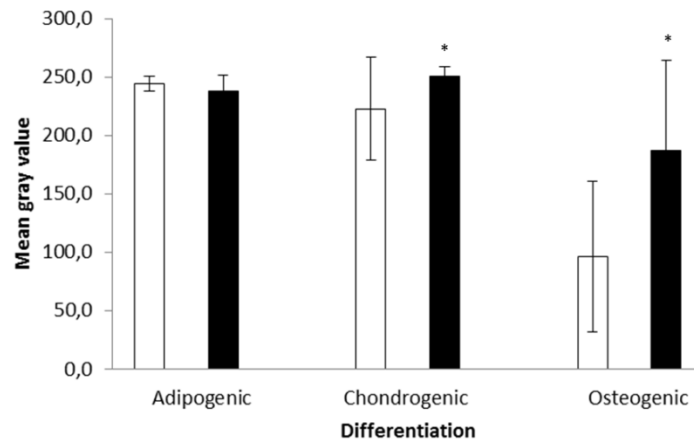


Figure 4.9. Mean grey values (inversely related to differentiation potential) obtained after colour intensity analysis of adipogenic, chondrogenic and osteogenic differentiation images of equine (white) and human (black) WJ-MSCs. * $P < 0.05$.

Discussion

In this study, MSCs were successfully isolated from equine and human Wharton's jelly by tissue digestion using the same protocol. Further analysis of proliferation, migration, adhesion, immunophenotyping, tri-lineage differentiation and TEM behaviour of isolated MSCs was performed for comparative evaluation of WJ-MSCs from both species. TEM analysis confirmed the presence of an intense metabolism and secretory activity, all morphological features linked with the maintenance of cell stemness and survival. Interestingly, major differences between cellular properties of hWJ-MSCs and eWJ-MSCs were observed in the proliferation, migration, adhesion abilities and also in differentiation potential.

For this study, the horse was chosen as an appropriate animal model, since there are pathophysiological similarities between human and equine orthopaedic diseases (Patterson et al., 2012). Furthermore, in equine medicine the treatment of orthopaedic injuries with MSCs

is currently widely used (Smith, 2008; Crovace et al., 2010; Godwin et al., 2012). Wharton's jelly is a plentiful and inexpensive source of cells that fit into the category of primitive stromal cells (Troyer and Weiss, 2008), so in the present study it was chosen as donor tissue.

In both species, TEM analysis showed cells with a fibroblast shape, large nucleus, well developed RER and Golgi apparatus surrounded by several mitochondria, ultrastructural characteristics connected with a proliferating status and an intense synthetic and metabolic activity, which characterize mesenchymal stem cells (Pasquinelli et al. 2007; Pascucci et al., 2010). Equine WJ-MSCs showed a higher number of nucleolus, ranging from 2 to 6, comparing to the human WJ-MSCs, in which one nucleolus was always detected. The number of nucleolus is correlated with an intense protein synthesis and metabolic activity due to an increased demand for proteins during cell growth and proliferation which reflects an increase in protein synthetic capacity by upregulating ribosome biogenesis (Orsolich et al., 2016). The higher number of nucleolus in eWJ-MSCs is in agreement with our findings on cellular properties of eWJ-MSCs and hWJ-MSCs in which eWJ-MSCs demonstrated a higher proliferation, adhesion abilities and differentiation potential compared to hWJ-MSCs.

Furthermore, in both species a large amount of vesicles was observed in the cytoplasm, as previously reported in equine adipose derived mesenchymal stem cells where an high amount of primary endocytic vesicles, early endosomes, late endosomes, endolysosomes and lysosomes (Pascucci et al., 2010). In human mesenchymal stem cells, it was also reported the presence of autophagic vacuoles inside amnion MSCs (Pasquinelli et al., 2007; Teti et al., 2012), in agreement with our observations in which a high number of autophagy vesicles and autophagosomes were detected. Recently, it has been demonstrated the presence of a constitutive autophagy as a cytoprotective and cellular quality control mechanisms to balance

protein and organelle turnover, crucial for the maintenance of stemness (Garcia-Prat et al., 2016; Sbrana et al., 2016).

The first observation arose from proliferation assay is that equine WJ-MSCs grew more rapidly in comparison to human cells. Mean doubling time for equine cells was lower, but while human cells did not exhibit variation in the first 6 passages, an increase was observed by P4 for eWJ-MSCs. The quite early slowing down in growth of eWJ-MSCs observed in this study has never been observed before in our laboratory, and subsequently mean doubling time was higher than in previous studies (Iacono et al., 2012). A possible explanation could be that, for the present research, the culture medium was changed, and equine cells were cultured in the same medium routinely used for human MSCs (Mattioli-Belmonte et al., 2015). Further studies culturing eWJ-MSCs in different conditions are needed to ascertain such hypothesis.

Migration potential of MSCs is considered important for their integration into the host tissue during therapeutic applications (Li et al., 2009). In the present study, hWJ-MSCs showed a trend towards increased migration activity in comparison to eWJ-MSCs, suggesting their graft integration *in vivo* may be enhanced. This finding was surprising, given that human cells showed a slower doubling time, but could be partially explained by the observed lower cell-to-cell adhesion potential.

In fact, hWJ-MSCs spheroids after hanging drop culture were larger than those formed by eWJ-MSCs, and quite often fragmented, demonstrating a lower self-assembly ability. Self-assembly of MSCs into aggregates has significant implication in their applications in cell therapy and tissue regeneration (Sart et al., 2014). 3D spheroid culture system contributes to an optimization for efficient *in vitro* differentiation of MSCs (Wang et al., 2009) and *in vivo* MSC 3D transplantation of synovial MSC aggregates promoted cartilage tissue regeneration in a rabbit model (Suzuki et al., 2012).

In this study, no significant differences were observed in the adipogenic differentiation capacity between hWJ-MSCs and eWJ-MSCs, on the contrary, eWJ-MSCs produced more extracellular matrix both in chondrogenic and osteogenic differentiation, as confirmed by an higher intensity of staining. Differentiations were performed using standard protocols described in the literature for human MSCs (Mizuno and Hyakusoku, 2003), with some modifications (Iacono et al., 2012): for the chondrogenic differentiation 0.1 mM dexamethasone was added, while rabbit serum was used for the adipogenic differentiation protocol. Indeed, it has been reported that rabbit serum enhances adipogenic differentiation (Janderova et al., 2003).

Analysis of surface marker expression patterns provided further insights into the characteristics of human MSCs, but only one antibody of the panel available was cross-reacting with equine epitopes. This study confirms what already observed by others in the horse (De Schauwer et al., 2011; Ibrahim and Steinbach, 2012; Iacono et al., 2015), and adds to the list a new antibody that does not recognise the corresponding equine epitope (CD 19, clone B-C3).

In conclusion, our findings indicate that MSCs isolated from umbilical of different species, have a similar ultrastructure compatible with mesenchymal stem phenotype, which makes them to have different biological proprieties. This study helps to better clarify the specie-specific characteristics and in defining new animal models.

References

Crovace A., Lacitignola L., Rossi G., Francioso E., (2010). *Histological and immunohistochemical evaluation of autologous cultured bone marrow mesenchymal stem cells and bone marrow mononucleated cells in collagenase-induced tendinitis of equine superficial digital flexor tendon.* Vet Med Int; 2010: 250978.

De Schauwer C., Meyer E., Van de Walle G.R., Van S.A., (2011). *Markers of stemness in equine mesenchymal stem cells: a plea for uniformity.* Theriogenology; 75(8): 1431-1443.

De Schauwer C., Piepers S., Van de Walle G.R., Demeyere K., Hoogewijs M.K., Govaere J.L., Braeckmans K., Van Soom A., Meyer E., (2012). *In search for cross-reactivity to immunophenotype equine mesenchymal stromal cells by multicolor flow cytometry.* Cytometry; A81(4): 312-323.

Dominici M., Le Blanc K., Mueller I., Slaper-Cortenbach I., Marini F., Krause D., Deans R., Keating A., Prockop D., Horwitz E., (2006). *Minimal criteria for defining multipotent mesenchymal stromal cells. The International Society for Cellular Therapy position statement.* Cytotherapy; 8(4): 315-317.

García-Prat L., Martínez-Vicente M., Muñoz-Cánoves P., (2016). *Autophagy: a decisive process for stemness.* Oncotarget; 7(11): 12286-12288.

Godwin E.E., Young N.J., Dudhia J., Beamish I.C., Smith R.K., (2012). *Implantation of bone marrow-derived mesenchymal stem cells demonstrates improved outcome in horses with overstrain injury of the superficial digital flexor tendon.* Equine Vet J; 44(1): 25-32.

Iacono E., Merlo B., Romagnoli N., Rossi B., Ricci F., Spadari A., (2015). *Equine bone marrow and adipose tissue mesenchymal stem cells: cytofluorimetric characterization, in*

vitro differentiation, and clinical application. Journal of Equine Veterinary Science; 35: 130-140.

Iacono E., Rossi B., Merlo B., (2015). *Stem cells from foetal adnexa and fluid in domestic animals: an update on their features and clinical application.* Reprod Domest Anim; 50(3): 353-364.

Ibrahim S., Steinbach F., (2012). *Immunoprecipitation of equine CD molecules using anti-human MABs previously analyzed by flow cytometry and immunohistochemistry.* Vet Immunol Immunopathol; 145(1-2): 7-13.

Janderova L., McNeil M., Murrell A.N., Mynatt R.L., Smith S.R., (2003). *Human mesenchymal stem cells as an in vitro model for human adipogenesis.* Obes Res; 11(1): 65–74.

Li G., Zhang X.A., Wang H., Wang X., Meng C.L., Chan C.Y., Yew D.T., Tsang K.S., Li K., Tsai S.N. et al., (2009). *Comparative proteomic analysis of mesenchymal stem cells derived from human bone marrow, umbilical cord, and placenta: Implication in the migration.* Proteomics; 9(1): 20-30.

Orsolich I., Jurada D., Pullen N., Oren M., Eliopoulos A.G., Volarevic S., (2016). *The relationship between the nucleolus and cancer: Current evidence and emerging paradigms.* Seminars in Cancer Biology; 37: 36-50.

Pascucci L., Mercati F., Marini C., Ceccarelli P., Dall'Aglio C., Pedini V., Gargiulo A.M., (2010). *Ultrastructural morphology of equine adipose-derived mesenchymal stem cells.* Histol Histopathol; 25(10): 1277-1285.

Pasquinelli G., Tazzari P., Ricci F., Vaselli C., Buzzi M., Conte R., Orrico C., Foroni L., Stella A., Alviano F., et al., (2007). *Ultrastructural characteristics of human mesenchymal*

stromal (stem) cells derived from bone marrow and term placenta. Ultrastruct Pathol; 31(1): 23-31.

Patterson-Kane J.C., Becker D.L., Rich T., (2012). *The pathogenesis of tendon microdamage in athletes: the horse as a natural model for basic cellular research.* J Comp Pathol; 147(2-3): 227-247.

Piccinini F., Tesei A., Arienti C., Bevilacqua A., (2015). *Cancer multicellular spheroids: volume assessment from a single 2D projection.* Computer Methods Programs Biomed; 118(2): 95-106.

Rainaldi G., Pinto B., Piras A., Vatteroni L., Simi S., Citti L., (1991). *Reduction of proliferative heterogeneity of CHEF18 Chinese hamster cell line during the progression toward tumorigenicity.* In Vitro Cell Dev Biol; 27A(12): 949-952.

Sbrana F.V., Cortini M., Avnet S., Perut F., Columbaro M., De Milito A., Baldini N., (2016). *The Role of Autophagy in the Maintenance of Stemness and Differentiation of Mesenchymal Stem Cells.* Stem Cell Rev; 12(6): 621-633.

Smith R.K., (2008). *Mesenchymal stem cell therapy for equine tendinopathy.* Disability and Rehabilitation; 30(20-22): 1752-1758.

Suzuki S., Muneta T., Tsuji K., Ichinose S., Makino H., Umezawa A., Sekiya I., (2012). *Properties and usefulness of aggregates of synovial mesenchymal stem cells as a source for cartilage regeneration.* Arthritis Res Ther; 14(3): R136.

Teti G., Cavallo C., Grigolo B., Giannini S., Facchini A., Mazzotti A., Falconi M., (2012). *Ultrastructural analysis of human bone marrow mesenchymal stem cells during in vitro osteogenesis and chondrogenesis.* Microsc Res Tech; 75(5): 596-604.

Troyer D.L., Weiss M.L., (2008). *Wharton's jelly-derived cells are a primitive stromal cell population*. Stem Cells; 26(3): 591-599.

Vangsness C.T. Jr, Sternberg H., Harris L., (2015). *Umbilical cord tissue offers the greatest number of harvestable mesenchymal stem cells for research and clinical application: a literature review of different harvest sites*. Arthroscopy; 31(9): 1836-1843.

Wang W., Itaka K., Ohba S., Nishiyama N., Chung U.I., Yamasaki Y., Kataoka K., (2009). *3D spheroid culture system on micropatterned substrates for improved differentiation efficiency of multipotent mesenchymal stem cells*. Biomaterials; 30(14): 2705-2715.

CHAPTER 5

ULTRASTRUCTURAL COMPARISON BETWEEN EQUINE ADULT AND FOETAL MESENCHYMAL STEM CELLS

Article in preparation

Department of Veterinary Medical Sciences, University of Bologna, Ozzano Emilia, Bologna, Italy. Research in collaboration with Prof Janina Burk (Translational Centre of Regenerative Medicine of University of Leipzig, Germany) and with Prof. Mirella Falconi and Dr. Gabriella Teti (Department for Biomedical and Neuromotor Sciences, University of Bologna, Italy)

Introduction

Mesenchymal stem cells (MSCs), also known as multipotent stromal cells or mesenchymal progenitor cells (Dominici et al., 2006), are of increasing interest in the regenerative medicine field. Their application requires the ability to collect a large number of cells in a noninvasive way, the availability of highly proliferative cells that are able to differentiate, and the need to create cells for cryogenic banking (Lange Consiglio et al., 2013). For practical reasons, the most common harvest method employed clinically is bone marrow (BM) or adipose tissue (AT) harvest, although umbilical cord blood banks are rapidly expanding (Bourzac et al., 2010).

The aim of the study was to compare and describe property and characteristics of equine adult and foetal MSCs; in particular, MSCs derived from bone marrow and umbilical cord blood, and adipose tissue and Wharton's jelly.

Materials and Methods

Unless otherwise indicated, chemicals were purchased from Sigma-Aldrich, and laboratory plastics from Sarstedt Inc.

Foetal MSCs were collected, cultivated and analysed at the Laboratory of Biotechnology and Animal Reproduction (LRBA) of Department of Veterinary Medical Sciences (DIMEVET).

Adult MSCs were collected and cultivated at the Translational Centre of Regenerative Medicine (TRM) of University of Leipzig, Germany; then the cells were analysed at LRBA.

The Transmission Electron Microscopy (TEM) was performed for both foetal and adult MSCs at Department for Biomedical and Neuromotor Sciences, University of Bologna, Italy.

Animals

Umbilical cord blood (UCB) and Wharton's jelly (WJ) samples (*Figure 5.1*) were recovered immediately after delivery from three healthy mares, housed at the Department of Veterinary Medical Sciences, University of Bologna, for attended delivery. Experimental procedures were approved by the Ethics Committee, University of Bologna (8134-X/10). The written consent was given by the owners to allow tissues recovery for research purposes.

Bone marrow (BM) and adipose tissue (AT) samples were collected from three healthy horses at Translational Centre of Regenerative Medicine (TRM) of University of Leipzig, Germany.

Bone marrow was collected according to standard surgical procedures. Briefly, the horses were sedated, the sternal region was prepared aseptically and following local anaesthesia, the sternum was punctured with an 11 G bone marrow aspiration needle and a sample was aspirated into a heparinised syringe. Subcutaneous adipose tissue and tendon tissue used for the tenogenic differentiation were collected via skin incision from the supragluteal region and the superficial digital flexor tendon, respectively. Samples were stored at room temperature and subjected to cell isolation within 4 h after collection. Tendon samples for the tenogenic

differentiation were aseptically collected from the same animals and immediately frozen at -80°C .

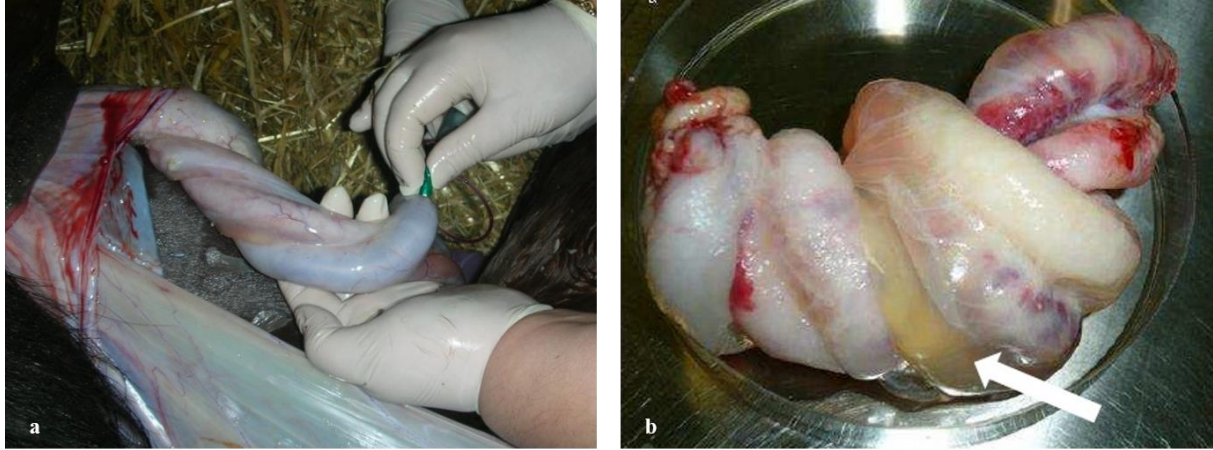


Figure 5.1. Collection of Umbilical Cord Blood and Wharton's Jelly.

Cell isolation and Doubling method

Samples were washed under flowing water and stored in D-PBS (Dulbecco's Phosphate Buffered Solution) added with antibiotics (100 iu/ml penicillin and 100 $\mu\text{g/ml}$ streptomycin), at 4°C , until processing. In the lab, cells were isolated as previously described (Iacono et al., 2012; Burk et al., 2013). Primary cells were plated in a 25 cm^2 flask in Dulbecco's Modified Essential Medium (D-MEM) F12 Glutamax® (Gibco) supplemented with 10% FBS (Gibco) and antibiotics and incubated in a 5% CO_2 humidified atmosphere at 38.5°C . At ~80-90% of confluence, cells were dissociated by 0.25% trypsin, counted and plated at the concentration of 5×10^3 cells/ cm^2 as "Passage 1" (P1), and so on for the following passages. Calculation of cell-doubling time (DT) and cell-doubling numbers (CD) was carried out according to the formulae of Rainaldi et al. (1991).

Adhesion and Migration Assays

In order to define differences between adult and foetal MSCs, spheroid formation and migration test were performed. For adhesion assay, cells were cultured in 'hanging drops'

(5.000 cells/drop) for 24 h. Images were acquired by a Nikon Eclipse TE 2000-U inverted microscope. Spheroid areas were determined using ImageJ software Version 1.6. Starting from the binary masks obtained by Image J, the volume of each spheroid was computed using ReViSP (Bellotti et al., 2016), a software specifically designed to accurately estimate the volume of spheroids and to render an image of their 3D surface.

To assess cell migration potential, a scratch assay was carried out, as previously described (Liang et al., 2007). The distances of each scratch closure were calculated by ImageJ, and the migration percentages were calculated as previously reported (Rossi et al., 2014).

In vitro differentiation

At P3, in vitro differentiation potential of cells towards osteogenic, adipogenic, chondrogenic and tenogenic lineages was studied. Cells (5×10^3 cells /cm²) were cultured under specific induction media (*Table 5.1*) and for tenogenic differentiation as described by Lovati et al. (2012).

About the tenogenic induction, the equine trimmed fresh tendon was co-cultured with MSCs separately on the opposite sides of permeable transwell inserts divided by a 0.4 µm pored size membrane (Corning Costar, Cambridge, MA, USA). The co-culture system consisted of a polycarbonate transwell chamber, which can be inserted into the well of standard 6-well plates. MSCs at P3 were seeded on the bottom of 6-well culture plates at 500 and 1000 cells/cm² for 15 days of co-culture. Tendon fragments of 2 to 3 mm³ were seeded on the upper membrane (pore size of 0.4 µm) of the transwell chamber. This chamber was inserted into the well of the plate and 3 ml of control medium, without foetal serum, were added to cover both the upper tendon pieces (*Figure 5.2*). The transwell co-culture system prevented the migration of both tendon fragments and released tenocytes in the lower chamber. It also inhibited cell-cell contact thanks to the physical separation between the upper and lower chambers, while

allowing exchange of the serum-free medium without growth factors and the diffusion of soluble factors between the two compartments due to the pored membrane.



Figure 5.2. Tenogenic differentiation.

Adipogenic medium (7 days) (Iacono et al., 2012)	Chondrogenic Medium (21 days) (Iacono et al., 2012)	Osteogenic Medium (21 days) (Mizuno and Hyakusoku, 2003)
DMEM F12 15% Rabbit Serum 0.5 mM IBMX ^a (removed after 3 days) 1 μ M DXM ^b (removed after 6 days) 10 μ g/mL insulin - 0.2 mM indomethacin	DMEM/TCM199 1% FBS 6.25 μ g/mL insulin 50 nM AA2P ^c 0.1 μ M DXM ^b -10 ng/mL hTGF β 1 ^d	DMEM/TCM199 10% FBS 50 μ M AA2P ^c 0.1 μ M DXM ^b 10 mM BGP ^e

Table 5.1. Specific induction media compositions.^aIBMX: isobutylmethylxanthine, ^bDXM: Dexamethasone, ^cAA2P: Ascorbic Acid 2-Phosphate, hTGF: ^d human Transforming Growth Factor, ^eBGP: Beta-Glycerophosphate.

As negative control, an equal number of cells was cultured in expansion medium for each differentiation.

To cytologically evaluate differentiation, cells were fixed with 10% formalin at room temperature (RT) and stained with Oil Red O, Alcian Blue, Von Kossa and Aniline Blue for adipogenic, chondrogenic, osteogenic and tenogenic induction, respectively. Adult MSCs were stained also with Van Gieson.

Immunocytochemistry (ICC)

Cells at P3, cultured on ICC slides, were fixed with 4 % paraphormaldehyde (20 min at RT), then washed in phosphate buffer (PB). Cells were blocked in goat serum (10 %) for 1 h and incubated overnight with primary antibodies (*Table 5.2*), then they were washed in PB2 (PB +

0.2 % BSA + 0.05 % saponin) and incubated with anti-mouse- or anti-rabbit- FITC conjugated secondary antibodies for 1 h. Nuclei were then labelled with Hoechst 33342 for foetal-MSCs and DAPI for adult-MSCs. The excess of secondary antibody and Hoechst/DAPI were removed by three washes with PB2. Images of MSCs were obtained with a Nikon Eclipse E400 microscope, using the software Nikon NIS-Elements.

Primary Antibody	Dilution
α -SMA (α -smooth muscle actin) (Gene tex)	1:500
N-Cadherin (Biorbyt orb11100)	1:100

Table 5.2. Primary antibodies for ICC.

Molecular Characterization

One hundred thousand cells were snap-frozen and RNA was extracted using Nucleo Spin® RNA kit (Macherey-Nagel) following the manufacturer's instructions. cDNAs were synthesized by RevertAid RT Kit (ThermoFisher Scientific) and used directly in PCR reactions, following the instructions of Maxima Hot Start PCR Master Mix (2X) (ThermoFisher Scientific). The primers used are listed in *Table 5.3*. PCR products were visualized with ethidium bromide on a 2% agarose gel.

Primers	References	Sequences (5'→3')	bp
MSC marker			
CD90	Mohanty et al., 2014	FW: TGCGAACTCCGCCTCTCT RW: GCTTATGCCCTCGCACTTG	93
CD73	Mohanty et al., 2014	FW: GGGATTGTTGGATACACTTCAAAG RW: GCTGCAACGCAGTGATTCA	90
Ematopoietic markers			
CD34	Mohanty et al., 2014	FW: CACTAAACCCTCTACATCATTTTCTCCTA RW: GGCAGATACCTTGAGTCAATTTCA	101
CD45	Mohanty et al., 2014	FW: TGATTCCCAGAAATGACCATGTA RW: ACATTTTGGGCTTGTCTGTAAAC	101
MHC markers			
MHC-I	Corradetti et al., 2011	FW: GGAGAGGAGCAGAGATACA RW: CTGTCACTGTTTGCAGTCT	218
MHC-II	Corradetti et al., 2011	FW: TCTACACCTGCCAAGTG RW: CCACCATGCCCTTTCTG	178
ILs			
TNF α	Jischa et al., 2008	FW: GCTCCAGACGGTGCTTGTG RW: GCCGATCACCCCAAAGTG	95
IL-8	Jischa et al., 2008	FW: CGGTGCCAGTGCATCAAG RW: TGGCCCACTCTCAATCACTCT	81
INF- γ	Castagnetti et al., 2012	FW: GTGTGCGATTTTGGGTTCTTCTA RW: TTGAATGACCTGGTTATCT	235
IL4	Castagnetti et al., 2012	FW: CAACTTCATCCAGGGATGCAA RW: CAGTCAGCTCCATGCACGAAT	107
IL- β 1	Castagnetti et al., 2012	FW: GAGGCAGCCATGGCAGCAGTA RW: TGTGAGCAGGGAACGGGTATCTT	257
IL-6	Visser and Pollitt, 2011	FW: AAACCACCTCAAATGGACCACTA RW: TTTTTCAGGGCAGAGATTTTGC	91
Pluripotency markers			
OCT4	Desmarais et al., 2011	FW: TCCCAGGACATCAAAGCTCTGCAGA RW: TCAGTTTGAATGCATGGGAGAAGCCAGA	679
NANOG	Desmarais et al., 2011	FW: GACAGCCCCGATTCATCCACCAG RW: GCACCAGGTCTGACTGTTCCAGG	492
SOX2	Desmarais et al., 2011	FW: GGCGGCAACCAGAAGAACAG RW: AGAAGAGGTAACCACGGGGG	663
Housekeeping			
GAPDH	Desmarais et al., 2011	FW: GTCCATGCCATCACTGCCAC RW: CCTGCTTACCACCTTCTTG	262

Table 5.3. Sequence of primers used for PCR analysis.

Transmission Electron Microscopy (TEM)

Equine MSCs at P3 obtained from UCB, WJ, AT and BM were fixed with 2.5% glutaraldehyde in 0.1 M cacodylate buffer for 2 h and post fixed with a solution of 1% osmium tetroxide in 0.1 M cacodylate buffer. The cells were then embedded in epoxy resins after a graded-ethanol serial dehydration step. The embedded cells were sectioned into ultrathin slices, stained by uranyl acetate solution and lead citrate, and then observed with transmission electron microscope CM10 Philips (FEI Company, Eindhoven, The Netherlands) at an accelerating voltage of 80 kV. Images were recorded by Megaview III digital camera (FEI Company, Eindhoven, The Netherlands). The TEM analysis was performed at Department for Biomedical and Neuromotor Sciences, University of Bologna, Italy.

Statistical Analysis

Harvested WJ, UCB, BM and AT (grams), CDs, DTs and percentages of migration are expressed as mean \pm standard deviation (SD). Statistical analyses were performed using IBM SPSS Statistics 21 (IBM Corporation). Data were analysed, for normal distribution, using a Shapiro-Wilk test, and then using one-way ANOVA. The 3D spheroid volumes and mean gray intensity of differentiated cells were compared using Bonferroni's test. Significance was assessed for $P < 0.05$.

Results*Cell isolation and Doubling method*

Adherent mononuclear cells were characterized by a homogeneous elongated fibroblast-like morphology. Undifferentiated cells of both lines were passaged up to three times; no changes in cell morphology was observed throughout the culture period.

Results were reported in *Table 5.4*. No statistically significant differences were found in DTs among earlier culture passages in both cell lines ($P > 0.05$).

	CD	DT
UCB	9.6 ± 0.9	2.4 ± 1.3
WJ	9.9 ± 1.1	2.693 ± 0.9
BM	8.6 ± 0.4	3.6 ± 1.4
AT	9.0 ± 1.4	2.2 ± 1.1

Table 5.4. Cell-doubling numbers (CD) and cell-doubling time (DT) reported as mean ± sd.

Adhesion and Migration Assays

Both foetal and adult MSCs formed spheroids when cultured in hanging drops (*Figure 5.3*).

Average areas and volume of the spheroids formed by foetal MSCs (derived from WJ and UCB) were significantly smaller than from adult MSCs (derived from BM and AT; $P < 0.05$).

Average percentage of migration, observed by scratch test, was statistically similar between cell lines (WJ-MSCs: $43.04 \pm 7.74\%$ vs UCB-MSCs: $28.36 \pm 5.01\%$ vs BM-MSCs: $25.02 \pm 10.20\%$ vs AT-MSCs: $24.48 \pm 21.44\%$; $P > 0.05$).

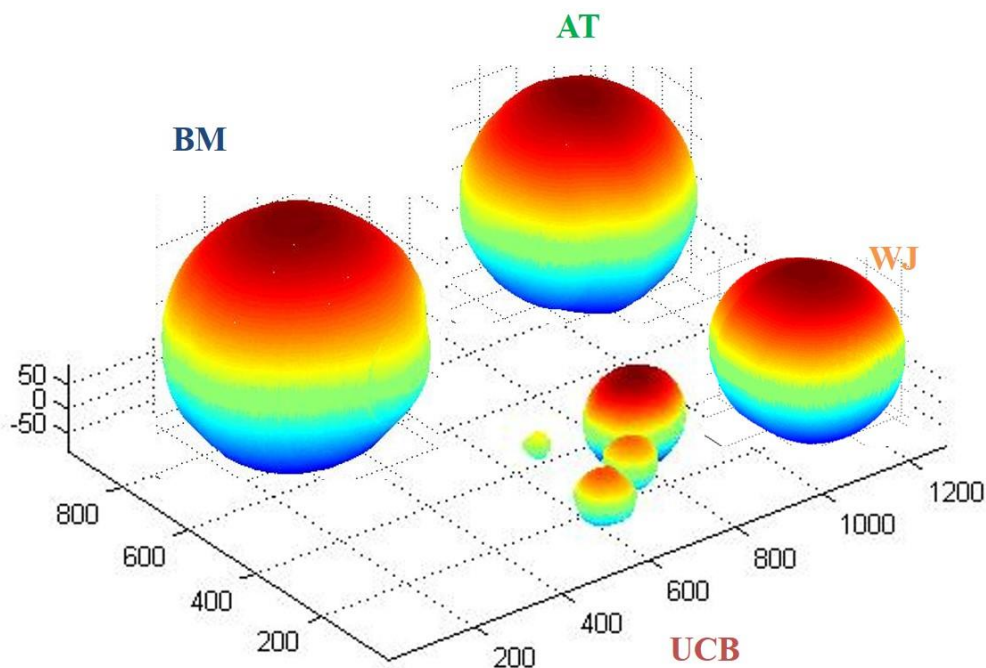


Figure 5.3. Spheroids of MSCs derived from BM, AT, WJ and UCB performed with ReViSP.

In vitro differentiation

All cell lines were able to differentiate toward osteogenic (*Figure 5.4*), chondrogenic (*Figure 5.5*), adipogenic (*Figure 5.6*) and tenogenic direction (*Figure 5.7* and *5.8*).

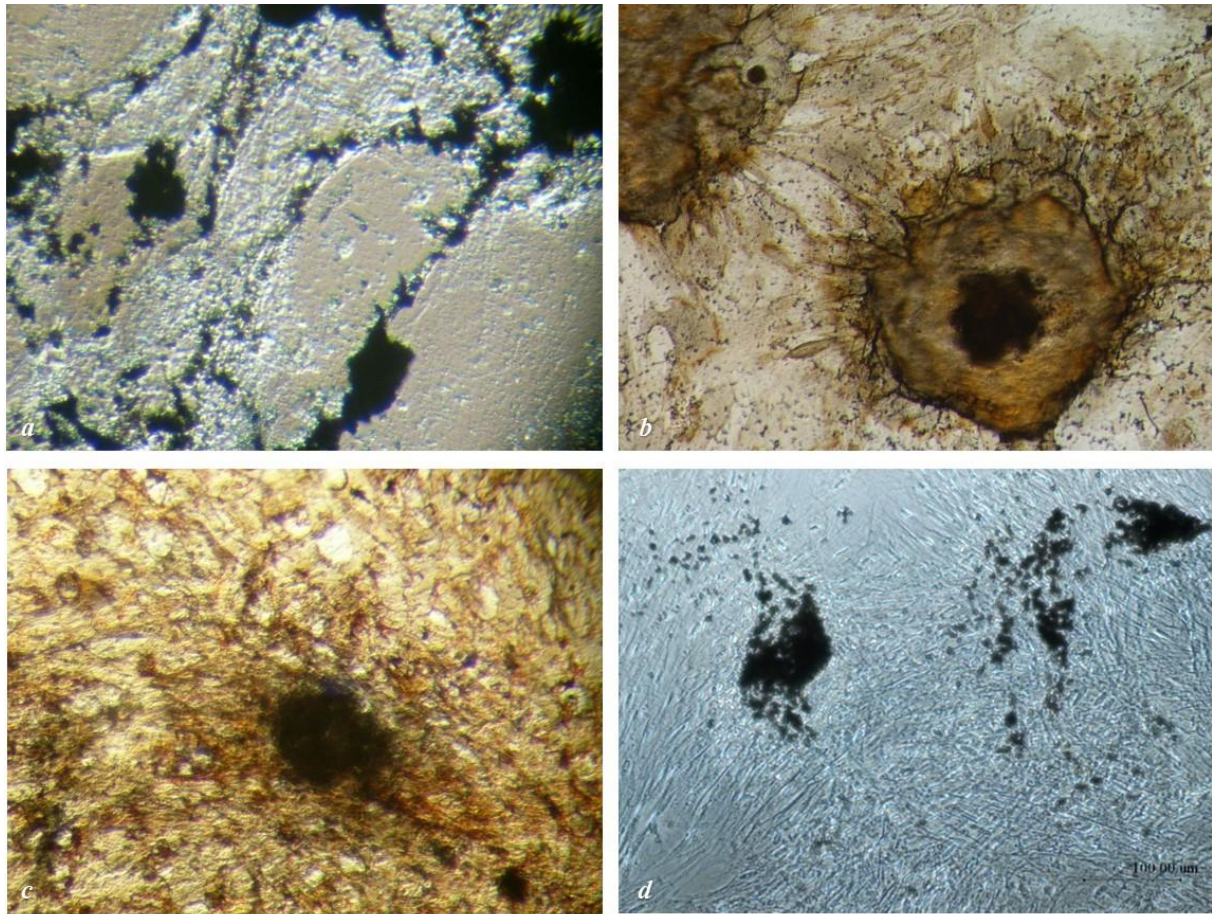


Figure 5.4. Osteogenic induction in UCB (*a*), WJ (*b*), BM (*c*) and AT-MSCs (*d*) over three weeks: von Kossa staining of extensive extracellular calcium deposition.

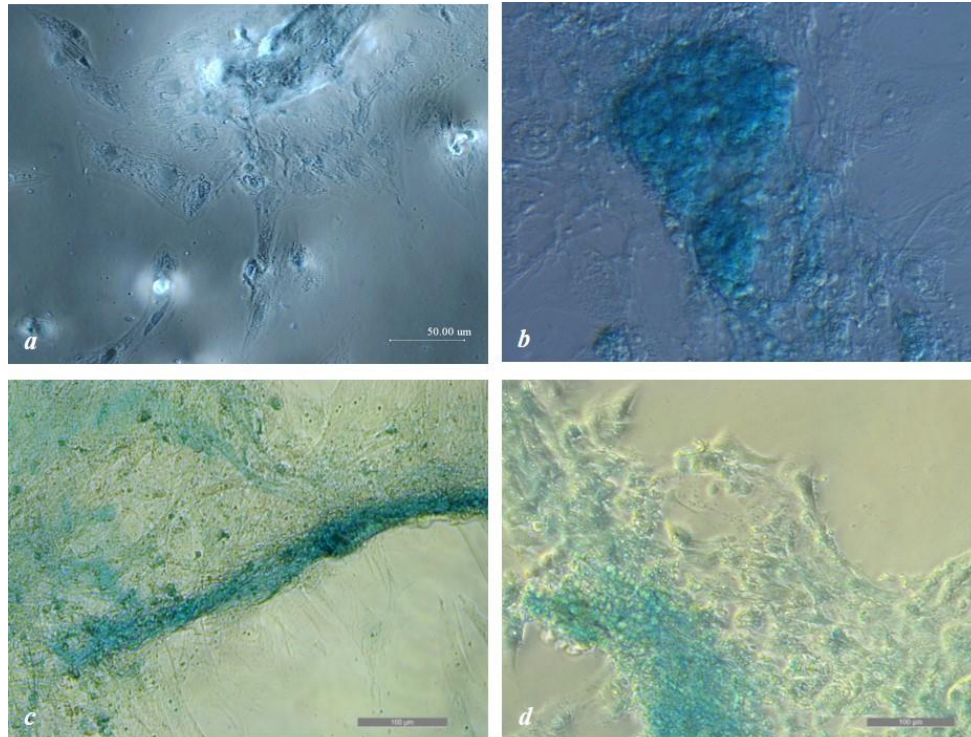


Figure 5.5. Chondrogenic induction in UCB (a), WJ (b), BM (c) and AT-MSCs (d) over three weeks: Alcian Blue staining of glycosaminoglycans in cartilage matrix.

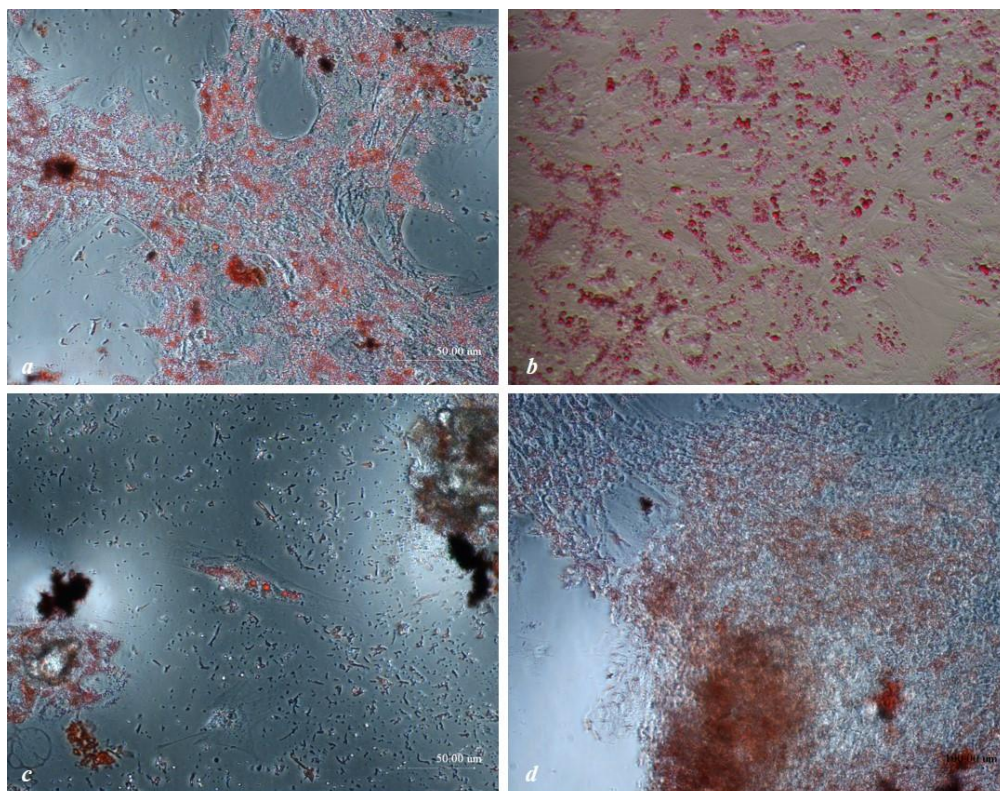


Figure 5.6. Adipogenic induction in UCB (a), WJ (b), BM (c) and AT-MSCs (d) over one week: Oil red O staining of extensive intracellular lipid droplet accumulation.

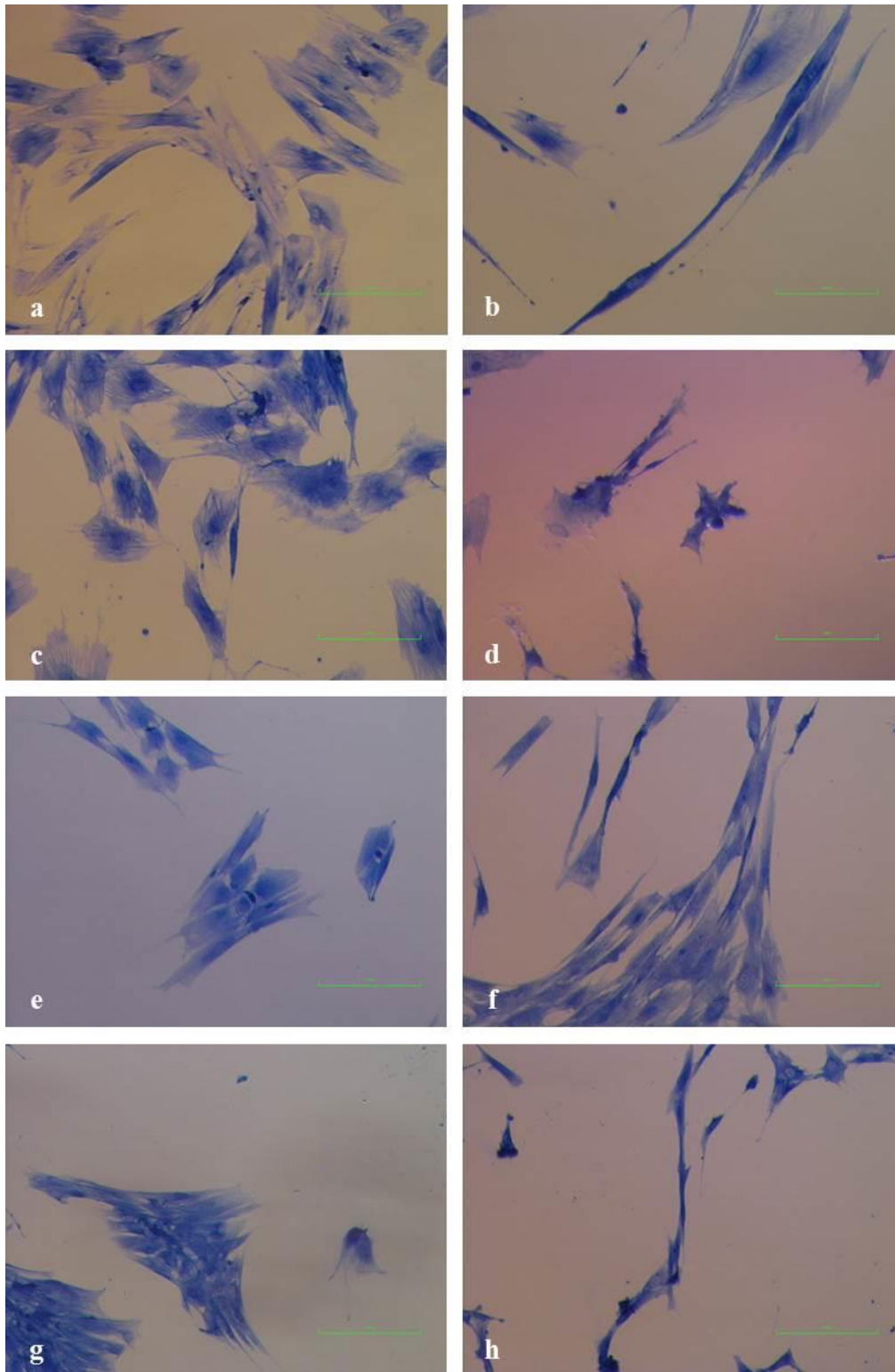


Figure 5.7. Tenogenic differentiation and staining with Aniline Blue method. UCB-MSCs control cells (a) and differentiated cells (b), WJ-MSCs control cells (c) and differentiated cells (d), BM-MSCs control cells (e) and differentiated cells (f) and AT-MSCs control cells (g) and differentiated cells (h).

BM-MSCs and UBC-MSCs showed the greater tenogenic potential; AT-MSCs showed an intermediate potential and WJ-MSCs showed the lower one.

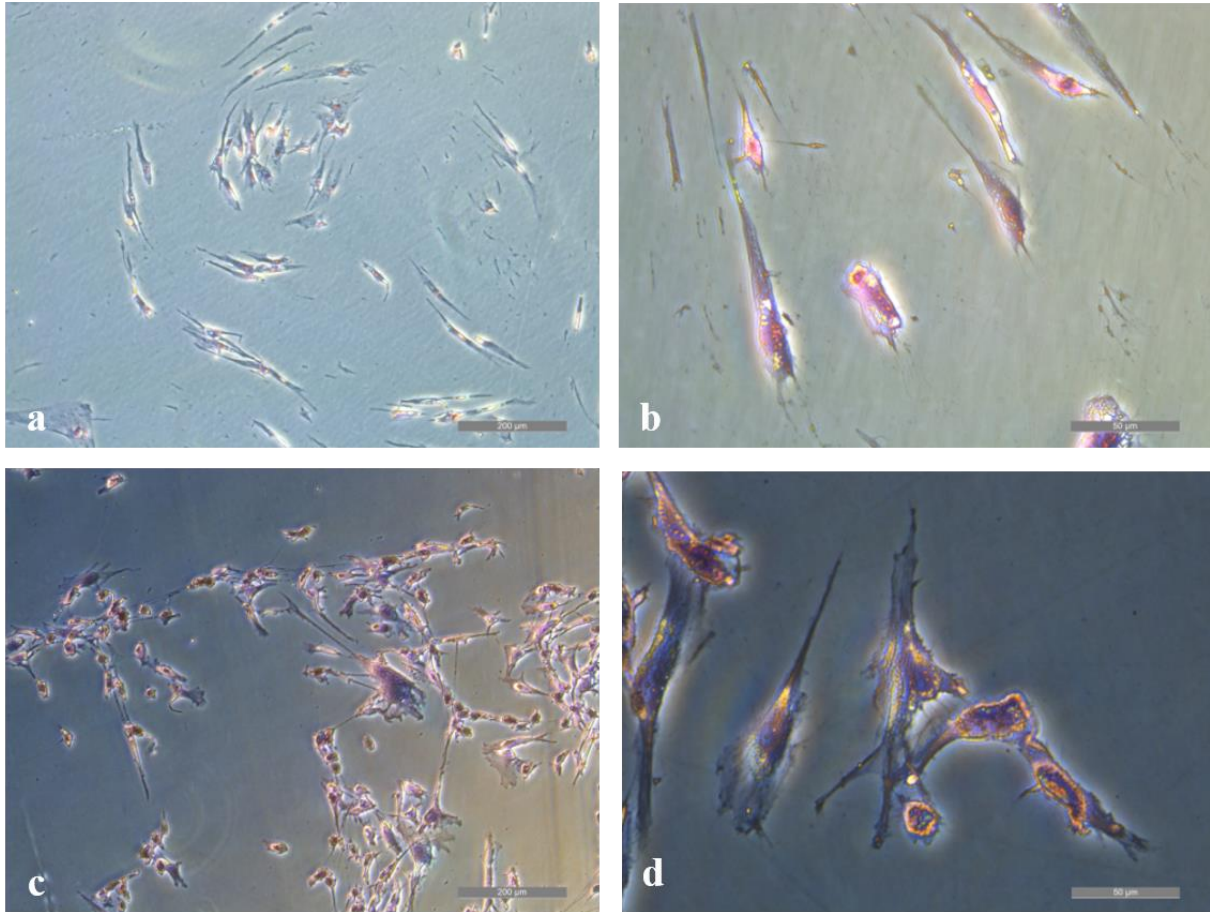


Figure 5.8. Tenogenic induction in AT-MSCs (**a**: magnification 10x; **b**: magnification 40x), BM-MSCs (**c**: magnification 10x; **d**: magnification 40x) over two weeks: Van Gieson staining.

Phenotypic and Molecular Analysis by Immunocytochemistry and PCR

Data observed by immunocytochemical staining of foetal and adult MSCs are showed in *Table 5.5*. Both cell lines clearly expressed the mesodermal marker alpha-SMA (*Figure 5.9 a, c, e, g*). On the contrary, UCB and BM- MSCs did not express the mesenchymal marker N-Cadherin (*Figure 5.9 b, d, f, h*). Data obtained by PCR were reported in *Table 5.6*.

	α-SMA	N-Cadherin
UCB	+	-
WJ	+	+
BM	+	-
AT	+	+

Table 5.5. Result about the expression of alpha-SMA and N-Cadherin in foetal and adult MSCs.

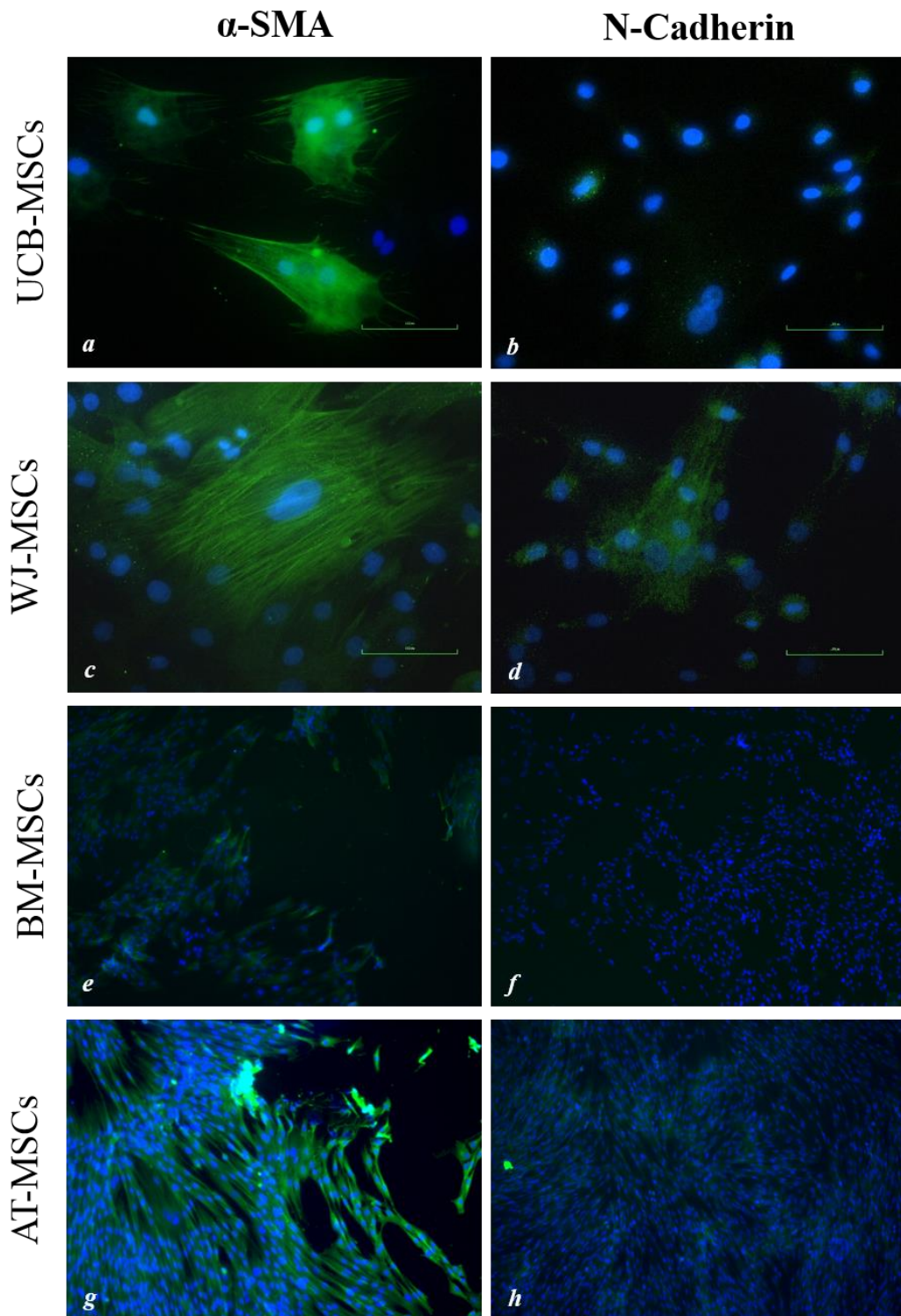


Figure 5.9. Photomicrographs of immunostaining of UCB, WJ, BM and AT-MSCs. Expression of the mesenchymal marker α -SMA in the UCB (*a*), WJ (*c*), BM (*e*) and AT-MSCs (*g*). Expression of the mesodermal marker α -SMA in the UCB (*a*), WJ (*c*), BM (*e*) and AT-MSCs (*g*). Expression of the mesenchymal marker N-Cadherin in the UCB (*b*), WJ (*d*), BM (*f*) and AT-MSCs (*h*).

Molecular Characterization

<u>Primers</u>	WJ-MSCs	UCB-MSCs	BM-MSCs	AT-MSCs
MSC marker				
CD90	+	+	+	+
CD73	+	-	+	-
Ematopoietic markers				
CD34	+	-	-	-
CD45	-	-	-	-
MHC markers				
MHC-I	+	+	+	+
MHC-II	-	-	-	-
ILs				
TNF α	-	-	-	-
IL-8	+	-	-	-
INF- γ	-	-	-	-
IL4	-	-	-	-
IL- β 1	+	-	-	-
IL-6	+	-	-	-
Pluripotency markers				
OCT4	+	-	-	-
NANOG	-	-	-	-
SOX2	-	-	-	-

Table 5.6. Results obtained by PCR running on foetal and adult MSCs.

Transmission Electron Microscopy (TEM)

Equine MSCs, obtained from umbilical cord blood, showed a fibroblast shape morphology with the nucleus and few nucleolus clearly detectable (*Figure 5.10A*). Localized in specific areas of the cytoplasm, several organelles such as Golgi apparatus surrounded by several vesicles (*Figure 5.10B*), rough endoplasmic reticulum (RER) (*Figure 5.10C*) and long mitochondria (*Figure 5.10D*) were well preserved and easily identified. Moreover, multivesicular bodies (*Figure 5.10B*) and lipid droplets (*Figure 5.10A* and *Figure 5.10B*) were observed in the cytoplasm. MSCs obtained from equine Wharton's jelly appeared with a spindle like morphology (*Figure 5.10E*) with the nucleus and nucleolus easily detectable (*Figure 5.10E*). At higher magnification, a regular RER and Golgi apparatus were observed (*Figure 5.10F* and *Figure 5.10G*). Several mitochondria with a long shape morphology and lipid droplets appeared widespread in the cytoplasm (*Figure 5.10E* and *Figure 5.10H*). MSCs collected from equine bone marrow showed a fibroblast like morphology comparable to the cells obtained from embryonal annexes tissues (*Figure 5.11A*). The cytoplasm was characterized by the presence of a widespread Golgi apparatus surrounded by several small vesicles (*Figure 5.11B*) and multivesicular bodies (*Figure 5.11B* insert). An extensive RER with enlarged membrane free from ribosomes and elongated mitochondria were well detected (*Figure 5.11C*) in the cytoplasm. Several cluster of extracellular vesicles and exosomes were observed on cell membrane (*Figure 5.11D*). MSCs collected from equine adipose tissues showed a well preserved morphology, with an elongated spindle body comparable to the cells obtained from equine bone marrow (*Figure 5.11E*). Golgi apparatus was widespread in the cytoplasm and several vesicles, organized in multivesicular bodies, were observed (*Figure 5.11F*). RER showed enlarged membranes almost free from ribosomes (*Figure 5.11G*). Several extracellular vesicles and exosomes were localized on the cell membrane (*Figure 5.11H*).

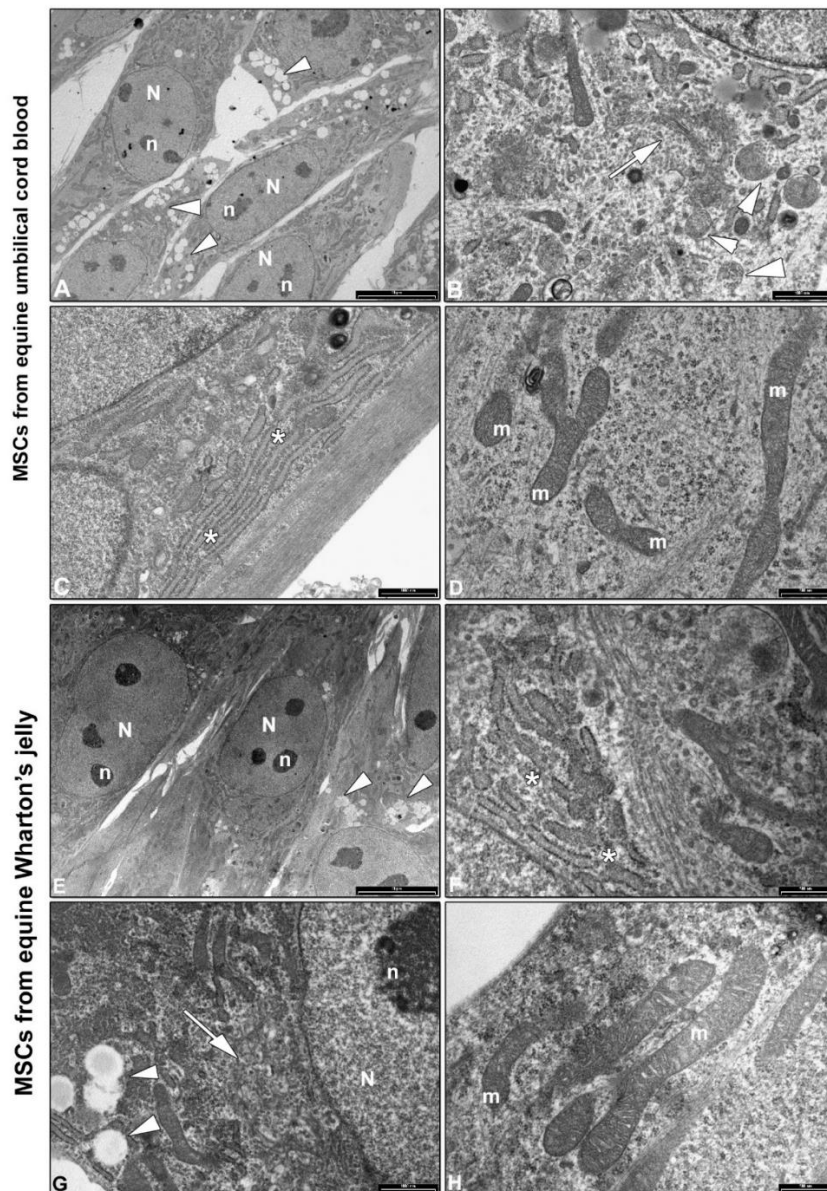


Figure 5.10. TEM analysis of equine UCB-MSCs. (A) cells showed a spindle morphology (N: nucleus; n: nucleolus; arrowhead: lipid droplets) (magnification 1950X; bar: 10 μ m); (B) the Golgi apparatus (arrow) surrounded by several vesicles and multivesicular bodies (white arrowheads) are observed (magnification: 13500X; bar: 1 μ m); (C) cytoplasmic area showing a regular RER (*) (magnification: 13500X; bar: 1 μ m); (D) Elongated mitochondria with evident internal cristae (m) (magnification: 19000X; bar: 500nm). TEM analysis of equine WJ-MSCs. (A) cells showed a fibroblast like morphology (N: nucleus; n: nucleolus; arrowheads: lipid droplets) (magnification 1950X; bar: 10 μ m); (B) cytoplasmic area showing a regular RER (*) (magnification: 13500X; bar: 1 μ m); (C) the Golgi apparatus (arrow) surrounded by several vesicles (N: nucleus; n: nucleolus; arrowheads: lipid droplets) (magnification: 13500X; bar: 1 μ m); (D) Elongated mitochondria with regular internal cristae (m) (magnification: 19000X; bar: 500nm).

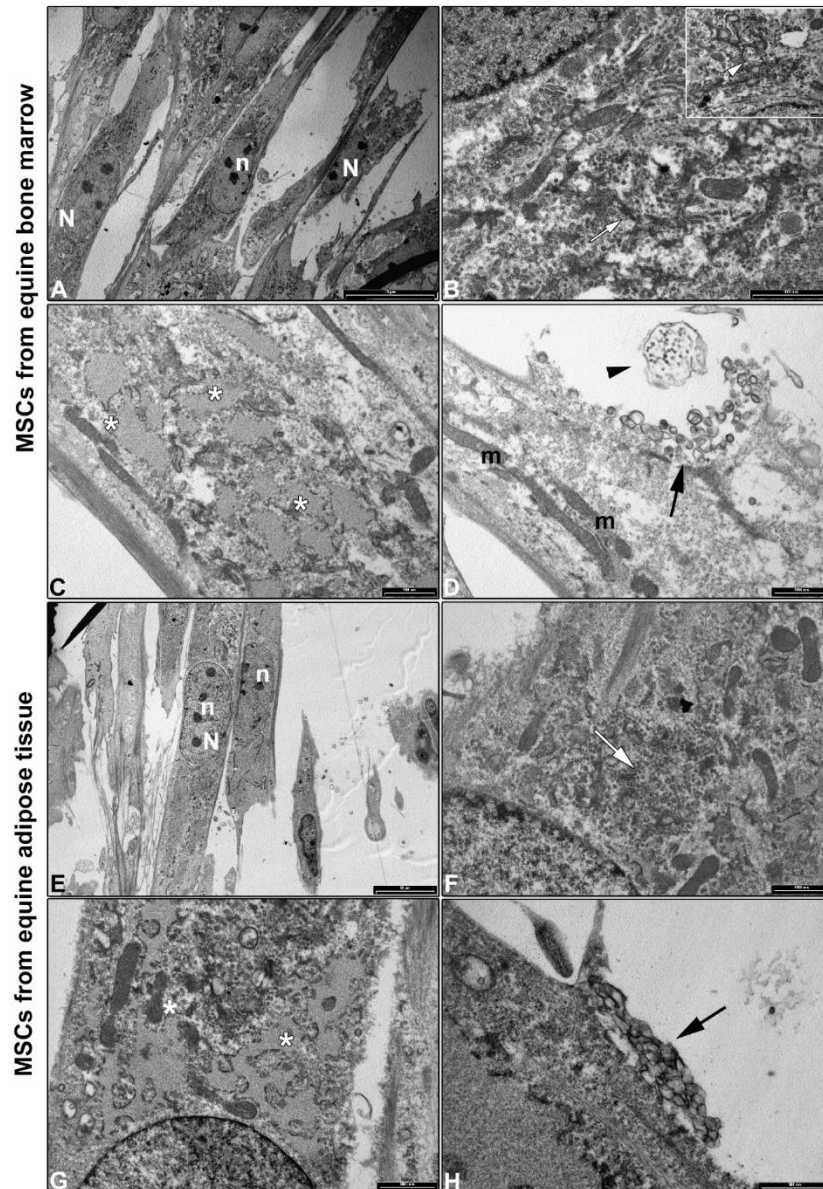


Figure 5.11. TEM analysis of equine BM-MSCs. (A) cells showed a fibroblast like morphology (N: nucleus; n: nucleolus) (magnification 1100X; bar: 20um); (B) the Golgi apparatus (arrow) surrounded by several vesicles (insert; magnification: 13500X; bar: 1um) are observed (magnification: 13500X; bar: 1um); (C) cytoplasmic area showing an enlarged RER (*) almost free from ribosomes (magnification: 19000X; bar: 500 nm); (D) exosomes (black arrows) clustered on cell membrane, extracellular vesicles (arrowheads) and elongated mitochondria (m) are detected (magnification: 13500X; bar: 1um). TEM analysis of equine AT-MSCs. (E) the cells showed a fibroblast like morphology (N: nucleus; n: nucleolus) (magnification 1450X; bar: 10um); (F) the Golgi apparatus (arrow) surrounded by several vesicles (magnification: 13500X; bar: 1um) is observed; (G) the cytoplasmic area showing RER with dilated membranes (*) (magnification:

13500X; bar: 1µm); (D) exosomes (black arrow) clustered on cell membrane (magnification: 19000X; bar: 500nm).

Discussion

In this study, MSCs from foetal (UCB and WJ) and adult tissue (BM and AT) were isolated and many features were compared: proliferation, migration, spheroids formation, differentiation capacity, expression of stemness markers, immunophenotype and ultrastructural features. Both foetal and adult MSCs were isolated, cultivated with standard protocols and they did not show statistical differences for CD and DT; however, in this study we considered only the first three passages of culture. All isolated cells showed the typical mesenchymal morphology. No differences were found between foetal and adult MSCs in migration ability.

At P3 all cells were differentiated to evaluate their osteogenic, chondrogenic and adipogenic. For the first time in equine species, cells from foetal adnexa were differentiated toward tenogenic line. Since the adhesion capability is related and enhanced to chondrogenic differentiation potential (Wang et al., 2009; Kavanagh et al., 2014; Sart et al., 2014), in the present study, the spheroid formation capability in vitro was assessed using the hanging drop method. Furthermore, the spheroids volume were determined by ReVisp (Bellotti et al., 2016). Cells derived from WJ showed a higher adhesion ability, forming smaller spheroids. Cells derived from umbilical cord blood were not able to give origin to a unique spheroid; in fact, they always create multiple small spheroids. According to these findings and to previous studies (Wang et al., 2009; Kavanagh et al., 2014; Sart et al., 2014), WJ-MSCs showed the highest chondrogenic and osteogenic differentiation potential, related to UCB-MSCs and adult cells. On the contrary, cells isolated from fluid matrix (BM and UCB) showed a higher ability to differentiate in tenocytes, while WJ-MSCs showed the lower one. It's still not clear

if this minor differentiation potential is due to a not suitable tenogenic induction protocol or because cells are not enough stimulated.

ICC investigation showed in all cell lines a positive expression of the mesodermal marker alpha-SMA. However, the ICC results regarding the expression of N-Cadherin by cells derived from fluid matrix (UCB and BM) are controversial: in fact, these cells presented a low expression of this typical mesenchymal marker. Further investigation on other samples are therefore necessary.

Regarding molecular analysis, foetal and adult MSCs at P3, demonstrate the characteristics defined by the International Society for Cellular Therapy (Dominici et al., 2006). Excepting for WJ-MSCs, all cells line resulted negative for CD34. As recently demonstrated, the expression of CD34 seems to depend on the environment, on the in vitro culture cell passages (Lin et al., 2012) and on the cell source. Furthermore, WJ-MSCs were the unique that expressed OCT-4, IL-8, IL- β 1 and IL-6. The OCT-4 is a typical marker of embryonic pluripotent cells (Miki et al., 2005; Izumi et al., 2009; De Coppi et al., 2007; Pirjali et al., 2013; Shaer et al., 2014) and it should not be expressed by MSCs. However, its expression, associated with the high differentiative potential of WJ-MSCs give them an intermediate characteristic between foetal and embryonic. IL-1 β , IL-6 and IL-8 are important mediator of the inflammatory response, involved in a variety of cellular activities, including cell proliferation, differentiation, apoptosis, chemotaxis, angiogenesis and hematopoiesis (Lamallice et al., 2007). These factors are involved in the complex interaction between MSCs and the tissue microenvironment as well as production of membrane vesicles, containing molecules such as short peptides, proteins, lipids, and various forms of RNAs (György et al., 2011). Their expression by WJ-MSCs make these cells the best choice for the application in regenerative medicine, also for the non-invasive collection of WJ. In fact, umbilical cord is

routinely discarded at parturition, and in our study no side effects for mare and foal were observed. Furthermore, at RT-PCR, all the cells resulted negative to TNF- α , IL-4 and INF, cytokines produced only after in vitro stimulation (De Schauwer et al., 2014).

All cells derived from all sources at TEM showed an elongated spindle body, a characteristic morphology of mesenchymal stem cells.

In adult equine cells, it was reported that the great number of vacuolar bodies that, actually, were not empty but contained small, medium and large intraluminal vesicles maturing from their internal membrane, might be interpreted as the ability of both cell types to produce a huge variety of “secreting” molecules (Pascucci et al., 2014). In this study as well, numerous intra and extracellular vacuolar bodies in foetal MSCs were found. These vesicles, originated from the internal layer of the cell membrane, had different dimensions (small, medium and big), containing a material of unknown composition. As demonstrated by other authors, they have the role of collecting efficiently cellular components: since cells have an intense replicative and metabolic capacity, they continuously need a renovation of their structures. Recent studies support the idea that these microvesicles contain some substances, made by the cell itself, that have a fundamental role in stimulating healing processes in damaged tissues (Du et al., 2014; Lange-Consiglio et al., 2016), and have also immunomodulatory activities (Aliotta et al., 2012).

At the present day, they are subject of many studies because it is thought that they have communication roles between cells: releasing their content, they provide lipids, proteins and mRNA/microRNA to damaged cells, helping the restore of their integrity (Simons et al., 2009; Camussi et al., 2010; Gyorgy et al., 2011).

In this study in AT and BM-MSCs, intracellular vesicular bodies were not found, but Bruno et al. (2013) reported that these are present in human BM-MSCs. MVs have a membrane, and

they have to be released in the extra cellular space in order to play their role, so they can bound to target cells using a specific receptor (Bruno et al., 2009). Once they have released their content, it is dispersed into the culture medium: if damaged cells are put in this “conditioned” culture medium, it is evident how it plays a therapeutic role on them, acting in a paracrine way (Bi et al., 2007). In the present study, we observed extracellular vesicles in BM-MSCs.

Even if there is a lot of interest for microvesicles, a lot has to be discovered, so further studies are necessities especially in equine medicine, in order to confirm their role in healing and immunomodulatory processes and their possible use in regenerative medicine.

In conclusion, it seems that foetal MSCs, especially WJ-MSCs, are the best source of stem cells in comparison with adult MSCs thanks to their characteristics. In particular, as for human also for the equine species, the cellular banking for Wharton’s Jelly, as Mesenchymal Stem cells niche, could be very useful. Both in human and equine species, mesenchymal stem cells (MSCs) from perinatal tissue, primarily Wharton’s jelly (WJ), may be particularly useful in the clinic for autologous transplantation for newborns and after banking in later stages of life.

References

- Aliotta J.M., Lee D., Puente N., Faradyan S., Sears E.H., Amaral A., Goldberg L., Dooner M.S., Pereira M., Quesenberry P.J., (2012). *Progenitor/ stem cell fate determination: interactive dynamics of cell cycle and microvesicles*. *Stem Cells Dev*; 21 (10), 1627-1638.
- Bellotti C., Duchi S., Bevilacqua A., Lucarelli E., Piccinini F., (2016). *Long term morphological characterization of mesenchymal stromal cells 3D spheroids built with a rapid method based on entry-level equipment*. *Cytotechnology*; 68 (6), 2479-2490.
- Bi B., Schmitt R., Israilova M., Nishio H., Cantley L.G., (2007). *Stromal cells protect against acute tubular injury via an endocrine effect*. *J Am Soc Nephrol*; 18 (9), 2486-2496.
- Bourzac C., Smith L.C., Vincent P., Beauchamp G., Lavoie J.P., Laverty S., 2010. *Isolation of equine bone marrow-derived mesenchymal stem cells: a comparison between three protocols*. *Equine Vet J*; 42 (6), 519-527.
- Bruno S., Collino F., Deregibus M.C., Grange C., Tetta C., Camussi G., (2013). *Microvesicles Derived from human bone marrow Mesenchymal Stem Cells inhibit tumor growth*. *Stem Cells Dev*; 22 (5), 758-771.
- Bruno S., Grange C., Deregibus M.C., Calogero R.A., Saviozzi S., Collino F., Camussi G., (2009). *Mesenchymal stem cell-derived microvesicles protect against acute tubular injury*. *J Am Soc Nephrol*; 20 (5), 1053-1067.
- Burk J., Ribitsch I., Gittel C., Juelke H., Kasper C., Staszky C., Brehm W., (2013). *Growth and differentiation characteristics of equine mesenchymal stromal cells derived from different sources*. *Vet J*; 195(1): 98–106.

Camussi G., Deregibus M.C., Bruno S., Cantaluppi V., Biancone L., (2010). *Exosomes/microvesicles as a mechanism of cell-to-cell communication*. *Kidney Int*; 78 (9), 838-848.

Castagnetti C., Mariella J., Pirrone A., Cinotti S., Mari G., Peli A., (2012). *Expression of interleukin-1 β , interleukin-8, and interferon- γ in blood samples obtained from healthy and sick neonatal foals*. *Am J Vet Res*; 73(9): 1418–1427.

Corradetti B., Lange-Consiglio A., Barucca M., Cremonesi F., Bizzarro D., (2011). *Size-sieved subpopulations of mesenchymal stem cells from intervacular and perivascular equine umbilical cord matrix*. *Cell Prolif*; 44(4): 330–342.

De Coppi P., Bartsch G., Siddiqui M.M., Xu T., Santos C.C., Perin L., Mostoslavsky G., Serre A.C., Snyder E.Y., Yoo J.J., Furth M.E., Soker S., Atala A., (2007). *Isolation of amniotic stem cell lines with potential for therapy*. *Nat Biotechnol* 2007; 25(1): 100-106.

De Schauwer C, Goossens K, Piepers S, Hoogewijs MK, Govaere JIJ, Smits K, Meyer E, Van Soom A, Van de Walle G., (2014). *Characterization and profiling of immunomodulatory genes of equine mesenchymal stromal cells from non invasive sources*. *Stem Cell Reas Ther*; 5(1): 6.

Desmarais J., Demers S., Suzuki J.J., Laflamme S., Vincent P., Laverty S., Smith L., (2011). *Trophoblast stem cell marker gene expression in inner cell mass-derived cells from parthenogenetic equine embryos*. *Reprod Camb Engl*; 141(3): 321–332.

Dominici M., Le Blanc K., Mueller I., Slaper-Cortenbach I., Marini F., Krause D. Deans R., Keating A., Prockop D., Horwitz E., (2006). *Minimal criteria for defining multipotent mesenchymal stromal cells. The International Society for Cellular Therapy position statement*. *Cytotherapy*; 8(4): 315-317.

Du T., Ju G., Wu S., Cheng Z., Cheng J., Zou X., Zhang G., Miao S., Liu G., Zhu Y., (2014). *Microvesicles derived from human Wharton's jelly mesenchymal stem cells promote human renal cancer cell growth and aggressiveness through induction of hepatocyte growth factor*. PloSOne; 9 (5), e96836.

György B., Szabó T.G., Pásztói M., Pál Z., Misják P., Aradi B., László V., Pállinger E., Pap E., Kittel A., Nagy G., Falus A., Buzás E.I., (2011). *Membrane vesicles, current state-of-the-art: emerging role of extracellular vesicles*. Cell Mol Life Sci; 68 (16), 2667-2688.

Iacono E., Brunori L., Pirrone A., Pagliaro P.P., Ricci F., Tazzari P.L., Merlo B., (2012). *Isolation, characterization and differentiation of mesenchymal stem cells from amniotic fluid, umbilical cord blood and Wharton's jelly in the horse*. Reprod Camb Engl; 143(4): 455–468.

Izumi M., Pazin B.J., Minervini C.F., Gerlach J., Ross M.A., Stolz D.B., (2009). *Turner ME, Thompson RL, Miki T. Quantitative comparison of stem cell marker-positive cells in fetal and term human amnion*. J Reprod Immunol; 81(1): 39-43.

Kavanagh D., Robinson J., Kalia N., (2014). *Mesenchymal stem cell priming: fine-tuning adhesion and function*. Stem Cell Rev; 10(4): 587–599.

Lamallice L., Le Boeuf F., Huot J., (2007). *Endothelial cell migration during angiogenesis*. Circ Res; 100(6): 782–794.

Lange-Consiglio A., Perrini C., Tasquier R., Deregibus M.C., Camussi G., Pascucci L., Marini M.G., Corradetti B., Bizzaro D., De Vita B., Romele P., Parolini O., Cremonesi F., (2016). *Equine amniotic microvesicles and their anti-inflammatory potential in a tenocyte model in vitro*. Stem Cells Dev; 25 (8), 610-621.

Miki T., Lehmann T., Cai H., Stolz D.B., Strom S.C., (2005). *Stem cell characteristics of amniotic epithelial cells*. Stem Cells; 23(10): 1549-1559.

Mizuno H., Hyakusoku H., (2003). *Mesengenic potential and future clinical perspective of human processed lipoaspirate cells*. J Nippon Med Sch; 70(4): 300–306.

Mohanty N., Gulati B., Kumar R., Gera S., Kumar P., Somasundaram R., Kumar S., (2014). *Immunophenotypic characterization and tenogenic differentiation of mesenchymal stromal cells isolated from equine umbilical cord blood*. Vitro Cell Dev Biol Anim; 50(6): 538–548.

Pascucci L., Alessandri G., Dall’Aglia C., Mercati F., Cloliolo P., Bazzucchi C., Dante S., Petrini S., Curina G., Ceccarelli P., (2014). *Membrane vesicles mediate pro-angiogenic activity of equine adipose-derived mesenchymal stromal cells*. Vet J; 202(2); 361–366.

Pirjali T., Azarpira N., Ayatollahi M., Aghdaie M.H., Geramizadeh B., Talai T., (2013). *Isolation and characterization of human mesenchymal stem cells derived from human umbilical cord Wharton’s jelly and amniotic membrane*. Int J Organ Transplant Med; 4(3): 111-116.

Rainaldi G., Pinto B., Piras A., Vatteroni L., Simi S., Citti L., (1991). *Reduction of proliferative heterogeneity of CHEF18 Chinese hamster cell line during the progression toward tumorigenicity*. Vitro Cell Dev Biol; 27A(12): 949–952.

Rossi B., Merlo B., Colleoni S., Iacono E., Tazzari P.L., Ricci F., Lazzari G., Galli C., (2014). *Isolation and in vitro characterization of bovine amniotic fluid derived stem cells at different trimesters of pregnancy*. Stem Cell Rev; 10(5): 712–724.

Sart S., Tsai A., Li Y., Ma T., (2014). *Three-dimensional aggregates of mesenchymal stem cells: cellular mechanisms, biological properties, and applications*. Tissue Eng. Part B Rev. 20(5): 365–380.

Shaer A., Azarpira N., Aghdaie M.H., Esfandiari E., (2014). *Isolation and characterization of human mesenchymal stromal cells derived from plavental deciduas basalis; umbilical cord Wharton's Jelly and amniotic membrane*. Pak J Med Sci; 30(5): 1022-1026.

Simons M., Raposo G., (2009). *Exosomes-vesicular carriers for intercellular communication*. Curr Opin Cell Biol; 21(4) 575-581.

Visser M., Pollitt C., (2011). *Lamellar leukocyte infiltration and involvement of IL-6 during oligofructose-induced equine laminitis development*. Vet Immunol Immunopathol; 144(1-2): 120–128.

Wang W., Itaka K., Ohba S., Nishiyama N., Chung U., Yamasaki Y., Kataoka K., (2009). *3D spheroid culture system on micropatterned substrates for improved differentiation efficiency of multipotent mesenchymal stem cells*. Biomaterials; 30(14): 2705–2715

SECTION III- Clinical Application

CHAPTER 6

EFFECTS OF AMNIOTIC FLUID MESENCHYMAL STEM CELLS IN CARBOXYMETHYL CELLULOSE GEL ON HEALING OF SPONTANEOUS PRESSURE SORES: CLINICAL OUTCOME IN SEVEN HOSPITALIZED NEONATAL FOALS.

Iacono E., **Lanci A.**, Merlo B., Ricci F., Pirrone A., Antonelli A., Mariella J., Castagnetti C.
Turkish Journal of Biology (2016) 40:484-492



Effects of amniotic fluid mesenchymal stem cells in carboxymethyl cellulose gel on healing of spontaneous pressure sores: clinical outcome in seven hospitalized neonatal foals

Eleonora IACONO^{1*}, Aliai LANCI¹, Barbara MERLO¹, Francesca RICCI², Alessandro PIRRONE³,
 Carlotta ANTONELLI³, Jole MARIELLA¹, Carolina CASTAGNETTI¹

¹Department of Veterinary Medical Sciences, University of Bologna, Bologna, Italy

²Immunohematology and Transfusion Center, Policlinico S. Orsola-Malpighi, Bologna, Italy

³Bologna, Italy

Received: 31.07.2015 • Accepted/Published Online: 13.10.2015 • Final Version: 23.02.2016

Abstract: In the present study, an innovative therapy for spontaneously arisen pressure sores in seven hospitalized neonatal foals is described, using mesenchymal stem cells obtained from equine amniotic fluid. Amniotic fluid mesenchymal stem cells (AFMSCs) were isolated from fluid samples recovered at delivery. Heterologous cells, at passage three of *in vitro* culture, were applied to sores twice a week for four consecutive times in a carboxymethylcellulose (CMC) gel. As a control, a commercial ointment was used. The results showed that the mean sore regression rate with AFMSCs in CMC gel was statistically higher than the mean value recorded in the control group. This was associated with a significant effect of the treatment used and a statistically significant effect of treatment over time. The results suggest that local application of mesenchymal stem cells isolated from amniotic fluid, using CMC as scaffold, could be considered as an effective treatment of deep sores in hospitalized neonatal foals.

Key words: Equine, amniotic fluid, mesenchymal stem cells, wound healing, carboxymethylcellulose

1. Introduction

The mechanical forces involved in the pathogenesis of pressure sores are locally exerted pressure, friction, and tension forces, which occur when the patient is lifted or put in decubitus (Kanj et al., 1998; Agrawal and Chauhan, 2012). Other predisposing factors are malnutrition and skin moisture (Fader et al., 2003; Hendrickson, 2011; Agrawal and Chauhan, 2012). Neonatal foals are particularly prone to this kind of injury, due to their thin skin and possible concomitant disorders, which force them into prolonged decubitus (Knottenbelt, 2009). Moreover, foals' sores could be a consequence of casts and rigid splints application for treating flexural deformities. After skin injury, a new epithelium has to form in order to close the wound and restore the skin's function. This requires the proliferation and directional migration of keratinocytes, fibroblasts, and mesenchymal stem cells (MSCs) (Balbino et al., 2005). MSCs are essential for skin homeostasis and repair by promoting cell differentiation, immunomodulation, secretion of growth factors to drive reepithelialization and neovascularization, and modulation of resident stem cells (Fuchs and Horsley, 2008; Balaji et al., 2012). In human

medicine, different studies have also focused on the use of MSCs in skin care (Wu et al., 2007; Gianaroli et al., 2009; Sorrell et al., 2010).

In horses, despite the fact that extended wounds of the distal limbs are one of the most common dermatological lesions, which tend to have a long recovery period and poor response to conventional therapies, only a few papers exist on the use of regenerative therapy. Recently, Spaas et al. (2013) reported the successful use of peripheral blood stem cells for treating large wounds on the legs of four horses not responding to conventional therapies.

Amniotic fluid mesenchymal stem cells (AFMSCs), due to their differentiation potential, may be an exciting source of regenerative cells (Tsai et al., 2004; Perin et al., 2007). Our research group demonstrated their potential in skin wound repair, associated with platelet-rich plasma (PRP; Iacono et al., 2012b).

Due to the difficult healing of pressure sores in foals, in the present study the effectiveness of local application of allogenic equine AFMSCs, using carboxymethylcellulose (CMC) gel as a scaffold, was compared to an ointment based on formosulfathiazole, usually employed in our

* Correspondence: eleonora.iacono2@unibo.it

IACONO et al. / Turk J Biol

equine perinatology unit (EPU) in the treatment of pressure sores spontaneously arisen in neonatal foals.

2. Materials and methods

2.1. Animals

All experimental procedures were approved by the local ethics committee and the Italian Ministry of Health. All procedures were carried out with due care for animal welfare and oral consent was provided by the owners.

Foals between 10 and 15 days old and hospitalized at the EPU "Stefano Belluzzi" of the Department of Veterinary Medical Sciences, University of Bologna, during the 2012 breeding season were considered.

2.2. Experimental design

Before starting treatments, Sessing classification (Table 1; Ferrell et al., 1995) and National Pressure Ulcer Advisory Panel (NPUAP; Table 2; Bluestein and Javaheri, 2008) criteria, usually employed in human medicine, were applied to determine the severity of treated sores. In the literature, specific classifications for horse sores are not reported. In particular, Sessing classification was used to

classify sores according to macroscopic appearance, while NPUAP criteria were used for the depth degree. After classification, sores were divided into two groups: Group 1, treated with local application of AFMSCs in CMC gel; Group 2 (control), treated with formsulfathiazole ointment. To evaluate the similar distribution of sores between groups and their homogeneity, a Student t-test for paired variable (SPSS 20.0) was performed before starting treatments.

In Group 1, treatment was applied twice a week for four consecutive times; in Group 2, ointment applications were performed every 48 h. In both groups, after day 30, limbs were no longer bandaged and no further treatments were applied.

2.3. Mesenchymal stem cell isolation and culture

All chemicals were obtained from Sigma-Aldrich (St. Louis, MO, USA) and plastic dishes and tubes from Sarstedt Inc. (Newton, NC, USA), unless otherwise noted.

Mares between 6 and 15 years of age and housed at the EPU for delivery were enrolled. All mares had a normal pregnancy, followed by spontaneous delivery, and all

Table 1. Sessing classification of skin wounds (Ferrell et al., 1995).

Stage	Description
0	Normal skin, but at risk.
1	Intact skin, but hyperpigmented or reddened.
2	The bottom and edges of the ulcer are intact and not red.
3	The bottom and edges of the ulcer with pink granulation tissue, modest presence of exudate and odor.
4	Presence of modest granulation tissue, initial and modest necrotic tissue, moderate exudate and odor.
5	Abundant presence of foul smelling exudate, necrotic eschar, and whitish or reddish edges.
6	Further ulceration around the primary ulcer, purulent exudate, intense odor, presence of necrotic tissue and systemic symptoms of sepsis.

Table 2. Classification of the National Pressure Ulcer Advisory Panel (NPUAP; Bluestein and Javaheri, 2008).

Stage	Description
1	Intact skin with nonblanchable redness of a localized area usually over a bony prominence. Darkly pigmented skin may not have visible blanching; its color may differ from the surrounding area. The area may be painful, firm, soft, warmer, or cooler as compared to adjacent tissue.
2	Partial thickness loss of dermis presenting as a shallow open ulcer with a red pink wound bed, without slough. May also present as an intact or open/ruptured serum-filled or serosanguineous filled blister. Presents as a shiny or dry shallow ulcer without slough or bruising.
3	Full thickness tissue loss. Subcutaneous fat may be visible but bone, tendon, or muscle are not exposed. Slough may be present but does not obscure the depth of tissue loss. May include undermining and tunneling.
4	Full thickness tissue loss with exposed bone, tendon, or muscle. Slough or eschar may be present. Often includes undermining and tunneling. The ulcer can extend into muscle and/or supporting structures (e.g., fascia, tendon, or joint capsule), making osteomyelitis or osteitis likely to occur. Exposed bone/muscle is visible or directly palpable.

neonatal foals had an APGAR score between 9 and 10 (Vaala et al., 2002) within 10 min of birth.

Amniotic fluid samples were taken shortly after the foal or the amniotic membrane passed through the vulva, stored at 4 °C, and processed within 12 h, as previously described (Iacono et al., 2012a). Briefly, each sample was diluted 1:1 with Dulbecco's phosphate buffer solution containing antibiotics (100 IU mL⁻¹ penicillin and 100 µg mL⁻¹ streptomycin). The obtained solution was centrifuged for 15 min at 470 × g (Heraeus Megafuge 1.0R; rotor: Heraeus # 2704) and the obtained pellet was resuspended in 5 mL of culture medium containing Dulbecco's modified Eagle's medium (DMEM) and tissue culture medium (TCM199) (1:1), plus 10% (v/v) fetal bovine serum (GIBCO, Invitrogen Corporation, Carlsbad, CA, USA) and antibiotics. Mononuclear cells were isolated by centrifuging the sample on 5 mL of 70% Percoll solution (30 min at 1880 × g). The interphase was collected, diluted with 5 mL of culture medium, and centrifuged at 470 × g for 10 min. The supernatant was aspirated and cells were washed with culture medium a second and third time. Cells were then resuspended in 1 mL of culture medium and counted by hemocytometer. Primary cells were plated in a 25-cm² flask at a maximum density of 5 × 10⁴ cells/cm² and incubated in a 5% CO₂ humidified atmosphere at 38.5 °C. The medium was completely replaced after 24 h in order to remove nonadherent cells. Afterwards, the medium was completely replaced every 3 days until the adherent cell population reached ~80% confluence. At this point, the adherent primary MSCs were passed by digestion with 0.05% (w/v) trypsin, counted with a hemocytometer, and reseeded as "Passage 1" (P1) at 25 × 10³ cells/cm². Cells at P3 were used for clinical applications. The culture was maintained until the administration of the cell therapy (P3). Prior to the cellular use, an aliquot of cells (P3) was collected to perform immunophenotypic characterization, testing the following markers: CD44, CD90, and MHC Class I and II (Iacono et al., 2012a, 2014). Furthermore, the AFMSCs' negative expression for hematopoietic marker CD34 was assessed. Adipogenic, chondrogenic, and osteogenic differentiations were also performed to demonstrate the multipotent potential of the cells used.

2.4. Staging of preparations for MSC application

Immediately before application, under a laminar flow hood and in sterile conditions, AFMSCs were detached from the flask and cells were counted using a hemocytometer. For each application, approximately 5 × 10⁵ cells/mL were used. A gel of CMC used as a scaffold was produced in a sterile petri dish under a laminar flow hood using 5 g of CMC and 5 mL of DMEM/TCM199. Once formed, the gel was placed for 30 min under a UV lamp to avoid bacterial contamination and to break the medium amino acid chains, which could affect skin healing. Immediately

before treatment, cells were added to the gel.

Before applying MSCs, wounds were rinsed with isotonic sterile saline (0.9% NaCl) solution. The skin around the wounds was greased with Vaseline to prevent further damage at the time of the next dressing. Immediately after application, the limb was bandaged with cotton gauze, a bandage, and VetRap (3M, Milan, Italy).

2.5. Staging of preparations for ointment cutaneous application

As a control, formsulfathiazole, derived from sulfathiazole and formaldehyde condensation and usually employed in our unit for pressure sore treatment (unpublished data), was used (Socatil Cavallo, Acme Srl, Reggio Emilia, Italy). Due to its poor solubility in water, it is poorly absorbed, and it is therefore suitable for topical use. Before applying the ointment, sores were treated as described above, and after treatment application, the limb was bandaged.

2.6. Assessment of healing and statistical analysis

In Group 1 and 2 wound areas were photographed using a digital camera twice a week for at least 1 month (nine measurements: T0 = day starting treatments and T8 = end of follow-up). A ruler was placed next to the wound as a reference. Images of the wounds were analyzed using image analysis software (ImageJ, processing and analysis in Java, Version 1.6). The area (cm²) was measured three times and the average was calculated to obtain a single measure. The line for measurement was drawn along the margin of the epithelium granulation, leaving scar tissue. The contributions of epithelialization and wound contraction were not quantified.

The mean percentage of regression was calculated as follows:

$$\% \text{ of regression} = (A - a \times 100) / A,$$

where A is the major area and a is the same area measured 48 h later.

The influence of time and treatment, and the interaction between them, were evaluated using a general linear model for repeated measures (SPSS 20.0). Descriptive statistical analysis results are expressed as mean ± standard deviation. P < 0.05 was considered statistically relevant.

3. Results

3.1. Confirmation of the equine AFMSCs' stem cell character

Adherent cells, derived from samples of equine amniotic fluid, showed elongated fusiform morphology with a central nucleus. Their multipotency was demonstrated by incubating cells in media promoting differentiation into the osteogenic, chondrogenic, or adipogenic lineage. AFMSCs differentiated into osteoblasts, chondrocytes, or adipocytes, as evidenced by calcium-rich mineralized matrix or glycosaminoglycans matrix deposits or by the presence of intracellular lipid droplets, respectively

IACONO et al. / Turk J Biol

(Figures 1A–1C). The analysis of cell phenotype by flow cytometry showed that they expressed CD90 (glycosylphosphatidylinositol-anchored glycoprotein)

and CD44 (cell-surface glycoprotein) and were negative for hematopoietic marker CD34 (Figure 1D). According to the literature, the capacity of differentiation and self-

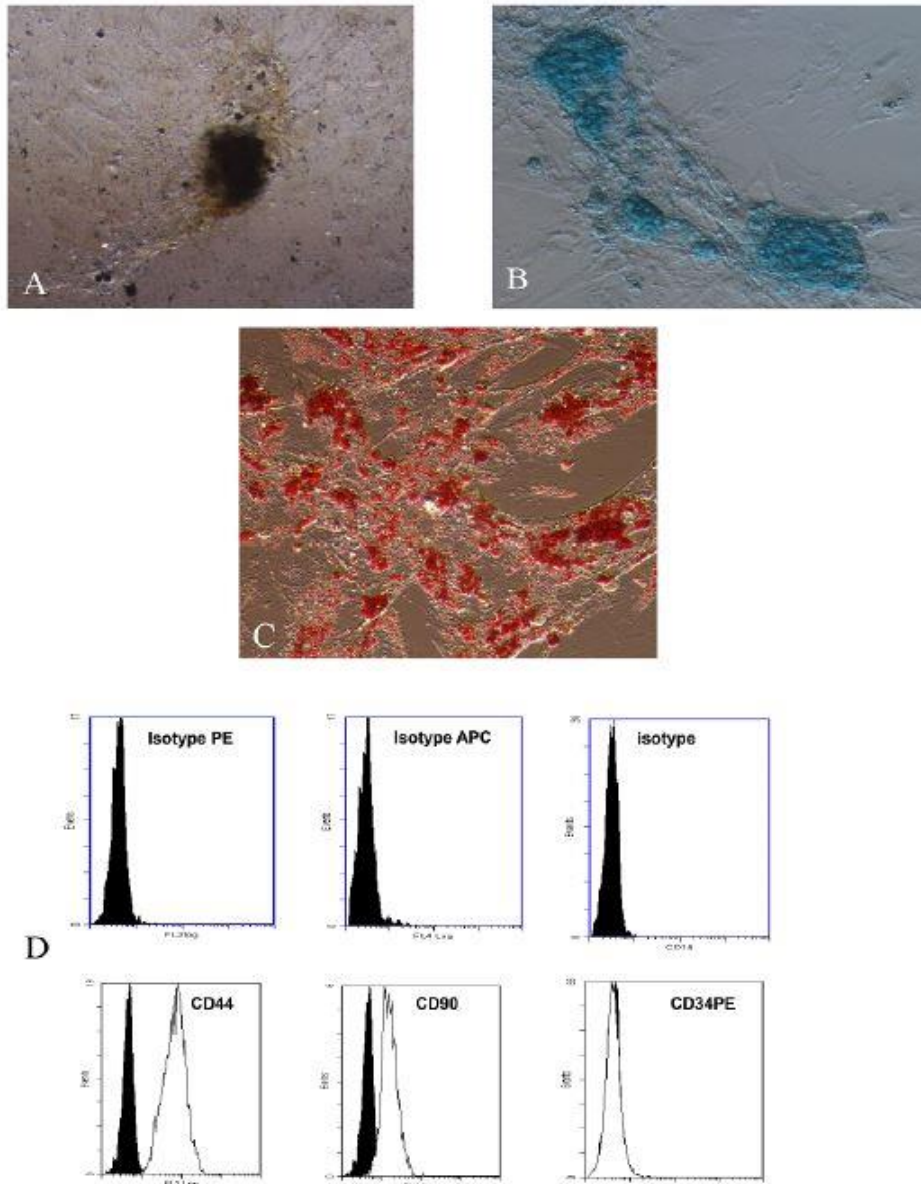


Figure 1. In vitro differentiation studies and flow cytometry analysis of equine AFMSCs at P3 of in vitro culture. A) Osteogenic induction: von Kossa staining of extensive extracellular calcium deposition. Magnification 10 \times . B) Chondrogenic induction: Alcian blue staining of glycosaminoglycans in cartilage matrix. Magnification 20 \times . C) Adipogenic induction: Oil red O staining of extensive intracellular lipid droplet accumulation. Magnification 10 \times . D) Overlay histograms of cytometry analysis. In black isotypic controls are represented. Empty histograms represent the analysis with mAbs on mesenchymal cell culture.

replication, as well as adherence on plastic, are parameters acceptable to confirm the identity of MSCs (Dominici et al., 2006). Furthermore, as previously reported by our research group (Iacono et al., 2014), by RT-PCR, isolated cells did not express major histocompatibility complex I and II, confirming the immunosuppressive function of the MSCs.

3.2. Healing

Seven foals between 10 and 15 days old and with severe skin sores were hospitalized at the EPU during the 2012 breeding season. Animals were affected by skin sores due to prolonged decubitus or the application of tube casts for treating limb flexural deformities. One foal was excluded from the study before starting treatments. This subject, affected by limb flexure deformities and septicemia, had sores on both the carpus and front fetlock of grade 5 and 4 of Sessing and NPUAP classifications, respectively. Due to the complete exposure of articular components, the owner decided on euthanasia. One foal was discharged before the end of the follow-up. Both of these foals were not considered for statistical analysis. A total of 9 pressure sores on the carpus (4), fetlock (2), and hock (3) of 5 hospitalized foals were considered. According to Sessing classification, 6/9 sores were grade 3, 1/9 grade 4, 1/9 grade 4.5, and 1/9 grade 5, while in the NPUAP classification they all corresponded to grade 3. Sores were divided into two groups: Group 1 ($n = 6$) was treated with local application of AFMSCs and Group 2 (control; $n = 3$) was treated with formosulfathiazole. Sores were uniformly distributed between the two groups. Due to the low number of cases, the location of the sores was not considered for treatment distribution and statistical analysis. Furthermore, given that the foals were hospitalized at an intensive care unit and that decubitus was changed by medical personnel every 1–2 h, the development side (left or right) of sores was not considered for statistical analysis. Finally, since in the present work naturally occurring sores were treated in owned foals, negative control groups (CMC gel scaffold only and placebo) were not used.

At the first measurement, the mean sore area in Group 1 was $24.86 \pm 11.60 \text{ cm}^2$, while in Group 2 it was $17.27 \pm 12.04 \text{ cm}^2$. While the mean area of sores in Group 1 decreased from T0 ($24.86 \pm 11.60 \text{ cm}^2$) to the last measurement (T8: $10.77 \pm 7.42 \text{ cm}^2$; Figure 2), in Group 2, the mean sore area increased from T0 ($17.27 \pm 12.04 \text{ cm}^2$; Figure 3) to T2 ($26.16 \pm 17.50 \text{ cm}^2$) and then started to decrease until T8 ($15.82 \pm 14.63 \text{ cm}^2$; Figure 3). The mean regression rate in Group 1 was statistically higher than the value recorded in Group 2 (7.7 ± 5.3 vs. 3.0 ± 27.8 ; $P < 0.05$). This was associated with a significant effect of the treatment used ($P < 0.05$), while no time effect was demonstrated ($P > 0.05$). However, a statistically significant effect of treatment over time was found ($P < 0.05$; Figure 4).

4. Discussion

In the present study, conventional therapy of sores by application of local ointment was compared with local application of AFMSCs in CMC gel. Enrolled animals, unlike in the study recently performed by Kim et al. (2013) in dogs, were not experimental animals, but were rather subjects spontaneously referred to the EPU. This may have led to a greater variability in the severity and healing of treated sores, depending on subjects, concomitant diseases, and systemic medications administered during hospitalization; however, the failure to use experimental animals makes our results more useful to evaluate the feasibility of application of MSC treatment in the clinical field. Unfortunately, it was not possible to perform a biopsy after the last treatment, given the concern of the owners about a possible recurrence of the disease. This would have allowed us to evaluate the regenerated tissue in relation to different treatments.

In a recent study, Spaas et al. (2013) demonstrated that local injection of peripheral blood stem cells might be a useful treatment for large wounds in horses. In the present study, we chose to apply stem cells directly to the sores using a gel support, as intradermal administration would require the application of protective substances between the surface of the wound and the bandage, making it difficult to understand the results. In the equine species, AFMSCs were used for treating skin wounds in one septicemic foal using PRP as a scaffold (Iacono et al., 2012b). Since foals treated in the present study were sick and/or orphaned, it was not possible to produce PRP from either the foals or their mothers. To avoid an adverse reaction to any erythrocyte factor present in the PRP of a donor's blood, in this investigation, AFMSCs were applied using a CMC gel as a scaffold. It was obtained in our laboratory by mixing CMC as a jelly holder and tissue culture medium as metabolic support for cells. In sores treated with local application of AFMSCs in CMC gel regression was higher, compared to regression of sores treated with local application of formosulfathiazole-based ointment. Furthermore, sores treated with AFMSCs in CMC gel healed quicker, in spite of the persistence of the cause in most cases (i.e. the compression due to the application of splinting of the limbs and prolonged recumbence). CMC is a low-cost biomaterial that has been used as dressing for wounds, with the purpose of protection (Ramli and Wonga, 2011) and as an excipient for some drugs (van Zuijlen et al., 2001). It has a strong ability to absorb and transport fluids and protect from bacterial exposure from the external environment (Wonga and Ramli, 2014). These attributes are important both for human and equine wounds, which are considered to be pathologically similar (Cochrane et al., 2003).

IACONO et al. / Turk J Biol

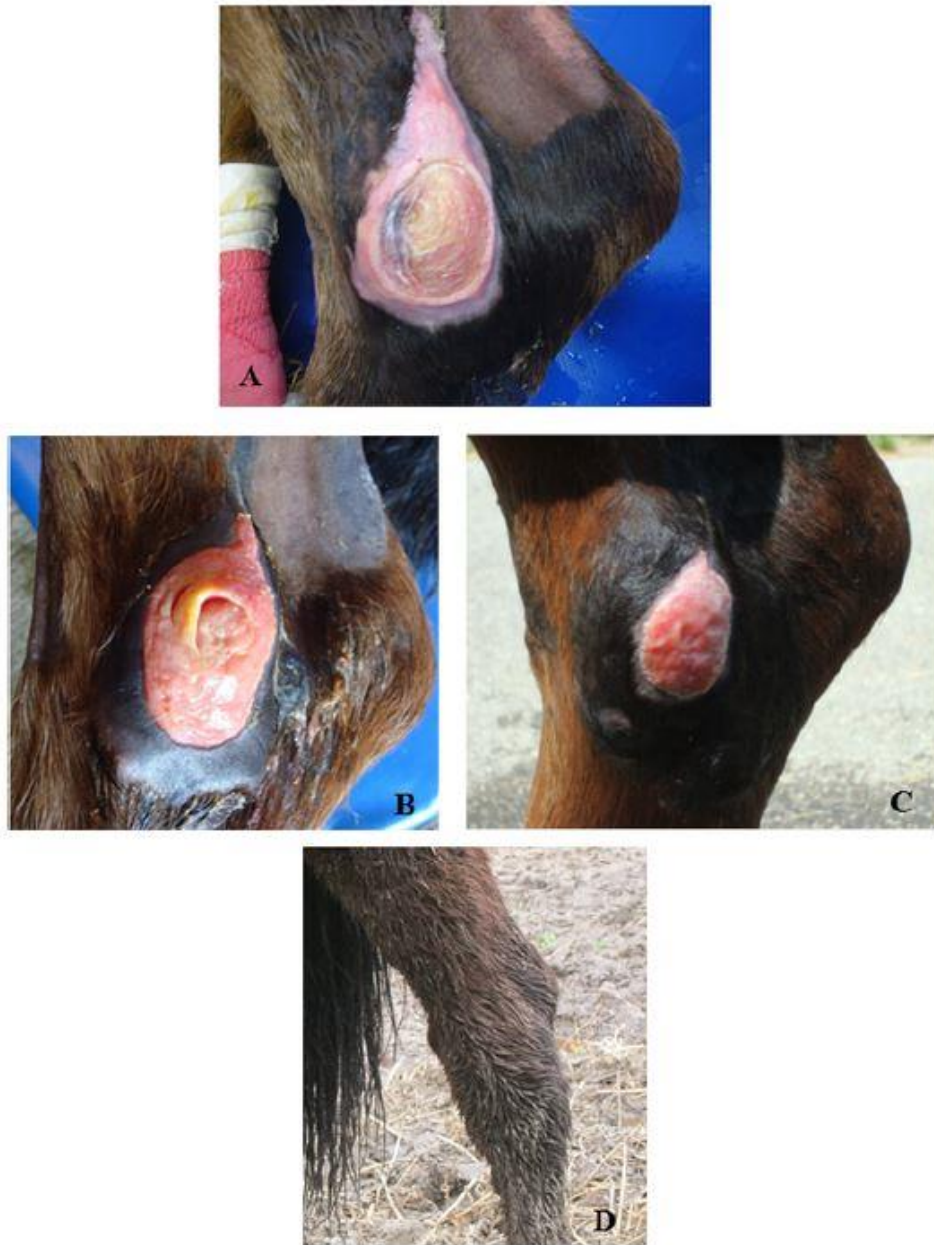


Figure 2. Pressure sore localized on the hock of an orphaned foal hospitalized at the EPU and treated with local application of AFMSCs in CMC gel. A) Before starting treatment; B) 2 weeks later; C) 4 weeks later; D) 6 months after hospitalization.

IACONO et al. / Turk J Biol



Figure 3. Pressure sore localized on the hock of an orphaned foal hospitalized at the EPU and treated with local application of formosulfathiazole. A) Before starting treatment; B) 2 weeks later; C) 1 month later.

IACONO et al. / Turk J Biol

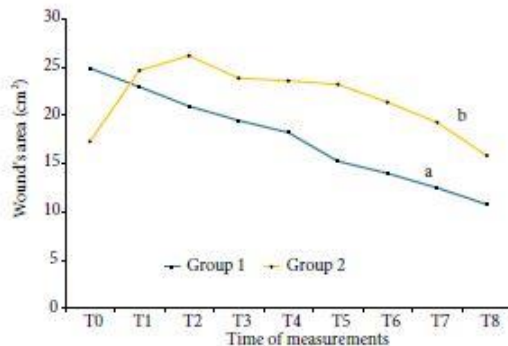


Figure 4. Trend of skin sores' regression in Group 1 (n = 6) and Group 2 (n = 3; control). a vs. b: P < 0.05.

Recently, an improvement of healing was observed at the histological level when CMC was used with adipose tissue MSCs in chemically induced wounds in mice (Rodrigues et al., 2014). The lack of systemic and local reaction (local inflammation, etc.), as pointed out by our study, confirms the safety of CMC gel (Rodrigues et al., 2014)

References

- Adam EN, Southwood LL (2006). Surgical and traumatic wound infections, cellulitis, and myositis in horses. *Vet Clin North Am Equine Pract* 22: 335–361.
- Agrawal K, Chauhan N (2012). Pressure ulcers: back to the basics. *Indian J Plast Surg* 45: 244–254.
- Balaji S, Keswani SG, Crombleholme TM (2012). The role of mesenchymal stem cells in the regenerative wound healing phenotype. *Adv Wound Care* 1: 159–165.
- Balbino CA, Pereira LM, Curi R (2005). Mechanisms involved in wound healing: a revision. *Rev Bras Cienc Farm* 41: 27–51.
- Bluestein D, Javaheri A (2008). Pressure ulcers: prevention, evaluation, and management. *Am Fam Physician* 78: 1186–1194.
- Cochrane CA, Pain R, Knottenbelt DK (2003). In-vitro wound contraction in the horse: differences between body and limb wounds. *Wounds* 15: 175–181.
- De Coppi P, Bartsch G, Siddiqui M, Xu T, Santos C, Perin L, Mostoslavsky G, Serre AC, Snyder EY, Yoo JJ et al. (2007). Isolation of amniotic stem cell lines with potential for therapy. *Nat Biotechnol* 25: 100–106.
- Dominici M, Le Blanc K, Mueller I, Slaper-Cortenbach I, Marini F, Krause D, Deans R, Keating A, Prockop D, Horwitz E (2006). Minimal criteria for defining multipotent mesenchymal stromal cells. The International Society for Cellular Therapy position statement. *Cytotherapy* 8: 315–317.
- Fader M, Clarke-O'Neill S, Cook D (2003). Management of nighttime urinary incontinence in residential settings for older people: an investigation into the effects of different pad changing regimes on skin health. *J Clin Nurs* 12: 374–386.
- Ferrell B, Artinian B, Sessing D (1995). The Sessing Scale for assessment of pressure ulcer healing. *J Am Geriatr Soc* 43: 37–40.
- Fuchs E, Horsley V (2008). More than one way to skin. *Genes Dev* 22: 976–985.
- Gianaroli L, Carai P, Stanghellini I, Ferraretti A, Magli M (2009). *Le cellule staminali: dalla ricerca all'applicazione clinica*. Rome, Italy: Repronews, Organo Ufficiale della Società Italiana di Riproduzione (in Italian).
- Hendrickson DA (2011). Management of deep and chronic wounds. In: Auer J, Stick J, editors. *Equine Surgery*. 4th ed. St. Louis, MO, USA: Saunders, pp. 317–323.
- Iacono E, Brunori L, Pirrone A, Pagliaro P, Ricci F, Tazzari P, Merlo B (2012a). Isolation, characterization and differentiation of mesenchymal stem cells from amniotic fluid, umbilical cord blood and Wharton's jelly in the horse. *Reproduction* 143: 455–468.
- Iacono E, Merlo B, Pirrone A, Antonelli C, Brunori L, Romagnoli N, Castagnetti C (2012b). Effects of mesenchymal stem cells isolated from amniotic fluid and platelet-rich plasma gel on severe decubitus ulcers in a septic neonatal foal. *Res Vet Sci* 93: 1439–1440.

IACONO et al. / Turk J Biol

- Iacono E, Rossi B, Lanci A, Castagnetti C, Merlo B (2014). Expression of proinflammatory cytokines by equine mesenchymal stem cells from foetal adnexa: preliminary data. In: Proceedings of the 5th International Symposium AICC-GISM, Italy, p. 103.
- Kanj L, Wilking S, Phillips T (1998). Pressure ulcers. *J Am Acad Dermatol* 38: 517-536.
- Kim J, Lee J, Lyoo Y, Jung D, Park H (2013). The effects of topical mesenchymal stem cell transplantation in canine experimental cutaneous wounds. *Vet Dermatol* 24: 242-253.
- Knottenbelt D (2009). *Pascoe's Principles and Practice of Equine Dermatology*. 2nd ed. St. Louis, MO, USA: Saunders.
- Perin L, Giuliani S, Jin D, Sedrakyan S, Carraro G, Habibian R, Warburton D, Atala A, De Filippo RE (2007). Renal differentiation of amniotic fluid stem cells. *Cell Proliferation* 40: 936-948.
- Ramli NA, Wonga TW (2011). Sodium carboxymethylcellulose scaffolds and their physicochemical effects on partial thickness wound healing. *Int J Pharm* 403: 73-82.
- Rodrigues C, de Assis AM, Moura DJ, Halmenschlager G, Saffi J, Xavier LL, da Cruz Fernandes M, Wink MR (2014). New therapy of skin repair combining adipose-derived mesenchymal stem cells with sodium carboxymethylcellulose scaffold in a pre-clinical rat model. *PLoS One* 9: e96241.
- Sorrell JM, Caplan AI (2010). Topical delivery of mesenchymal stem cells and their function in wounds. *Stem Cell Res Ther* 1: 30.
- Spaas JH, Broeckx S, Van de Walle GR, Poletini M (2013). The effects of equine peripheral blood stem cells on cutaneous wound healing: a clinical evaluation in four horses. *Clin Exp Dermatol* 38: 280-284.
- Tsai MS, Lee JL, Chang YJ, Hwang SM (2004). Isolation of human multipotent mesenchymal stem cells from second-trimester amniotic fluid using a novel two-stage culture protocol. *Hum Reprod* 19: 1450-1456.
- Vaala W, House J, Madigan J (2002). Initial management and physical examination of the neonate. In: Smith BP, editor. *Large Animal Internal Medicine*. 3rd ed. St. Louis, MO, USA: Mosby, pp. 277-293.
- Van Zuijlen PP, Vloemans JE, van Trier AJ, Suijker MH, van Unen E, Groenevelt F, Kreis RW, Middelkoop E (2001). Dermal substitution in acute burns and reconstructive surgery: a subjective and objective long-term follow-up. *Plast Reconstr Surg* 108: 1938-1946.
- Wonga TW, Ramli NA (2014). Carboxymethylcellulose film for bacterial wound infection control and healing. *Carbohydr Polym* 112: 367-375.
- Wu Y, Chen L, Scott P, Tredget E (2007). Mesenchymal stem cells enhance wound healing through differentiation and angiogenesis. *Stem Cells* 25: 2648-2659.

CHAPTER 7

EFFECTS OF WHARTON'S JELLY MESENCHYMAL STEM CELLS ON PRESSURE SORE OF A SIX-MONTH-OLD FILLY

Article in Preparation

Department of Veterinary Medical Sciences, University of Bologna, Ozzano Emilia, Bologna, Italy

Introduction

Wounds are common in equine patients as a consequence of physical overstrain, and could negatively affect quality of life and athletic performance (Dart et al., 2005). Both equine and human persistent or slow healing injuries are a challenge for clinicians. These lesions frequently result in inadequate tissue reorganization and thus in a high re-injury rate and are related to a long period of incapacity or to an unsatisfactory return to performance.

The repair of full-thickness cutaneous wounds depends principally on three coordinated and overlapping phases: acute inflammation, cellular proliferation, and finally matrix synthesis and remodeling with scar formation (Theoret, 2004). The first phase prepares the wound for the subsequent reparative phases with the involvement of cells, such as neutrophils and macrophages, and mediators, such as cytokines and growth factors. If this phase is not resolved quickly, the persistence of inflammatory cells and mediators might contribute to the pathogenesis of diseases characterized by excessive fibrosis and/or scarring. The proliferation stage involves fibroblast migration and growth with the formation of granulation tissue and epithelialization (Theoret, 2004). The final phase determines the reduction of wound size by a process referred to as "wound contraction" that is due to a contractile phenotype of fibroblasts. Collagen remodelling with the formation of larger bundles, oriented along the lines of tension, ensures an increase in tensile strength during this last phase (Theoret, 2004).

Enormous variation exists in treatments, medications, bandages, and bandaging techniques applied to wounds in horses (Dart et al., 2005; Stashak and Theoret, 2008). In the last few years, different research groups reported good results in the skin healing using MSCs, both in human and veterinary medicine. In the present study, a 6 months old foal, with a skin wound on the left hock, was treated with local application of heterologous WJ-MSCs in autologous plasma, and the wound's regression was determined.

Case history and clinical findings

A 45 kg Standardbred filly was born in April 2016 at the Equine Perinatology Unit (EPU) "Stefano Belluzzi" - Department of Veterinary Medical Sciences (DIMEVET) - University of Bologna. The delivery was eutocic and the foal's APGAR score at birth was 10 (Vaala, 2006). At birth, the filly had severe flexural/angular deformity of the hind limbs (*Figure 7.1a*) and she was unable to stand up and to suckle; for this reason, she was fed with nasogastric tube for the first 24 hours. At one-day of life she was able to stand up and nurse but she spent long periods in decubitus, and at 3 days of life a superficial pressure sore appears on the left hock (*Figure 7.1b*). Before starting treatments, Sessing classification (Ferrell et al., 1995; *Table 7.1*) and National Pressure Ulcer Advisory Panel (NPUAP; Bluestein and Javaheri, 2008; *Table 7.2*) criteria, usually employed in human medicine, were applied to determine the severity of the pressure sore. In particular, Sessing classification is useful to classify sores according to macroscopic appearance, while NPUAP criteria are applied to evaluate the depth degree. According to Sessing classification, skin sore was grade 4, while in the NPUAP classification it corresponded to grade 3. The wound was washed with sterile water, medicated with hyaluronic acid in gauze (Connettivina®; Fidia farmaceutici S.p.A., Italy) and bandaged with cotton gauze, bandage and Vetrap (3m, Milan, Italy) every day until discharge.

At discharge the wound, according to Sessing classification, was grade 3, while in the NPUAP classification it corresponded to grade 2 (*Figure 7.1c*).

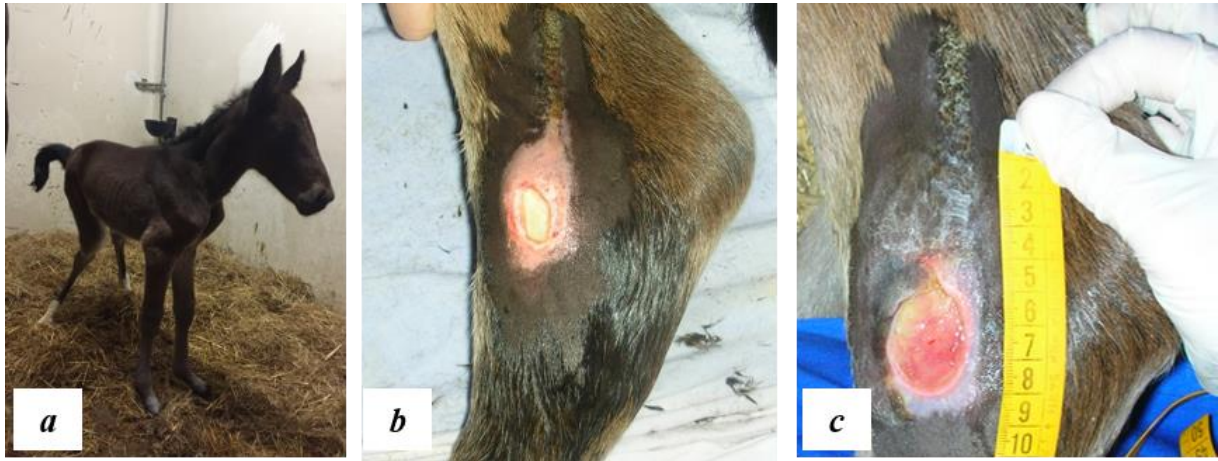


Figure 7.1. a) filly at 2 days of life; b) the wound at 3 days of life; c) the wound at discharge at 10 days of life.

As referred by the owner, the wound, treated with ozone therapy at stud farm, healed completely on June at 2 months of life (*Figure 7.2*). However, the owner referred that the filly spent long period in decubitus also at the farm until August.



Figure 7.2. a) at the beginning of the treatment with ozone therapy; b) in the middle and c) at the end.

At the end of September, the 6 months old filly was admitted at EPU because the owner referred that in July a wound in the same left hock appeared again. At admission, the wound, according to Sessing classification was grade 5, while in the NPUAP classification it corresponded to grade 4 (*Figure 7.3*).

Stage	Description
0	Normal skin, but at risk.
1	Intact skin, but hyperpigmented or reddened.
2	The bottom and edges of the ulcer are intact and not red.
3	The bottom and edges of the ulcer with pink granulation tissue, modest presence of exudate and odor.
4	Presence of modest granulation tissue, initial and modest necrotic tissue, moderate exudate and odor.
5	Abundant presence of foul smelling exudate, necrotic eschar, and whitish or reddish edges.
6	Further ulceration around the primary ulcer, purulent exudate, intense odor, presence of necrotic tissue and systemic symptoms of sepsis.

Table 7.1. Sessing classification of skin wounds (Ferrell et al., 1995).

Stage	Description
1	Intact skin with nonblanchable redness of a localized area usually over a bony prominence. Darkly pigmented skin may not have visible blanching; its color may differ from the surrounding area. The area may be painful, firm, soft, warmer, or cooler as compared to adjacent tissue
2	Partial thickness loss of dermis presenting as a shallow open ulcer with a red pink wound bed, without slough. May also present as an intact or open/ruptured serum-filled or serosanguineous filled blister. Presents as a shiny or dry shallow ulcer without slough or bruising.
3	Full thickness tissue loss. Subcutaneous fat may be visible but bone, tendon, or muscle are not exposed. Slough may be present but does not obscure the depth of tissue loss. May include undermining and tunneling.
4	Full thickness tissue loss with exposed bone, tendon, or muscle. Slough or eschar may be present. Often includes undermining and tunneling. The ulcer can extend into muscle and/or supporting structures (e.g., fascia, tendon, or joint capsule), making osteomyelitis or osteitis likely to occur. Exposed bone/muscle is visible or directly palpable.

Table 7.2. Classification of the National Pressure Ulcer Advisory Panel (NPUAP; Bluestein and Javaheri, 2008).



Figure 7.3. The wound at admission in September. Wound's area was $4.73 \pm 0.15 \text{ cm}^2$.

Treatment

The treatment was divided into three phases:

Surgical phase

Since the skin and subcutaneous tissue appeared necrotic, before starting the Mesenchymal Stem Cells (MSCs) treatments, a surgical curettage was carried out. Under sedation, the depth of the wound was evaluated with sterile stylet and a deep surgical curettage was carried out with sterile scalpel to remove the necrotic tissue (*Figure 7.4 a*). The wound was cleaned with sterile water, medicated with salicylic acid powder and bandaged. For the following 8 days the wound was daily washed with tap water, mechanical debridement was performed using a woven wet gauze and Dermaflon[®] (salicylic acid, malic acid, benzoic acid; Zoetis, Italy) was applied on the wound. The surgical curettage was repeated at Day 5 (at fifth day after admission). At Day 8 the wound's area was $7.28 \pm 0.20 \text{ cm}^2$ (*Figure 7.4 f*).

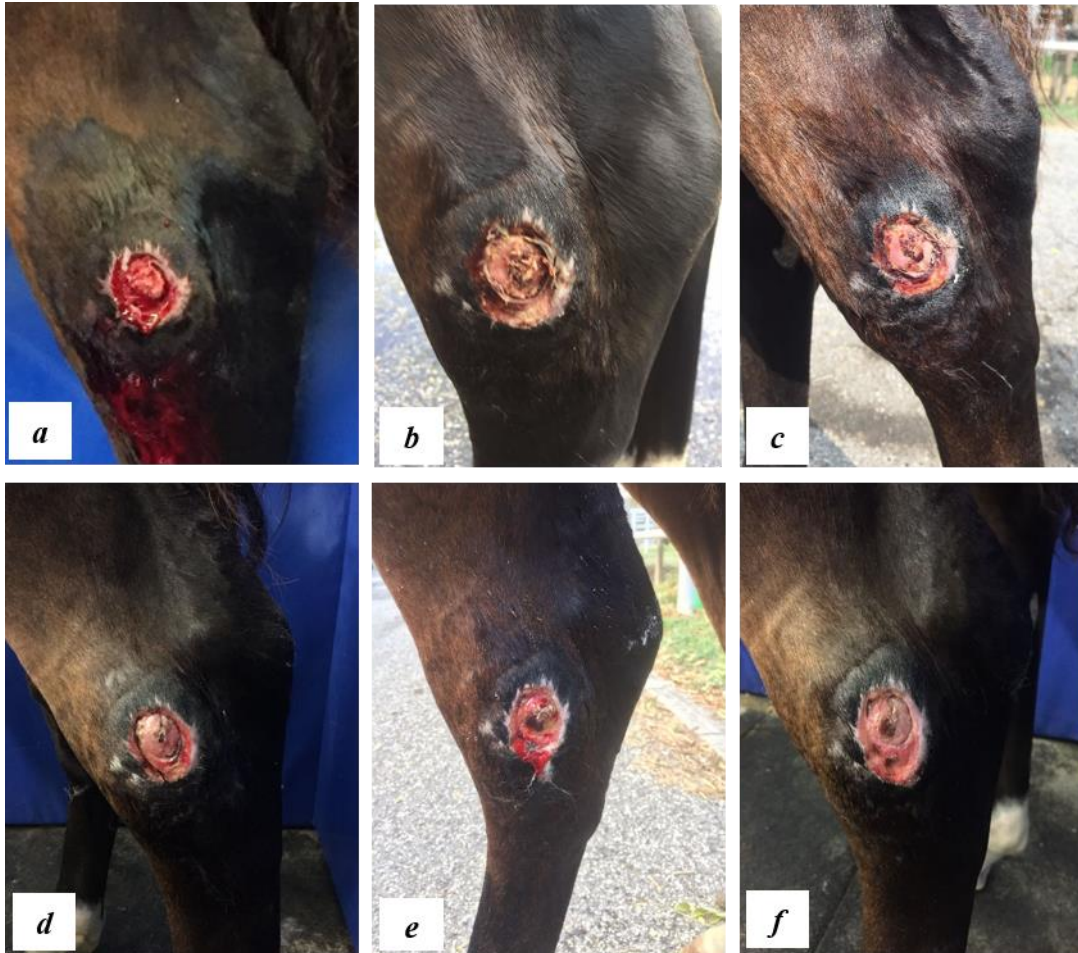


Figure 7.4. First period of treatment: surgical curettage and Dermaflon[®] for deep debridement of the wound. **a)** The wound during first surgical curettage at Day 0; **b)** The wound at Day 3; **c)** The wound at Day 4; **d)** The wound at Day 5; **e)** The wound at Day 7; **f)** The wound at Day 8, area was $7.28 \pm 0.20 \text{ cm}^2$: time of first application of WJ-MSCs.

Regenerative phase

At Day 8, the wound was grade 4 according to Sessing classification, while in the NPUAP classification it corresponded to grade 4. It had less granulation tissue and little necrotic flesh. Four cutaneous applications of MSCs were performed in 18 days, within about 4 days of each other.

Mesenchymal stem cell isolation and culture

The employed MSCs were collected in the foaling season 2016 from Wharton's jelly (*Figure 7.5*); the cells were isolated and cultured until Passage 2 (P2) of culture. At P2 the cells were cryopreserved in liquid nitrogen.

Before the cutaneous application, WJ-MSCs were thawed (P3) and re-expanded in Dulbecco's Modified Essential Medium (D-MEM) F12 Glutamax® (Gibco). Then immunophenotypic characterization was performed, testing the following markers: the cells resulted positive for CD90, and negative for CD45 and mycoplasma by RT-CPR.

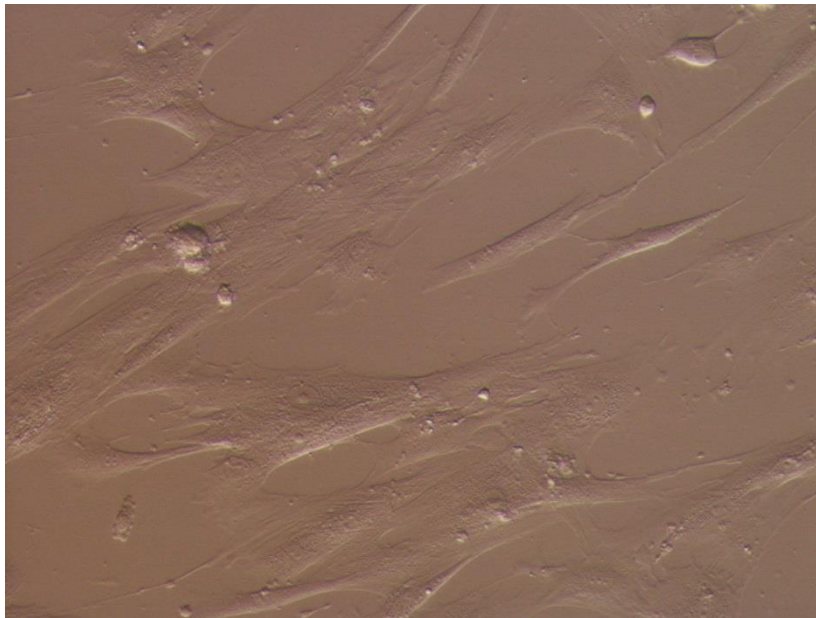


Figure 7.5. WJ-MSCs at P2.

Staging of preparations for MSC application

Immediately before application, under a laminar flow hood and in sterile conditions, WJ-MSCs were detached from the flask and cells were counted using a hemocytometer. For each application, approximately 5×10^5 cells/mL were used. Autologous plasma was collected with sterile closed system from the filly. A gel of CMC used as a scaffold was produced in a sterile petri dish under a laminar flow hood using 5 g of CMC and 5 mL of autologous plasma. Before preparing gel, the CMC was placed for 30 min under

a UV lamp to avoid bacterial contamination. Immediately before treatment, cells were added to the gel.

Before applying MSCs, wounds were rinsed with isotonic sterile saline solution. The skin around the wounds was greased with Vaseline to prevent further damage at the time of the next dressing. Immediately after application, the limb was bandaged with cotton gauze, a bandage, and Selfix (Pic solution, Artsana S.p.A., Italy) (*Figure 7.6c*).

After the first application, at Day 12 (*Figure 7.6 d*) the wound's area was $4.25 \pm 0.03 \text{ cm}^2$ and it was grade 3 according to Sessing classification because there was an odorless yellow exudate, while in the NPUAP classification it corresponded to grade 2.

After the four applications, at Day 22 (*Figure 7.6 g*), the wound's area was $1.90 \pm 0.03 \text{ cm}^2$ and it was grade 2 according to Sessing classification, while in the NPUAP classification it corresponded to grade 2.



Figure 7.6. Second period of treatment: cutaneous application of Mesenchymal Stem Cells derived from Wharton's Jelly. **a)** WJ-MSCs in gel of autologous plasma and carboxymethyl cellulose. **b)** Application of WJ-MSCs gel. **c)** Bandage. **d)** Day 12, the wound after the first application of WJ-MSCs and the area was $4.25 \pm 0.03 \text{ cm}^2$. **e)** Day 14, the wound after the second application of WJ-MSCs and the area was $4.07 \pm 0.04 \text{ cm}^2$. **f)** Day 19, the wound after the third application of WJ-MSCs and the area was $2.53 \pm 0.06 \text{ cm}^2$. **g)** Day 22, the wound after the fourth application of WJ-MSCs and the area was $1.90 \pm 0.03 \text{ cm}^2$.

Medical phase

In this phase, the wound had abundant granulation tissue, wound's sizes were modest, and the wound was superficial.

The wound was daily cleaned and treated by hydrotherapy with cold tap water for 10 minutes and application with RHD[®] cream (hyperozonized lipids; Acme s.r.l., Italy) and Vaseline on skin around the wound. Immediately after application, the limb was bandaged with cotton gauze and Selfix (Pic solution, Artsana S.p.A., Italy; *Figure 7.7*).



Figure 7.6. Third period of treatment: daily hydrotherapy and application of RHD[®]. **a)** Cutaneous application of ointment RHD[®]. **b)** Day 26, area was $1.67 \pm 0.04 \text{ cm}^2$. **c)** Day 32, area was $0.97 \pm 0.01 \text{ cm}^2$. **d)** Day 34, area was $0.78 \pm 0.02 \text{ cm}^2$. **e)** Day 36, area was $0.59 \pm 0.01 \text{ cm}^2$. **f)** Day 39, day of discharge, area was $0.38 \pm 0.01 \text{ cm}^2$.

The wound was photographed using a digital camera at every treatment (T0 = day at the hospitalization and Td = day at discharge). A ruler was placed next to the wound as a reference. Images of the wounds were analyzed using image analysis software (ImageJ, processing and analysis in Java, Version 1.6). The area (cm²) was measured three times and the average was calculated to obtain a single measure. The line for measurement was drawn along the margin of the epithelium granulation, leaving scar tissue (*Figure 7.8*).

At the end of each phase, the mean percentage of regression was calculated as follows:

$$\% \text{ of regression} = (A - a \times 100) / A,$$

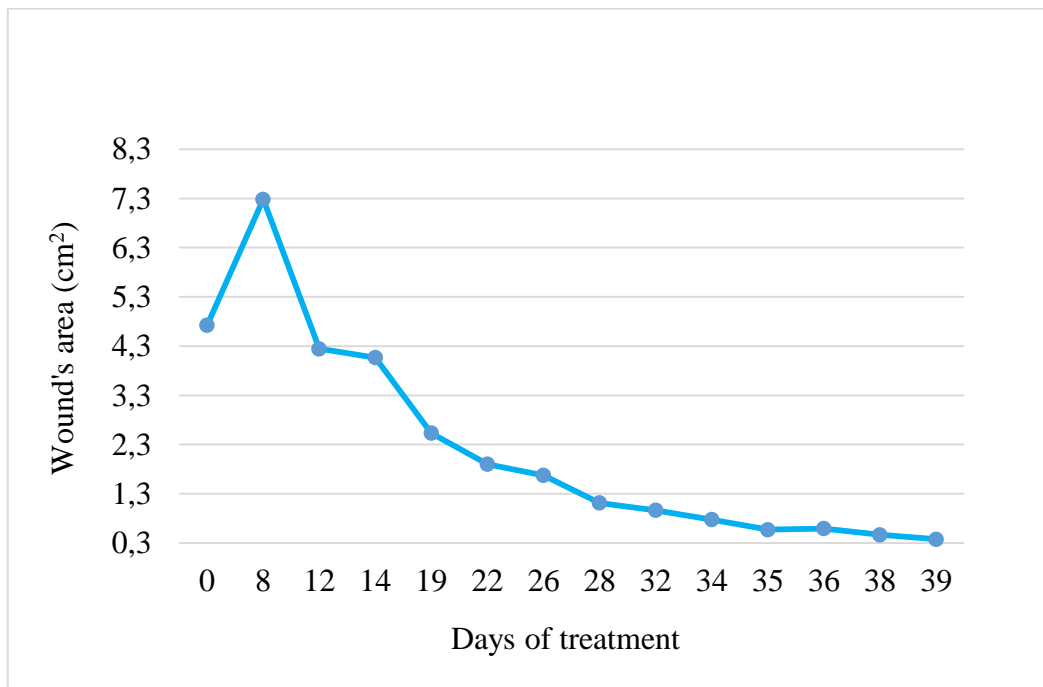
Where A is the initial Area and a is the same area measured at the end of the phase of treatment (*Table 7-3*).



Figure 7.8. Measure of wound's area using software ImageJ.

Outcome

At Day 39 the wound's area was $0.38 \pm 0.01 \text{ cm}^2$ (Figure 7.7f).



Graph 1. Regression of wound's area (cm²) in 39 days of hospitalization.

Phase of treatment	Wound's Area (cm²)	% of regression
Day 0	4.73 ± 0.15	/
Surgical phase	7.28 ± 0.20	-54%
Regenerative phase	1.90 ± 0.03	+ 74%
Medical phase	0.38 ± 0.01	+ 80%

Table 7.3. Percentage of regression of each phase of the treatment.

As shown by the photos sent by the owner, the hair grew completely without changing color of the coat and did not leave evident scars on the skin (*Figure 7.9*).



Figure 7.9. Day 47. Picture sent by the owner 8 days after discharge.

Discussion

Wound infection and the development of chronic inflammation leading to ulcerative-type lesions, as well as fibro-proliferative conditions such as exuberant granulation tissue, are frequent in wounds occurring in horse limbs (Theoret, 2008). It is reported that 7% of injuries leading to the retirement of racehorses are the direct result of a wound (Perkins et al., 2005). Wounds, particularly on the distal limb, are a common occurrence in horses and, when they involve structures underlying the skin, are costly and time-consuming to manage and may lead to decreased performance, retirement or euthanasia (Theoret et al., 2016).

Several factors influence wound healing as wound type, degree of contamination, location and age of the wound. Wound type is an important indicator of the vascular supply, degree of contamination, and viability of surrounding tissue, which reliably determine the best mode of management. The inflammatory phase is prolonged in the presence of necrotic debris, foreign material, or infection. Distal limb wounds are the most difficult to heal because the skin has a decreased vascular supply, numerous bony prominences, absence of supporting deep

musculature, highly mobile joints, and a generally higher degree of contamination than in other body sites (Moy, 1993; Cochrane et al., 2003; Knottenbelt, 2003). There are many sources of chronic inflammation in a wound, including necrotic tissue, foreign bodies, repetitive mechanical trauma, and the application of cytotoxic agents (Knottenbelt, 2003). Furthermore, chronic wounds do not progress normally through the various phases of repair, usually because of underlying conditions. The goal of chronic wound therapy is to identify and resolve the causal factors so that healing could proceed (Knottenbelt, 2003; Hendrickson and Virgin, 2005).

Necrotic tissue and foreign bodies prolong inflammation because of the body's attempt to rid the area of the alien matter. Debridement of devitalized tissue is the most effective method to improve healing in these cases.

The new epithelium, which eventually covers a wound healing by second intention, is fragile and susceptible to reinjury so that wound contraction is considered a mechanism to reduce the wound surface area (Theoret, 2004). In the present study, the filly was hospitalized for a reinjury of a pressure wound, probably due to the newly formed thin skin. When the filly was readmitted in September, she did not spend too much time in decubitus; the stimulating pressure due to the frequent recumbences was no longer present.

Wound assessment is one of the most important step in wound repair: the failure of a regenerative process is at the basis of an erroneous assessment and the beginning of an inappropriate treatment (Hendrickson, 2012). In this case, at first evaluation of the wound, our group decided to start with accurate debridement because the necrotic tissue was very abundant. Debridement is an effective way to reduce the bacterial contamination and to minimize necrotic tissue. The most common type of debridement in equine practice is surgical

and other types of debridement (mechanical and autolytic) tend to create more trauma, consequently increasing the healing time required (Hendrickson, 2012).

In the present study, a surgical debridement was associated with a mechanical one to permit a complete removal of necrotic tissue and to create a perfect wound bed for MSCs' application. The debridement phase led to an increase of 54% of the size of the wound in 8 days.

In the regenerative phase of the treatment, we performed four cutaneous applications of WJ-MSCs in carboxymethylcellulose gel, as a scaffold, and autologous plasma, as metabolic support for the cells.

Since long time, in human medicine it has been shown that MSCs can differentiate not only into mesenchymal lineage cells but also into other lineage cells *in vitro*, while *in vivo* studies have also shown that MSCs can differentiate into tissue-specific cells in response to stimuli provided by different organs (Jiang et al., 2002). Sasaki et al. (2008) demonstrated that MSCs could differentiate into multiple skin cell types including keratinocytes and contribute to wound repair. Currently, in equine medicine there is not an ideal source of stem cells and a standard protocol for the application; however, most of the research focuses on MSCs derived from adult tissue, as bone marrow, adipose tissue and peripheral blood (Adams et al., 2013; Burk et al., 2013; Radtke et al., 2013; Spaas et al., 2013; Carter-Arnold et al., 2014; Ferris et al. 2014; Lopez and Jarazo, 2014; Burk et al, 2016). The adult tissue provides autologous cells, whereas to use autologous cells from foetal adnexa they need to be collected at birth and cryopreserved.

Carrade et al. (2011) evaluated the hypersensitivity response to intradermal injections of autologous and allogenic MSCs derived from umbilical cord tissue (UCT). MSC injection resulted in minor wheal formation, characterized by mild dermatitis, dermal edema and endothelial hyperplasia, that fully resolved by 48 – 72 h. They concluded that equine

allogeneic UCT MSC might be safely administered intradermal without stimulating a measurable cellular immune response.

Azari et al. (2011) evaluated the effects of intradermal injections of caprine WJ-MSCs on first intention cutaneous wound healing in healthy goats. This study demonstrated the beneficial effect of injections of caprine WJ-MSCs on wounds surgically made. The histopathological and microscopic evaluation revealed that re-epithelialization was complete at days 7 and less inflammation, thinner granulation tissue formation with minimum scar in the treated wounds in comparison with control wounds (Azari et al., 2011). The umbilical cord, since it is a discarded material after delivery, represents an excellent alternative non-invasive source of MSCs. Moreover, WJ-MSCs are highly proliferative, show tri-lineage differentiation ability and may have broader differentiation capacity than BM-MSCs (Carrade et al., 2011). Additionally, human WJ-MSCs have potent immunosuppressive properties including the reduction of lymphocyte proliferation in vitro (Li et al., 2007; Weiss et al., 2008).

Our research group performed two studies about the wound healing with cutaneous application of Amniotic Fluid MSCs (Iacono et al., 2012b; Iacono et al., 2016). In the first paper, heterologous AF-MSCs were applied with platelet rich plasma (PRP) on a sore localized at right hock in a septic neonatal foal. The regression of wound healing was compared with other treatment applied on other sores in the same foal. The mean regression rate of MSCs + PRP (26.1%) was statistically higher than the others (20.6% and 18.1% Aloe gel, 18.1% PRP; Iacono et al., 2012b). In the more recent paper, heterologous AF-MSCs were applied in a carboxymethylcellulose (CMC) gel on spontaneously arisen pressure sores in seven hospitalized neonatal foals. As control, a commercial ointment was used. The mean regression rate with AF-MSCs in CMC gel was statistically higher than the mean value recorded in the control group, associated with a significant effect of the treatment used and a

statistically significant effect of treatment over time (Iacono et al., 2016). The results suggested that local application of MSCs isolated from amniotic fluid, using CMC as scaffold, could be considered as an effective treatment of deep sores in hospitalized neonatal foals (Iacono et al., 2016). In the present study, the size of the sore was reduced by 74%. We obtained this higher rate in comparison with Iacono et al. (2016) results probably because of the previous wound bed preparation. In addition, the 6 months old filly was healthy, unlike other foals that had continuous pressure stimulus on the wounds, so the healing process was slower.

The gel containing MSCs adheres well to the wound and acts as a dressing. Instead, intradermal injections resulted to be painful, and therefore required appropriate restraint of the animal and good sedation with detomidine and butorphanol; furthermore, it is itself an inflammatory stimulus. In our case, in fact, cutaneous application did not require any sedation of the animal, and it was necessary just a minimum restraint to carry out the bandage.

In the last phase, the treatment of the sore was carried out with an ointment containing ozone and the size of the sore was reduced by 80%. Bactericidal and pro-oxidant properties of ozone therapy on wound healing is well documented (Sagai and Bocci, 2011; degli Agosti et al., 2016). Recently, in human medicine, Rosul and Patskan (2016) reported that superficial and deep ulcers in 47 diabetic patients treated with ozone healed more rapidly than in control group. Ozone promotes the improvement of lipid peroxidation and antioxidant protection, and reduces the time of hospitalization (Rosul and Patskan, 2016). Furthermore, the ozone therapy activates the proliferation of fibroblasts by releasing oxygen and promotes the production of intercellular matrix with consequent proliferation of keratinoblasts and successive complete wound healing (Travagli et al., 2010). The use of cutaneous application of ozone in our case contributed to maintain vital the granulation tissue until the complete healing of the sore.

Unfortunately, it was not possible to perform a biopsy after the 3 phases of treatment, given the concern of the owner about a possible re-injury of the skin.

In conclusion, the most important step in wound healing is the accurate assessment of the wound to avoid an erroneous therapy. It is also important to evaluate the macroscopic changes of the wound and to choose a proper therapy. Since the absence of side effects and the good results obtained, the local use of heterologous MSCs derived from Wharton's jelly could represent a perfect healing treatment on deep wounds also in adult horses.

References

- Adams M. K., Goodrich L.R, Rao S., Olea-Popelka F., Phillips N., Kisiday J.D., McIlwraith C.W., (2013). *Equine bone marrow-derived mesenchymal stromal cells (BMDMSCs) from the ilium and sternum: Are there differences?* Equine Vet J; 45(3) :372–375.
- Azari O., Babaei H., Derakhshanfar A., Nematollahi-Mahani S.N., Poursahebi R., Moshrefi M., (2011). *Effects of transplanted mesenchymal stem cells isolated from Wharton's jelly of caprine umbilical cord on cutaneous wound healing; histopathological evaluation.* Vet Res Commun; 35(4): 211-22.
- Bluestein D., Javaheri A., (2008). *Pressure ulcers: prevention, evaluation, and management.* Am Fam Physician 78(10): 1186–1194.
- Burk J., Berner D., Brehm W., Hillmann A., Horstmeier C., Josten C., Paebst F., Rossi G., Schubert S., Ahrberg A.B., (2016). *Long-Term Cell Tracking following Local Injection of Mesenchymal Stromal Cells in the Equine Model of Induced Tendon Disease.* Cell Transplant; 25(12): 2199-2211.
- Burk J., Ribitsch I., Gittel C., Juelke H., Kasper C., Staszuk C., Brehm W., (2013). *Growth and differentiation characteristics of equine mesenchymal stromal cells derived from different sources.* Vet J; 195(1): 98–106.
- Carrade D.D., Affolter V.K., Outerbridge C.A., Watson J.L., Galuppo L.D., Buerchler S., Kumar V., Walker N.J., Borjesson D.L., (2011). *Intradermal injections of equine allogeneic umbilical cord-derived mesenchymal stem cells are well tolerated and do not elicit immediate or delayed hypersensitivity reactions.* Cytotherapy; 13(10): 1180-1192.

Carter-Arnold J., Neilsen N.L., Amelse L.L., Odoi A., Dhar M.S., (2014). *In vitro analysis of equine, bone marrow- derived mesenchymal stem cells demonstrates differences within age- and gender-matched horses.* Equine Vet J; 46(5): 589–595.

Cochrane C.A., Pain R., Knottenbelt D.C., (2003). *In-vitro wound contraction in the horse: differences between body and limb wounds.* Wounds; 15(6): 175–81.

Dart A.J., Dowling B.A., Smith C.L., (2005). *Topical treatments in equine wound management.* Vet Clin North Am Equine Pract; 21(1): 77–89.

Degli Agosti I., Ginelli E., Mazzacane B., Peroni G., Bianco S., Guerriero F., Ricevuti G., Perna S., Rondanelli M., (2016). *Effectiveness of a Short-Term Treatment of Oxygen-Ozone Therapy into Healing in a Posttraumatic Wound.* Case Rep Med; 9528572.

Ferrell B., Artinian B., Sessing D., (1995). *The Sessing Scale for assessment of pressure ulcer healing.* J Am Geriatr Soc; 43(1): 37–40.

Ferris D. J., Frisbie D.D., Kisiday J.D., McIlwraith C.W., Hague B.A., Major M.D., Schneider R.K., Zubrod C.J., Kawcak C.E., Goodrich L.R., (2014). *Clinical outcome after intra-articular administration of bone marrow derived mesenchymal stem cells in 33 horses with stifle injury.* Vet.Surg 43(3): 255–265.

Hendrickson D., Virgin J., (2005). *Factors that affect equine wound repair.* Vet Clin North Am Equine Pract; 21(1): 33-44.

Hendrickson D.A., (2012). *Management of Superficial Wounds in Equine Surgery, 4th edition,* Auer JA and Stick JA. St Louis, Missouri, 306-316.

Iacono E., Brunori L., Pirrone A., Pagliaro P., Ricci F., Tazzari P., Merlo B., (2012a). *Isolation, characterization and differentiation of mesenchymal stem cells from amniotic fluid, umbilical cord blood and Wharton's jelly in the horse*. *Reproduction* 143(4): 455–468.

Iacono E., Merlo B., Pirrone A., Antonelli C., Brunori L., Romagnoli N., Castagnetti C. (2012b). *Effects of mesenchymal stem cells isolated from amniotic fluid and platelet-rich plasma gel on severe decubitus ulcers in a septic neonatal foal*. *Res Vet Sci* 93(3): 1439–1440.

Iacono E., Lanci A., Merlo B., Ricci F., Pirrone A., Antonelli C., Mariella J., Castagnetti C., (2016). *Effects of Amniotic Fluid Mesenchymal Stem Cells in carboxymethyl cellulose gel on spontaneous pressure sores healing: clinical outcome in seven hospitalized neonatal foals*. *Turkish Journal of Biology*; 40(2): 484 – 492.

Jacobs K.A., Leach D.H., Fretz P.B., et al., (1984). *Comparative aspects of the healing of excisional wounds on the leg and body of horses*. *J Vet Surg*; 13(2): 83–90.

Jiang Y., Jahagirdar B.N., Reinhardt R.L., Schwartz R.E., Keene C.D., Ortiz-Gonzalez X.R., Reyes M., Lenvik T., Lund T., Blackstad M., et al., (2002). *Pluripotency of mesenchymal stem cells derived from adult marrow*. *Nature*; 418(6893): 41–49.

Knottenbelt D.C., (2003). *Handbook of equine wound management*. Liverpool, UK: WB Saunders.

Li C., Zhang W., Jiang X., Mao N., (2007). *Human-placenta-derived mesenchymal stem cells inhibit proliferation and function of allogeneic immune cells*. *Cell Tissue Res*; 330(3): 437 – 46.

Lopez M. J., Jarazo J., (2014). *State of the art: Stem cells in equine regenerative medicine*. Equine Vet J; 47(2); 145-154.

Moy L.S., (1993). *Management of acute wounds*. Dermatol Clin; 11(4): 759–76.

Perkins N.R., Reid W.E., Morris R.S., (2005). *Profiling the New Zealand Thoroughbred racing industry. 2. Conditions interfering with training and racing*. NZ Vet J; 53(1): 69–76.

Radtke C. L., Nino-Fong R., Esparza Gonzalez B.P., Stryhn H., McDuffee L.A., (2013). *Characterization and osteogenic potential of equine muscle tissue- and periosteal tissue-derived mesenchymal stem cells in comparison with bone marrow- and adipose tissue-derived mesenchymal stem cells*. Am J Vet Res; 74(5): 790–800.

Rosul M.V., Patskan B.M., (2016). *Ozone therapy effectiveness in patients with ulcerous lesions due to diabetes mellitus*. Wiad Lek; 69(1): 7-9.

Sagai M., Bocci V., (2011). “*Mechanisms of action involved in ozone therapy: is healing induced via a mild oxidative stress?*”. Med Gas Res; 1:29.

Stashak T.S., Theoret C., (2008). *Equine wound management*. 2nd edition. Ames (IA): Wiley-Blackwell.

Theoret C.L., (2004). *Update on wound repair*. Clin Tech Equine Pract; 3(2): 110–122.

Theoret C.L., (2008). *Wound repair in the horse: problems and innovative solutions*. In Stashak TS, Theoret CL (eds): *Equine Wound Management (ed 2)*. Ames, IA, Wiley-Blackwell; 47–68.

Travagli V., Zanardi I., Valacchi G., Bocci V., (2010). *Ozone and ozonated oils in skin diseases: a review*. Mediators Inflamm; 2010: 610418.

Vaala W.E., (2006). *Perinatology*. In: Higgins AJ, Snyder JR, editors. *The Equine Manual*. 2nd edition, W.B. Saunders; 803–804.

Weiss M.L., Anderson C., Medicetty S., Seshareddy K.B., Weiss R.J., VanderWerff I., et al., (2008). *Immune properties of human umbilical cord Wharton's jelly-derived cells*. *Stem Cells*; 26(11): 2865 – 2874.

GENERAL RESULTS AND DISCUSSION

The purpose of this PhD thesis was to perform a dissertation about the equine umbilical cord (UC), with particular attention to its macroscopic characteristics moving into its microscopic features, since UC is a good Mesenchymal Stem Cells (MSCs) niche.

The first section aimed to describe the macroscopic features of equine UC (length and number of coils), to calculate the umbilical coiling index (UCI) in normal pregnancy and healthy foals of three different breeds. One hundred twenty four healthy mares with normal pregnancy were enrolled in the study and were divided into three groups according to the breed: 70 Standardbreds (STB), 38 Thoroughbreds (THB) and 16 Saddlebreds (SAD). All the STB and SAD were housed in Italy while the THB were housed in New Zealand. Mare's age was higher in SAD than in THB and STB; the latter had a significantly lower gestational length. The foal's weight was positively correlated with placental weight in all breeds; in STB, the foal's weight was positively related to parity and gestational length. Regarding the mean total UC length, data reported in the present study are comparable to the previous reported in Thoroughbred, Standardbred and Warmblood. The length of the two UC portions was statistically different between STB and THB, where the amniotic portion is longer than the allantoic one. In each breed, total UC length was correlated with number of total coils (THB and STB = 5 ± 1 ; SAD = 6 ± 1), the UC's amniotic length was positively correlated with the number of amniotic coils as the allantoic length with the number of allantoic coils. The normal UCI was 0.09 in STB and THB and 0.1 in SAD. The number of coils and the UCI has never been investigated in veterinary medicine.

The first section aimed also to microscopically and immunohistochemically describe the physiological aspects of equine umbilical cord. Twenty-eight healthy mares housed for attended delivery were enrolled in the study. Immediately after breaking of the umbilical cord,

the intramniotic portion closest to the foal (about 15 cm) was collected. The following data were recorded: gestational length, days of pregnancy, length of stage II labour (minutes), placental weight and presence of foetal membranes alterations. Macroscopic evaluation of umbilical cords was performed for evaluating WJ's distribution. Furthermore, immediately after foaling, APGAR score, foal's weight, sex and outcome were recorded. Umbilical cord's sections were stained with Masson's trichrome stain, Orcein technique to identify elastic fibres and with Silver Impregnation technique to identify reticular fibres. The immunohistochemical analysis was conducted giving particular attention at WJ. The WJ was found just in the intramniotic portion of UC, closest to the foal, while it was absent in the allantoic portion. The amount of WJ (g), mean 5.1 ± 3.2 , was negatively correlated with the mare's age ($P < 0.05$; $r = -0.387$). All the vessels (two umbilical arteries and one umbilical vein) showed the three typical layers: tunica intima, tunica media and tunica adventitia. A perivascular tissue, composed by dense collagen fibres arranged concentrically, surrounded the tunica adventitia. Wharton's jelly was made of collagen fibres, which were arranged to create a loose reticular texture with also fibroblast, white blood cells and capillaries. Finally, the UC were externally surrounded by amniotic membrane. Elastic fibres were less concentrated with an uneven pattern around the vessels and a dense network of reticular fibres was found in the entire section of the cord. The immunohistochemical analysis revealed the presence of fibroblast cells positive for antibodies anti-type I, V and VI collagen and anti-fibrillin. For the first time in equine medicine, we reported the physiological amount of Wharton's jelly in normal umbilical cord. In human medicine, in fact, a quantitative variation of WJ was associated with pathological conditions such as hypertensive disorders, foetal distress, gestational diabetes and foetal growth restriction. Furthermore, the total absence of WJ has been associated with foetal death. The reduction of WJ facilitate torsion, compression

or stretching of UC that would adversely affect foetal blood flow. Given the presence in human species of a strong correlation between these and specific pathological conditions of newborn and mother, further studies are needed, both on normal and high risk pregnancies to verify the presence of these correlations also in the equine species.

In the second and major component of this dissertation, the ultrastructural characterization and immune profile of equine MSCs derived from foetal tissues (Wharton's jelly and blood) were investigated; equine foetal MSCs were then compared to human foetal MSCs and equine adult MSCs.

In the first study we compared clinically relevant characteristics of equine MSCs derived from AM and WJ; we found that MSCs were more easily isolated from WJ, even if MSCs derived from AM exhibited most rapid proliferation ($P < 0.05$). Osteogenic and chondrogenic differentiation was most prominent in MSCs derived from WJ, as also suggested by the lower adhesion of AM cells, demonstrated by the greater volume of spheroids after hanging drop culture ($P < 0.05$). Data obtained by PCR confirmed the immunosuppressive function of AM and WJ-MSCs and the presence of active genes specific for anti-inflammatory and angiogenic factors (IL-6, IL 8, IL- β 1). For the first time, by means of transmission electron microscopy (TEM), we ascertained that equine WJ-MSCs constitutively produce a very impressive number of large vacuolar bodies, scattered throughout the cytoplasm. Through the examination of cell monolayers by TEM, we observed that the most noteworthy difference between AM-MSCs and WJ-MSCs was the presence of an abundant extracellular fibrillar matrix located in the intercellular spaces among WJ-MSCs. These findings indicate that MSCs from different sources display significantly different properties that may impact on their therapeutic application. The data presented in this paper have an additional value, as they can be noteworthy for horses as well as for other mammalian species, including humans.

The second study of this section aimed to compare human and equine WJ-MSCs. Human and equine WJ-MSCs were isolated and cultured using the same protocols and culture media. Cells were characterized by analysing morphology, growth rate, migration and adhesion capability, immunophenotype, differentiation potential and ultrastructure. Results showed that human and equine WJ-MSCs have similar ultrastructural details connected with intense synthetic and metabolic activity, but differ in growth, migration, adhesion capability and differentiation potential. In fact, at the scratch assay, the migration rate of human WJ-MSCs was higher ($P < 0.05$) than that of equine cells, while the volume of spheroids obtained after 48 h of culture in hanging drop was larger than the volume of equine ones ($P < 0.05$), demonstrating a lower cell adhesion ability. This also revealed the lower doubling time of equine cells (3.5 ± 2.4) as compared to human (6.5 ± 4.3) ($P < 0.05$), and subsequently the higher number of cell doubling after 44 days of culture observed for the equine (20.3 ± 1.7) as compared to human cells (8.7 ± 2.4) ($P < 0.05$). Even if in both species tri-lineage differentiation was achieved, equine cells showed a higher chondrogenic and osteogenic differentiation ability ($P < 0.05$). Our findings indicate that, although the ultrastructure demonstrated a staminal phenotype in human and equine WJ-MSCs, they showed different properties reflecting the different sources of MSCs.

The third study of this section aimed of the study was to compare and describe property and characteristics of equine foetal and adult MSCs; in particular, MSCs derived from umbilical cord blood and Wharton's jelly, bone marrow (BM) and adipose tissue (AT). Umbilical cord blood (UCB) and Wharton's jelly (WJ) samples were collected immediately after delivery from three healthy mares. BM and AT were collected from three healthy horses. WJ-MSCs showed the highest chondrogenic and osteogenic differentiation potential, related to UCB-MSCs and adult cells. On the contrary, cells isolated from fluid matrix (BM and UCB)

showed a higher ability to differentiate in tenocytes, while WJ-MSCs showed the lower one. ICC investigation showed in all the cells a positive expression of the mesodermal marker alpha-SMA. However, the ICC results regarding the expression of N-Cadherin by cells but derived from fluid matrix (UCB and BM) are controversial. WJ-MSCs were the unique that expressed OCT-4, IL-8, IL- β 1 and IL-6. Their expression by WJ-MSCs make these cells the best choice for the application in regenerative medicine, also for the non-invasive collection of WJ because umbilical cord is routinely discarded at parturition. In this study, numerous intra and extracellular vacuolar bodies in foetal MSCs and only extracellular vesicles in adult MSCs were found. These vesicles, originated from the internal layer of the cell membrane, had different dimensions (small, medium and big), containing a material of unknown composition. As demonstrated by other authors, they have the role of collecting efficiently cellular components: since cells have an intense replicative and metabolic capacity, they continuously need a renovation of their structures. Recent studies support the idea that these microvesicles contain some substances, made by the cell itself, that have a fundamental role in stimulating healing processes in damaged tissues (Du et al., 2014; Lange-Consiglio et al., 2016), and have also immunomodulatory activities

The third section included the clinical applications of MSCs derived from AF and WJ on cutaneous wounds of different ages' foals. The employ of foetal MSCs on cutaneous wounds decreased their healing both in neonatal foals and six-month foals, in comparison with other traditional treatments.

In the first study of this section, an innovative therapy for spontaneously arisen pressure sores in seven hospitalized neonatal foals is described, using amniotic fluid Mesenchymal Stem Cells (AF-MSCs). Cells were isolated from amniotic fluid collected at delivery in healthy mares. Heterologous cells, at passage three of in vitro culture, were local applied to sores

twice a week for four consecutive times in a carboxymethylcellulose (CMC) gel. As a control, a commercial ointment was used. The results showed that the mean sore regression rate with AF-MSCs in CMC gel was statistically higher than the mean value recorded in the control group. This was associated with a significant effect of the treatment used and a statistically significant effect of treatment over time.

In the second study of this section, a 6 months old filly, with a skin wound on the left hock, was treated with WJ-MSCs and the wound's regression was determined. The treatment was divided into three phases: surgical, regenerative and medical. In order to monitor daily the healing, the wound was evaluated macroscopically following two human classifications. In the surgical phase two surgical curettages were carried out and then the wound was daily treated with commercial cream. In the regenerative phase of the treatment, lasted 18 days, we performed four cutaneous applications of heterologous WJ-MSCs in carboxymethyl cellulose gel, as a scaffold and autologous plasma, as metabolic support for the cells. After the first application, the vital granulation tissue that filled the wound was already visible and the disappearance of the small amount of necrotic tissue that was present at the end of the surgical phase was evident. In the medical phase the wound was daily cleaned and treated with ozone bases ointment. The three phases of the treatment led to a progressive reduction of wound's dimension: $7.28 \pm 0.20 \text{ cm}^2$ at the end of the first phase, $1.90 \pm 0.03 \text{ cm}^2$ after the WJ-MSCs application and $0.38 \pm 0.01 \text{ cm}^2$ at discharge.

Since the absence of side effects and the good results obtained, the local use of heterologous MSCs derived from foetal adnexa could represent a perfect healing treatment on deep wounds both in hospitalized neonatal foals and adult horses.

CONCLUSIONS

Based on our results, it is evident that the umbilical cord, usually discarded, warrants major attention in equine medicine: both for the evaluation of the foal at birth and as optimal source of Mesenchymal Stem Cells.

The results obtained in these studies on healthy foal's umbilical cord could be useful as control in further studies to evaluate if any alteration could be related to neonatal illness, as in human medicine.

We also underlined differences and similarities between equine and human fetal MSCs, and equine adult and fetal MSCs; finally, we applied the fetal MSCs on spontaneous wounds in foals and we obtained a very high regression rate without any side effects.